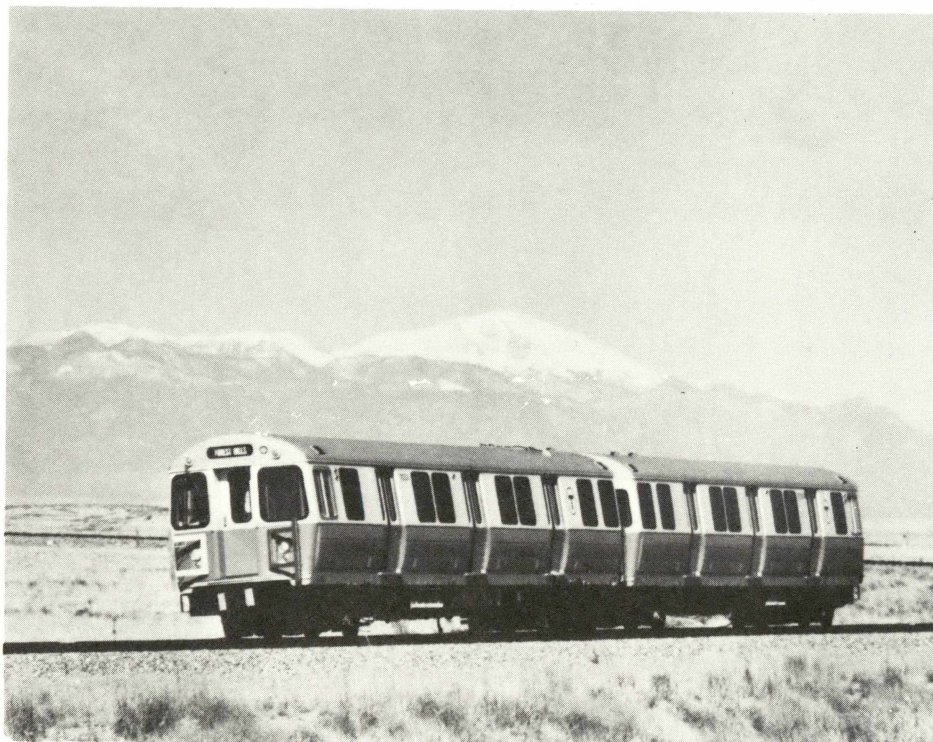


Massachusetts Bay Transportation Authority

No. 12 Orange Line Vehicle Evaluation



U.S. DEPARTMENT OF TRANSPORTATION
TRANSPORTATION TEST CENTER



MASSACHUSETTS BAY
TRANSPORTATION AUTHORITY

NOTICE

This document is disseminated under the sponsorship of the Department of Transportation in the interest of information exchange. The United States Government assumes no liability for its contents or use thereof.

The United States Government does not endorse products or manufacturers. Trade or manufacturers' names appear herein solely because they are considered essential to the object of this report.

1. Report No. FRA/TTC-81/12		2. Government Accession No.		3. Recipient's Catalog No.	
4. Title and Subtitle Massachusetts Bay Transportation Authority No. 12 Orange Line Vehicle Evaluation			5. Report Date October, 1981		
			6. Performing Organization Code		
7. Author(s) K.J. Simmonds and G.R. Arnold*			8. Performing Organization Report No.		
9. Performing Organization Name and Address Transportation Test Center P.O. Box 11449 Pueblo, Colorado 81001			10. Work Unit No. (TRAIS)		
			11. Contract or Grant No.		
12. Sponsoring Agency Name and Address U.S. Department of Transportation Urban Mass Transportation Administration Office of Technology Development and Deployment Office of Rail and Construction Technology Washington, DC 20590			13. Type of Report and Period Covered Final Report February-April, 1981		
			14. Sponsoring Agency Code		
15. Supplementary Notes *Boeing Services International, Inc., Operations and Maintenance Contractor, Transportation Test Center, Pueblo, Colorado, Contract DTFR-80-C-20016 with the Federal Railroad Administration					
16. Abstract This report presents the results of an engineering evaluation of the Massachusetts Bay Transportation Authority's No. 12 Orange Line rapid transit cars, accomplished at the Transportation Test Center, Pueblo, Colorado. The test program was carried out from February through April, 1981. The scope of the program included vehicle performance, ride quality, acoustic transmissibility and absorptivity tests, and an evaluation of the squeal properties of several brake shoe types. Wherever appropriate, test data were compared to the vehicle specifications criteria; ride quality data were compared to International Organization for Standardization (ISO) guidelines for ride comfort. The test data show that the vehicles generally met the requirements of their specification criteria; deficiencies were noted in the friction-only and emergency braking performance. The vehicle ride quality was dominated by a vertical vibration at the carbody center, thought to be due to excitation of the first vertical bending mode. The phenomenon was aggravated by passenger load and by speed. At higher passenger loads and speeds the vertical vibration approached the 25-minute reduced comfort boundary of the ISO guidelines. The contribution of the vehicle doors to the transmissibility of noise to the vehicle interior was defined, together with the effectiveness of acoustic ceiling panels in attenuating interior noise. The brake squeal tests identified a type of lead- and asbestos-free shoe which did not squeal, but which exhibited a braking performance decrement compared to the standard brake shoes.					
17. Key Words Rapid Transit Vehicles Performance Ride Quality Interior Noise Brake Squeal			18. Distribution Statement Document may be purchased from the National Technical Information Service 5285 Port Royal Road Springfield, Virginia 22161		
19. Security Classif. (of this report) Unclassified		20. Security Classif. (of this page) Unclassified		21. No. of Pages 148	22. Price

TABLE OF CONTENTS

	<u>Page</u>
EXECUTIVE SUMMARY	xv
INTRODUCTION	1-1
Background	1-1
Test Program Scope	1-1
Test Variables	1-2
Train Consist	1-2
Master Controller	1-2
Braking System	1-2
Input Voltage	1-3
Speed	1-3
Vehicle Weight	1-3
Chronology	1-4
DESCRIPTION OF VEHICLE	2-1
Design Parameters	2-1
Carbody	2-1
Trucks and Suspension	2-3
Propulsion and Control System	2-3
Traction Motors and Gear Units	2-4
Braking System	2-4
DESCRIPTION OF FACILITIES	3-1
Transit Test Track	3-1
Climatic Conditions	3-6
Instrumentation, Data Acquisition, and Data Processing	3-6
PERFORMANCE CHARACTERISTICS	4-1
Acceleration	4-1
Objectives	4-1
Test Method	4-2
Results	4-2
Braking	4-12
Objectives	4-12
Test Method	4-12
Results	4-13

TABLE OF CONTENTS, CONTINUED

	<u>Page</u>
Spin/Slide Protection System Efficiency	4-29
Objective.	4-29
Test Method.	4-30
Results.	4-30
Train Resistance.	4-36
Objectives	4-36
Test Method.	4-36
Results.	4-37
Energy Consumption.	4-41
Objectives	4-41
Test Method.	4-41
Results.	4-42
Duty Cycle.	4-44
Objective.	4-44
Test Method.	4-44
Results.	4-44
RIDE QUALITY TESTS	5-1
Component-Induced Vibration	5-4
Objective.	5-4
Test Method.	5-4
Results.	5-4
Comparison of Ride Quality to ISO 2631 Reduced Comfort Boundaries.	5-4
Effect of Constant Vehicle Speeds and Vehicle Loading on Ride Quality.	5-9
Objective.	5-9
Test Method.	5-9
Results.	5-10
Effect of Track Section on Ride Quality	5-14
Objective.	5-14
Test Method.	5-14
Results.	5-14

TABLE OF CONTENTS, CONTINUED

	<u>Page</u>
Effect of Acceleration and Braking on Ride Quality.	5-16
Objective.	5-16
Test Method.	5-16
Results.	5-16
The Low Frequency Ride of the Vehicle	5-16
Comparison of the Orange Line Ride Quality to that of the Blue Line	5-19
Summary	5-26
ACOUSTIC TESTS	6-1
Absorptive Panel and Door Transmissibility Evaluation	6-1
Objectives	6-1
Test Methods	6-1
Results.	6-3
Brake Squeal.	6-11
Objectives	6-11
Test Method.	6-11
Results.	6-12
APPENDIX A	
APPENDIX B	

LIST OF FIGURES

<u>Figure</u>	<u>Page</u>
2-1 MBTA Orange Line Vehicles at TTC	2-2
3-1 Transit Test Track	3-2
3-2 Transit Test Track Profile Showing Grades.	3-3
4-1 Effect of Vehicle Weight on Acceleration Characteristics . . .	4-3
4-2 Effect of Vehicle Weight on Time/Distance and Time/Speed Relationships.	4-4
4-3 Effect of Master Controller Position on Acceleration Characteristics.	4-6

LIST OF FIGURES, CONTINUED

<u>Figure</u>		<u>Page</u>
4-4	Effect of Master Controller Position on Time/Distance and Time/Speed Relationships	4-7
4-5	Effect of Line Voltage on Acceleration Characteristics	4-8
4-6	Effect of Line Voltage on Time/Distance and Time/Speed Relationships.	4-9
4-7	Effect of Direction of Travel/Lead Car on Acceleration Characteristics.	4-10
4-8	Effects of Direction of Travel/Lead Car on Time/Distance and Time/Speed Relationships	4-11
4-9	Full Service EP Blended Braking Characteristics, AWO Weight.	4-14
4-10	Full Service EP Blended Braking Characteristics, AW3 Weight.	4-14
4-11	Full Service SAP Blended Braking Characteristics, AWO Weight	4-16
4-12	Full Service SAP Blended Braking Characteristics, AW3 Weight	4-16
4-13	Time and Distance Required to Stop, Blended Braking, AWO Weight	4-17
4-14	Time and Distance Required to Stop, Blended Braking, AW3 Weight	4-17
4-15	Full Service EP Friction Braking Characteristics, AWO Weight	4-18
4-16	Full Service EP Friction Braking Characteristics, AW3 Weight	4-18
4-17	Full Service SAP Friction Braking Characteristics, AWO Weight	4-19
4-18	Full Service SAP Friction Braking Characteristics, AW3 Weight	4-19
4-19	Average Braking Deceleration Characteristics, Friction Braking.	4-21
4-20	Time and Distance Required to Stop, Friction Braking, AWO Weight	4-22
4-21	Time and Distance Required to Stop, Friction Braking, AW3 Weight	4-22

LIST OF FIGURES, CONTINUED

<u>Figure</u>		<u>Page</u>
4-22	Emergency Braking Characteristics, AWO Weight.	4-23
4-23	Emergency Braking Characteristics, AW3 Weight.	4-23
4-24	Time and Distance Required to Stop, Emergency Braking, AWO Weight	4-24
4-25	Time and Distance Required to Stop, Emergency Braking, AW3 Weight	4-24
4-26	Average Deceleration Characteristics, Emergency Braking. . . .	4-27
4-27	Jerk Rate Determination for A Typical Brake Application. . . .	4-28
4-28	Effect of Weight and Control Mode on Jerk Rate	4-28
4-29	Effect of Weight and Control Mode on Control Response.	4-29
4-30	Spin Characteristics Under Acceleration.	4-32
4-31	Slide Characteristics Under Braking.	4-33
4-32	Drift Deceleration Characteristics, AWO Weight	4-38
4-33	Drift Deceleration Characteristics, AW3 Weight	4-38
4-34	Train Resistance Variation with Speed.	4-39
4-35	Comparison of Train Resistance Test Data with Davis Formula Calculated Values.	4-40
4-36	Energy Consumed by A Two-Car Train, Orange Line Round Trip Simulation.	4-43
4-37	Brake Shoe Temperature Time Histories During An Orange Line Duty Cycle	4-45
5-1	Ride Roughness vs Reduced Comfort Exposure Time (ISO 2631) . . .	5-2
5-2	Carbody Accelerometer Locations.	5-3
5-3	1/3 Octave Band Vibration Levels	5-6
5-4	1/3 Octave Band Vibration Levels	5-6
5-5	Effect of ISO Frequency-Weighting Applied to Lateral and Vertical Spectra	5-7

LIST OF FIGURES, CONTINUED

<u>Figure</u>		<u>Page</u>
5-6	1/3 Octave Band Vibration Levels	5-8
5-7	1/3 Octave Band Vibration Levels	5-8
5-8	Ride Roughness Time History, Midcar Vertical	5-9
5-9	Ride Roughness Levels, Variation with Speed, AW3 Weight.	5-11
5-10	Ride Roughness Levels, Effect of Three Worst Speeds.	5-13
5-11	Comparison of Frequency Spectra at Two Vehicle Weights	5-13
5-12	Ride Roughness Time Histories.	5-15
5-13	Ride Roughness Time History.	5-15
5-14	Ride Roughness Time Histories, Forward Lateral and Midcar Vertical During Acceleration	5-17
5-15	Ride Roughness Time Histories During Blended and Friction Braking	5-18
5-16	1/3 Octave Band Vibration Levels	5-20
5-17	1/3 Octave Band Vibration Levels	5-20
5-18	Curve of Constant Motion Sickness Incidence as a Function of Frequency	5-21
5-19	1/3 Octave Band Vibration Levels, Comparing Orange and Blue Line Cars.	5-23
5-20	1/3 Octave Band Vibration Level, Comparing Orange and Blue Line Cars.	5-23
5-21	1/3 Octave Band Vibration Levels, Comparing Orange and Blue Line Cars.	5-24
5-22	1/3 Octave Band Vibration Level, Comparing Orange and Blue Line Cars.	5-24
6-1	Undercar Sound Pressure Levels at 40 mi/h.	6-5
6-2	Undercar Sound Pressure Levels at 65 mi/h.	6-6
6-3	Effect of Absorptive Ceiling Panels on Interior Sound Pressure Levels, Track Stations 14-17	6-7

LIST OF FIGURES, CONTINUED

<u>Figure</u>		<u>Page</u>
6-4	Exterior Sound Pressure Levels, Compared to Standard Carbody Interior Levels, Track Stations 14-17	6-8
6-5	Interior Sound Pressure Levels with Side Doors Open, Track Stations 14-17	6-9
6-6	Interior Sound Pressure Levels with all Doors Insulated, Track Stations 14-17	6-10
6-7	Interior Sound Pressure Levels with End Doors Insulated, Track Stations 14-17	6-10
6-8	Maximum Noise Levels, Onboard and Wayside.	6-14
6-9	Typical Wayside Frequency Spectra During Brake Squeal (Unweighted)	6-15
6-10	Friction Braking Characteristics	6-16
A-1	Data Acquisition System, Block Diagram	A-7
A-2	Data Acquisition System.	A-8
A-3	Data Acquisition System.	A-9

LIST OF TABLES

<u>Table</u>		<u>Page</u>
1-1	Vehicle Weights.	1-4
1-2	Schedule Summary	1-4
2-1	Vehicle Description.	2-1
2-2	Controller Power Positions	2-3
3-1	TTT Construction Details	3-4
3-2	Amplitude and Waveforms of TTT Perturbations, Design Specifications	3-5
4-1	Vehicle Time-To-Speed Data Compared to Specification Requirement.	4-3
4-2	Control Response Times and Jerk Rates Under Acceleration, From a Standing Start.	4-6
4-3	Summary of Emergency Braking Data, AWO Weight.	4-26
4-4	Summary of Emergency Braking Data, AW3 Weight.	4-26
4-5	Spin/Slide Test Data	4-35
4-6	Energy Consumption Summary	4-42
4-7	The Orange Line Round Trip, Recorded Times and Distances . . .	4-46
5-1	Percent Change in Ride Roughness Level Due to Change in Speed (AW3 Weight)	5-11
5-2	Percent Difference of AW4 Ride Roughness Values from Those of AWO Weight.	5-12
5-3	Percent Differences from Average Ride Roughness Levels due to Effect of Track Section	5-14
5-4	ISO 2631 Lateral and Vertical Ride Roughness Values from 20 seconds of Data, Curve Part of Track Section III.	5-25
6-1	A-Weighted Sound Pressure Levels, Averaged Over Each Track Section.	6-4
6-2	Brake Shoe Types	6-11
6-3	Average Deceleration Levels from 50 mi/h	6-17

LIST OF TABLES, CONTINUED

<u>Table</u>		<u>Page</u>
A-1	Instrumentation Sensor Listing, Performance	A-2
A-2	Instrumentation Sensor Listing, Ride Quality.	A-5
A-3	Tape Recorder Configuration	A-11
A-4	One-Third Octave Band Center Frequencies.	A-14
A-5	Weighting Factors Relative to The Frequency Range of Maximum Acceleration Sensitivity* for the Vibration ISO 2631 Response Curves.	A-16
B-1	MBTA Orange Line Revenue Service Profile Simulation, Southbound.	B-2
B-2	MBTA Orange Line Revenue Service Profile Simulation, Northbound.	B-2

ACRONYMS

B&K	Brüel and Kjaer
CCW	counterclockwise
CTA	Chicago Transit Authority
CW	clockwise
EP	electropneumatic
FFT	Fast Fourier Transform
FM	frequency modulation
FRA	Federal Railroad Administration
IRIG	Inter Range Instrumentation Group
IRIG-B	Inter Range Instrumentation Group Time Code B
ISO	International Organization for Standardization
LVDT	Linear Variable Displacement Transducer
MBTA	Massachusetts Bay Transportation Authority
NYCTA	New York City Transit Authority
SAP	straight air pipe
TTC	Transportation Test Center
TTT	Transit Test Track
UMTA	Urban Mass Transportation Administration
URB	Urban Rail Building
WABCO	Westinghouse Air Brake Company
WMATA	Washington Metropolitan Area Transit Authority

ABBREVIATIONS

A	ampere(s)	lb/yd	pounds per yard
a.c.	alternating current	MHz	megahertz
Ⓢ	centerline	mi	miles
°F	degrees Fahrenheit	mi/h	miles per hour
dB	decibel	mi/h/s	miles per hour per second
dBA	decibel, A-weighted	min	minutes
d.c.	direct current	mm	millimeters
', ft	foot	ms	milliseconds
g	gravitational acceleration	psig	pounds per square inch gage
hr	hour	rms	root mean squared
Hz	Hertz	rpm	revolutions per minute
", in	inch	s	seconds
kHz	kilohertz	V	volts
kWh	kilowatt hours		
lb, lbs	pound(s)		

Executive Summary

This report presents an engineering evaluation of the No. 12 Orange Line rapid transit cars operated by the Massachusetts Bay Transportation Authority (MBTA). The evaluation was accomplished through a test program carried out from February through April 1981, at the Department of Transportation, Transportation Test Center (TTC), Pueblo, Colorado. The program was sponsored by the Office of Rail and Construction Technology in the Office of Technology Development and Deployment, Urban Mass Transportation Administration (UMTA), Washington, D.C.

The tests were conducted by Boeing Services International, Inc., the operations and maintenance contractor at the TTC, in conjunction with MBTA and Hawker Siddeley Canada Inc., the vehicle manufacturer. MBTA provided a full-time representative from their engineering consultant, L.T. Klauder and Associates, who provided technical support and coordination.

The test vehicles were designed and built by Hawker Siddeley Canada Inc. They share many major components and construction features with MBTA's No. 4 Blue Line cars, and have the same general appearance. Principal differences are in the vehicle length, (65 ft compared to 48 ft 10 in for the Blue Line cars) and the provision of a spin/slide protection system on the Orange Line cars. The Blue Line cars were the subject of an engineering test program at the TTC¹ in 1979.

The carbody is a welded steel structure with two main floor supports which run from front to rear. These allow a commonality of construction methods, and a modular approach to the fabrication of both types of cars. The carbody is mounted on two side-bearing, inside-journal trucks of cast steel construction. Primary suspension is provided by rubber/steel chevron springs mounted between the axle journals and the side frames; secondary suspension is provided by the air springs, two per truck. Two traction motors per truck are resiliently suspended in the truck frame and drive the axles through parallel reduction gearboxes. The motors are 4-pole d.c., series-wound units. Propulsion control in acceleration and braking is provided by series, series/parallel switching of motor pairs together with resistor bank stepping by means of a conventional cam controller. Compensation for vehicle weight is provided to give constant acceleration and deceleration levels independent of passenger load. The major braking effort of the cars is provided by the dynamic braking capability of the propulsion system, supplemented by friction tread brakes at low speeds, when dynamic braking becomes ineffective. The friction brakes

¹ Massachusetts Bay Transportation Authority Blue Line Vehicle Evaluation,
Report No. FRA/TTC-80/05.

provide a backup system in the event that the dynamic braking fails, and also provide all emergency braking effort.

Tests to define vehicle performance and ride quality were conducted on a married pair of cars according to standardized procedures, developed at the TTC for the evaluation of rapid transit vehicles. In addition, special acoustic noise measurement tests were formulated to investigate carbody noise transmissibility and brake squeal characteristics.

The tests were conducted on the Transit Test Track (TTT), a 9.1 mi oval of FRA Class 6 track. Six types of track typical of urban rail construction are represented in the TTT, together with typical switches and grade crossings; a level, tangent track section is used for all performance testing. The vehicles were tested at three vehicle weights identified as AW0, AW3, and AW4. The weights represented empty, standing passenger, and crush load passenger weight, respectively. The loading was simulated by means of lead ingots placed on the carbody floor.

The performance testing focused on vehicle performance in the areas of acceleration, braking, spin/slide protection system efficiency, train resistance, energy consumption, and friction brake duty cycles. The test results were compared to the vehicle specification criteria wherever appropriate. Acceleration performance was evaluated by making a series of test runs from a standing start on level, tangent track. The effects of vehicle weight, master controller position, line voltage, and direction of travel/lead car were studied to determine their influence on vehicle performance.

The vehicles met or exceeded all the acceleration criteria. Initial acceleration levels were 0.1 to 0.5 mi/h/s greater than the 2.5 mi/h/s requirement up to AW3 vehicle weight and still met this requirement at AW4 weight, showing excellent compensation for passenger load. Initial acceleration levels were maintained up to 25 mi/h at all weights, again surpassing the specification requirement for constant acceleration to 20 mi/h. Time-to-speed criteria (40 mi/h in 25 seconds and 65 mi/h in 170 seconds, maximum) were exceeded with comfortable margins; the vehicles achieved 40 mi/h in 21.5 seconds and 65 mi/h in 130.4 seconds at AW3 vehicle weight.

The master controller positions were shown to give reasonably progressive initial acceleration levels of 0.9, 1.6, and 2.6 mi/h/s for positions P1, P2 and P3, respectively; P3 and P4 controller positions give the same initial acceleration up to motor base speed, by design. There are no specification criteria for intermediate controller steps.

Initial acceleration levels were little affected by line voltage and the vehicles met the 2.5 mi/h/s acceleration requirement up to 20 mi/h at all voltages tested (550, 575, and 610 V d.c.). Above this speed, performance was marginally degraded at the lower voltage. There were no differences in acceleration performance due to direction of travel or lead car.

Jerk rates (rates of change of acceleration) were measured from the slopes of the initial acceleration time histories; the vehicles met the requirement for jerk rates not to exceed 2.0 mi/h/s². With one exception at 11 mi/h, the vehicles met the requirement for a maximum variation in acceleration of 0.6 mi/h/s, due to controller steps, with values up to ± 0.3 mi/h/s; the single exception gave a variation of ± 0.5 mi/h/s, which occurred at the transition from series to series-parallel connection of the traction motors.

The vehicles' braking performance was evaluated in blended and friction-only modes of operation for full service application, at initial speeds from 10 to 65 mi/h. The brakes were operated in their normal electropneumatic mode of control (EP) and in a back-up mode which relies on straight air pipe control (SAP). Emergency braking was evaluated over the speed range for the 'deadman' method of initiation, and from 65 mi/h initial speeds for stops initiated by the master controller 'emergency' detent, the external tripcock and the emergency brake valve in the passenger compartment. Braking performance was tested at vehicle weights of AW0 and AW3.

The vehicle specification calls for a full service braking deceleration level of 1.5 mi/h/s at 65 mi/h, increasing linearly to 2.75 mi/h/s at 50 mi/h and maintained at 2.75 mi/h/s from 50 mi/h to a stop. Emergency braking deceleration is required to be 3.25 mi/h/s throughout the speed range. The vehicles met the full service braking criteria in the blended mode with both EP and SAP operation, and showed good compensation for passenger weight. In the EP mode deceleration levels were of the order of 3.0 mi/h/s across the speed range, with levels 0.1 to 0.2 mi/h/s lower for the SAP mode of operation. Dynamic braking was effective down to 10-12 mi/h, exceeding the specification requirement that it should be effective down to 15 mi/h. Variation of deceleration due to controller steps was a maximum of ± 0.4 mi/h/s. There were no significant differences in performance due to direction of travel or operation from either motorman's cab.

Jerk rates were examined for the full service brake applications and were found in some cases to be significantly higher than the specification requirement of a maximum of 2.0 mi/h/s². The worst initial speed was found to be 20 mi/h with jerk rates in the 4.2 to 4.9 mi/h/s² range. The vehicles generally met the 2.0 mi/h/s² requirement at speeds over 40 mi/h. The MBTA recognized the jerk rate characteristics as inherent in this control system and set rates to be acceptable for normal operating conditions.

The friction-only braking characteristics showed variations in deceleration level with speed which are typical of friction braking operation. From an initial deceleration level at brake application, the deceleration fell to a minimum midway through the speed range and then peaked immediately prior to the stop. In order to assess the vehicles' overall friction braking performance, average deceleration values were computed from stopping distances and times. Based on these values the vehicles

met the intent of the specification criteria for initial brake entry speeds up to 40 mi/h. Above this speed, performance deteriorated significantly; for example, at a 50 mi/h initial speed, average decelerations were in the 2.4 to 2.5 mi/h/s range. Differences in deceleration levels due to EP or SAP mode of operation were insignificant; full service braking levels were marginally higher at AW0 vehicle weight than at AW3 (0.2 to 0.3 mi/h/s higher for the 30 mi/h initial speed case).

As for the friction-only braking, the emergency braking showed large changes in deceleration across the speed range, and so average deceleration values were computed to gain an understanding of overall performance. These show that the vehicles did not meet the 3.25 mi/h/s deceleration requirement on an average deceleration basis, except for initial speeds in the 18-30 mi/h range at AW3 vehicle weight. Emergency braking performance was better by 0.2 to 0.3 mi/h/s at the AW3 weight than at AW0. The brake cylinder pressures used to achieve the friction-only and emergency braking deceleration levels were those which had been found by L.T. Klauder and Associates to give acceptable performance levels in Boston.

The spin/slide protection system efficiency was examined in acceleration and braking. A soap solution was sprayed ahead of each wheel/rail interface, reducing the adhesion levels to the point where continuous sequences of spins or slides could be induced. The spin/slide protection system detects differences in axle rpm or excessive rates of change of rpm of any single axle. In the braking mode, braking is removed from the affected truck until the slide is corrected; in the propulsive mode, tractive effort is removed from the affected car until the spin is corrected. The system efficiency is defined as the achieved average tractive effort (whether propulsive or braking) divided by the available average tractive effort at the limit of adhesion, expressed as a percentage. Since vehicle mass is a constant, this can be expressed in terms of vehicle acceleration from the simple Force = Mass x Acceleration relationship. Using numerical integration techniques, achieved average acceleration and maximum average acceleration values were defined from the oscillograph traces of vehicle acceleration, and the system efficiencies were calculated from these values. For vehicle acceleration, the spin/slide protection system efficiency varied between 62 and 69 percent at coefficients of adhesion between 0.064 and 0.075. Under EP-controlled blended braking the cars achieved a system efficiency of 70 percent at a coefficient of adhesion of 0.077. The specification criterion calls for a system efficiency of at least 70 percent.

Drift tests were conducted to define the train resistance characteristics of the two-car train. The cars were coasted through a section of level tangent track in a series of overlapping test runs covering the speed range from 65 mi/h to a stop. The deceleration data gathered were converted into train resistance values, and compared to values calculated from the empirical Davis formula. The coefficients used in the formula for flanging and aerodynamic losses, and the value for

vehicle frontal area, were those given in the vehicle specification. The comparison showed that the Davis formula with the defined coefficients gives a good approximation of the actual train resistance at sea level. With an altitude correction applied to the aerodynamic resistance term, the Davis formula train resistance agrees well with the test data.

The energy consumption of the vehicles was measured while operating over a simulated service profile run. This represented an actual revenue service profile, with the distance between stations, section speeds, and station stop times accurately represented; only the track gradients differed.

Operating at AW3 vehicle weight and using full service (P4) acceleration, the energy consumption for a simulation of an Orange Line round trip from Oak Grove to Forest Hills was 4.8 kWh/car-mile. Limiting vehicle operation to a P3 controller position for acceleration, the energy consumed for the same route was 4.5 kWh/car-mile, for a 30-second penalty in trip time over the 21.8-mi distance. The P3 controller setting represents an 'economy' configuration as opposed to the P4 configuration which uses field weakening.

The equilibrium temperatures of the vehicles' friction brakes were determined while operating over the Orange Line revenue service profile, using full service braking in a friction-only mode. The temperatures of each brake shoe on the left-hand side of one car were recorded immediately following each station stop. Operating at AW4 vehicle weight on a 50° F day, the brake shoe temperatures stabilized in the 150°-200° F range, with the exception of the lead axle brake shoe which increased to, and stabilized at 225°-235° F during the last 12 minutes of the return trip. The general range of temperatures recorded will give no cause for concern when operating the vehicles over the Orange Line route in a friction-only braking mode.

The ride quality testing addressed component-induced vibration and carbody vibration due to vehicle operation. The effects of vehicle weight, track section, speed, and acceleration and deceleration were studied. Vibration levels were compared to the vehicle specification for component-induced criteria and to ISO² guidelines for ride quality. The guidelines specify a series of 'reduced comfort' boundaries, or exposure time limits to vibration across the frequency spectra. The exposure limits are expressed in acceleration levels (g rms) for each one-third octave frequency band.

Three carbody floor locations, over the front and rear truck kingpins and at the carbody longitudinal center, were instrumented with vertical and lateral accelerometers. Tests were conducted over all sections of the TTT, at vehicle weights of AW0, AW3, and AW4. Test runs were made at 'worst speeds'

2 Guide for the Evaluation of Human Exposure to Whole-body Vibration, ISO 2631-1974, International Organization for Standardization.

determined by observation of the online oscillograph traces. The data were processed using a spectrum analyzer integrated with a desktop computer to produce one-third octave frequency domain data. Time history data were rms-averaged and weighted to accentuate frequency content to which the human body is susceptible. This is analogous to the A-weighting of noise data.

For the component-induced test, the undercar equipment was operated individually and in various combinations while the accelerometer outputs were recorded. The worst-case vibration due to the undercar equipment was found to be in the vertical direction and was one-twentieth of the specification criterion. The specification states that vibration due to auxiliary equipment shall not exceed 0.04 g peak at any frequency up to 60 Hz. Since the vibration levels were small in relation to the equipment vibration criterion, no further analysis was undertaken.

One vibration phenomenon, a 10 Hz vertical vibration, predominately in the center of the carbody, dominated all other aspects of the vehicle ride quality. The high vibration levels were produced by excitation of the first body bending mode. The vibration was aggravated by speed and by increased vehicle weight. As the speed was increased, the periods of 10 Hz vibration became more sustained and of higher amplitude; 62 mi/h was identified as a worst-speed case. At AW3 vehicle weight and 62 mi/h the level of the one-third octave band centered on 10 Hz approached 0.1 g rms, which is coincident with the 25-minute ISO reduced comfort boundary. The vertical vibration levels at the front and rear of the carbody approached the ISO one-hour boundary at this condition, due to the 10 Hz band carbody response. Observation of the vehicle ride quality at 62 mi/h showed that the track section from stations 26 through 29 produced the most sustained periods of vibration. This particular section is constructed of 100 lb/yd jointed rail on wood ties, and is a 1°30' curve with 4" of superelevation, maintained to FRA Class 6 standards.

It is likely that the vehicle ride at the midcar location will cause passenger complaints at the high vehicle weights and speeds. Remedial steps should be taken to identify and 'de-tune' the forcing function which excites the 10 Hz carbody first vertical bending mode.

In contrast to the vertical ride, the lateral and longitudinal ride quality was excellent. In general, throughout the speed range, all one-third octave band levels were lower than the eight-hour ISO reduced comfort boundary line.

Acoustic noise tests were conducted to determine the contribution of the vehicle doors to the transmission of noise to the carbody interior, and to evaluate the effectiveness of ceiling acoustic treatment panels. In addition, onboard and wayside noise tests were undertaken to determine the brake squeal characteristics of a series of alternate brake shoe types, with the objective of choosing the best type for revenue service.

For the door transmissibility and acoustic treatment test, interior and exterior sound pressure levels were compared for a longitudinal carbody location centered on the rear doors. Standard carbody noise levels were compared to cases with insulation applied over the door exteriors, and for the acoustic ceiling panels masked with Masonite. The comparisons were made at speeds of 40 and 65 mi/h.

A 2 - 5 dB reduction in sound pressure level was experienced for one-third octave bands with center frequencies from 250 Hz to 4 kHz, after insulating both side and end doors. At 40 mi/h, the standard carbody interior noise levels were in the range 65-71 dBA, compared to 63-66 dBA for the 'all doors insulated' case. The interior ceiling acoustic panels were shown to have little or no absorptive effect for the sound frequency spectra experienced on the TTC.

Four sets of brake shoes were submitted for evaluation of their brake squeal properties. Westinghouse Air Brake Company (WABCO) submitted types V-222/W-539 (the standard vehicle brake shoe), V-239/W-539, and V-239/W-560. Hawker Siddeley Canada Inc. submitted TBL-693 shoes manufactured by TBL, Ltd of England. The shoes were evaluated in a new and worn condition, using friction-only braking stops from 50 mi/h at AW3 vehicle weight. Noise measurements were made onboard and at the wayside. The following test results were defined:

- o The WABCO V-239/W-560 had the highest onboard noise levels, 120 dB at a location adjacent to the rear truck, and were withdrawn from the test.
- o The other WABCO shoes, configurations V-222/W-539 and V-239/W-539 (the first a two-piece configuration, the second a one-piece) gave comparable brake squeal noise levels when new (104 dB, at 15 ft from the track centerline). However the V-239/W-539 configuration improved dramatically when worn, with levels 8-10 dB less at the 15 ft location, whereas the V-222/W-539 configuration showed no improvement. There was little or no brake squeal noise with the V-239/W-539 worn configuration.
- o The TBL-693 shoes were by far the quietest of all the shoes evaluated. Wayside sound pressure levels at the 15 ft location were less than 80 dB. There were no incidences of brake squeal. However, in comparing the braking deceleration characteristics, the TBL-693 showed a 0.2 mi/h/s performance decrement for both full service and emergency braking modes, based on average deceleration levels from 50 mi/h.
- o A one-third octave analysis of several typical brake squeal records showed that the predominant frequency excited by the brake squeal phenomenon lies in the one-third octave band centered on 31.5 kHz.

The cars demonstrated excellent reliability while at the TTC. Of 292 hours of scheduled testing, the cars were

available for 286 hours which represents 98 percent availability. During 6,381 miles of testing only one component failure was recorded. This was a high pressure limit switch on an air conditioning compressor.

Performance and ride quality testing was accomplished in 21 working days, the brake squeal evaluation in 17 days, and the door transmissibility and acoustic panel tests in 5 days. The total test program, including unloading, instrumentation installation, checkout, testing, and preparation to ship, was accomplished in 73 working days.

1 Introduction

This report presents an evaluation of the performance, ride quality, and acoustic characteristics of two examples of the No. 12 Orange Line rapid transit cars belonging to the Massachusetts Bay Transportation Authority (MBTA). The evaluation was accomplished through an engineering test program carried out at the Transportation Test Center (TTC), Pueblo, Colorado, from February through April 1981. The test program was sponsored by the Office of Rail and Construction Technology in the Office of Technology Development and Deployment, Urban Mass Transportation Administration (UMTA), Department of Transportation, Washington, D. C.

The evaluation tests were conducted according to test procedures developed at the TTC; additional special engineering tests were defined by the TTC in conjunction with MBTA and Hawker Siddeley Canada Inc., the vehicle manufacturer. MBTA furnished a full-time representative from their engineering consultant, L. T. Klauder and Associates, who provided technical support and coordination, and monitored the test program activity.

BACKGROUND

In 1973, specifications for the No. 4 Blue Line and No. 12 Orange Line cars were issued by the MBTA. The specifications were written to provide a commonality of major components and design features between the two car designs. A contract was signed on August 19, 1976, with Hawker Siddeley Canada Inc., for production of 70 Blue Line and 120 Orange Line cars. The MBTA, in cooperation with UMTA, requested the Federal Railroad Administration (FRA) conduct engineering tests on a married pair of each type of car at the TTC. The Blue Line vehicles were tested at the TTC from April through October, 1979.¹

TEST PROGRAM SCOPE

The test program evaluated the Orange Line vehicles in the areas of performance (acceleration, braking, and energy consumption, for example) and ride quality. Wherever applicable, the data were compared to the vehicle procurement technical specifications to determine how well these specifications had been met. Special engineering tests were conducted to evaluate noise transmissibility through the vehicle doors and the effectiveness of acoustic absorption panels in the vehicle ceilings. The categories of the vehicle evaluations were:

¹ Massachusetts Bay Transportation Authority Blue Line Vehicle Evaluation,
Report No. FRA/TTC-80/05.

- Acceleration
- Braking (blended, friction-only, and emergency modes of operation)
- Spin/Slide Protection System Efficiency
- Train Resistance
- Friction Brake Duty Cycle
- Component-Induced Vibration
- Ride Quality (effects of speed, track type, and acceleration/deceleration)
- Brake Shoe Squeal
- Door Acoustic Transmissibility
- Effectiveness of Acoustic Absorption Panels.

TEST VARIABLES

The vehicles were evaluated for the test condition variables described in the following paragraphs.

Train Consist

Testing was limited to the evaluation of a two-car train, comprised of cars 01208 and 01209. Orange Line cars are normally operated in trains of up to four cars. Each car in the train is married or permanently coupled to a complementary car and cannot be operated without it; this requirement is dictated by the allocation of undercar auxiliary equipment between the two cars.

Master Controller

The operator's master controller has four discrete levels of power application, P1 (minimum) through P4 (maximum), and vehicle acceleration characteristics were evaluated at each of these settings. The controller also has two indicated service brake positions, minimum application and full service, with variable positioning between the two, and an emergency position. Normal service brake characteristics were evaluated only for the full service position. Emergency braking was initiated by each of the vehicles' emergency trip systems in turn; i.e., master controller initiation, the motorman's 'deadman' handle, the emergency brake valve (located on the forward bulkhead of the passengers compartment), and the external wayside-initiated tripcock.

Braking System

The braking system is normally an electropneumatic (EP) controlled system, actuated by movement of the master controller. If the EP system fails, braking control is provided by a back-up straight air pipe (SAP) pneumatic system which provides full control, with a small control response delay not present in the EP mode. The test program evaluated the performance of the braking system with both modes of control. Braking performance was evaluated for blended; i.e., dynamic plus friction braking, and friction-only modes of operation, and for emergency operation.

Input Voltage

Acceleration performance characteristics were evaluated at nominal line voltages of 550, 575, and 610 V d.c. 'Nominal' voltage levels are set at the third rail collector shoe with the vehicles' stationary and auxiliary systems operating. All other test objectives were accomplished with line voltages between 575 and 610 V d.c. It should be noted that the nominal voltage is set under near 'no-load' conditions, and that significant voltage drops are experienced under load.

Speed

The vehicles were evaluated over a speed range from zero to 65 mi/h; braking performance was evaluated for initial braking entry speeds of 65, 50, 40, 30, 20, and 10 mi/h; ride quality test speeds were selected on the basis of those speeds which most excited the carbody.

Vehicle Weight

The vehicles were tested at three vehicle weights, simulating various passenger lading configurations, by means of lead ingots placed on the carbody floor. The three loadings represented empty weight, standing passenger weight, and maximum rush hour crush passenger weight; the configurations are designated AWO, AW3, and AW4, respectively.* The nominal condition and the actual test weights are listed in Table 1-1.

* Car 01209 was subjected to a load of approximately 1,400 lbs over the rear truck due to the weight of the data acquisition system. In order to provide an axle loading distribution similar to the empty configuration, ballast was added over the front truck and car 01208 was ballasted to match the same distribution. The actual test weight at AWO is therefore 3,760 lbs heavier than the empty weight for each car, with the same axle load distribution. This weight excludes an average test crew weight of 1,200 lbs as this was a variable from day to day.

TABLE 1-1. VEHICLE WEIGHTS.

Condition		Weight Code	Actual Weight (lbs)	
			Car 01208	Car 01209
Empty	front		35,500	34,600
	rear		33,280	32,760
	total		68,780	67,360
Empty Plus Instrumentation	front	AW0	36,880	35,980
	rear		34,660	34,140
	total		71,540	70,120
Standing Passenger	front	AW3	46,685	45,785
	rear		44,465	43,945
	total		91,150	89,730
Crush load	front	AW4	50,410	49,510
	rear		48,190	47,670
	total		98,600	97,180

CHRONOLOGY

A summary of the program scheduled activity days is shown in Table 1-2 compared with the actual number of days to accomplish each phase.

Much of the on-time performance of the program must be accredited to the reliability of the vehicles. Of 292 hours of scheduled testing, the cars were available for testing 286 hours, which represents 98 percent availability. During the course of the test the cars accumulated 6,381 miles with only one known component failure; on car 01208, the air conditioning compressor unit developed a faulty high pressure limit switch.

TABLE 1-2. SCHEDULE SUMMARY.

Activity	Scheduled Days	Actual Days
Unload Cars	3	4
Functional Test/Install Instrumentation	6	15
Track Checkout	5	5
Vehicle Evaluation/ Test Operations	18	21
Brake Shoe Squeal Evaluation	15	17
Door Noise Loss, Absorptive Panel Evaluation	8	5
Remove Instrumentation/ Cleanup	6	3
Load and Ship	5	3
Total	66	73

2 Description of Vehicle

The following paragraphs describe the general features of the cars in terms of principal dimensions, required performance, passenger load, and design features. The salient features of the carbody, trucks and suspension, propulsion and control system, traction motors, and braking system are identified.

DESIGN PARAMETERS

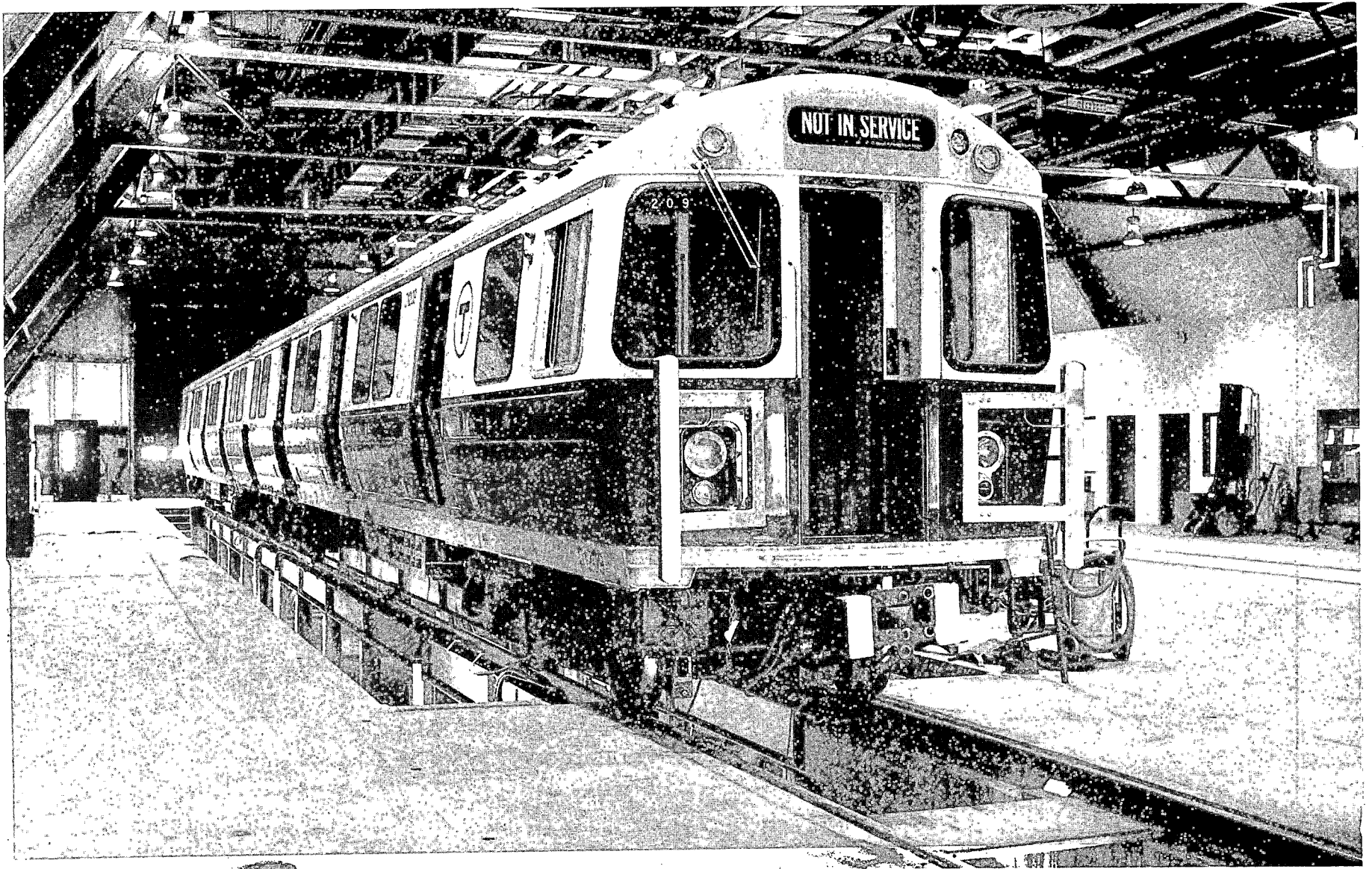
The two test vehicles were built by Hawker Siddeley Canada Inc., to meet MBTA specification, "Equipment Engineering No. 577, No. 12 Main Line Rapid Transit Cars," MBTA, August 1976. The No. 12 Orange Line cars share many design features with the No. 4 Blue Line cars. General appearance, construction, and major components are common to both cars; principal differences are in the vehicle length (65 ft 2 in compared to 48 ft 10 in for the Blue Line cars) and the provision of a spin/slide protection system on the Orange Line cars. A photograph of the test vehicles is shown in Figure 2-1, and the general vehicle design features are shown in Table 2-1.

TABLE 2-1. VEHICLE DESCRIPTION.

Length (over anticlimbers)	65 ft 0 in
Width	9 ft 3 in
Height	11 ft 11 3/4 in
Empty Weight	66,330 lbs
Passenger Load, Seated	74,450 lbs
Passenger Load, Standing	88,600 lbs
Passenger Load, Crush	96,150 lbs
Maximum Speed	65 mi/h
Nominal Acceleration	2.5 mi/h/s
Full Service Braking	2.75 mi/h/s
Emergency Braking	3.25 mi/h/s

CARBODY

The carbody is a steel welded structure of low alloy, high tensile steel, which includes the entire underframe, body structure and side, end, and roof sheets. Due to design considerations, for commonality of construction methods and mating compatibility with the Blue Line cars, the main floor supports are I-beams that run fore and aft instead of the traditional transverse full depth floor beams. Thus, two center sill I-beams are located 40 inches apart, and the floor panels are supported on the I-beams and the side sills. The end frames, incorporating the bolsters, draft sills, and anticlimbers are welded to the side sills.



2-2

FIGURE 2-1. MBTA ORANGE LINE VEHICLES AT TTC.

TRUCKS AND SUSPENSION

The trucks are General Steel Industries, type 70. They are side-bearing, inside-journal trucks with two traction motors mounted on each truck, one motor geared to each axle. The truck frame is of cast steel construction; the frame is cast in sections which are then welded together in a unique cast-welding process. Primary suspension is provided by elastomeric chevron springs mounted between the axle journals and the side frames; secondary suspension is provided by two air springs per truck, mounted between the bolster and the carbody underframe. The bolster-to-carbody longitudinal relationship is maintained by two resiliently mounted radius rods connecting the bolster and underframe. Passenger load is sensed at each truck by load leveling valves which vary the air spring pressure to maintain a constant floor height of 44.75" above the rail. Carbody roll corrections are made by twin leveling valves on the rear truck.

PROPULSION AND CONTROL SYSTEM

The propulsion and control system is a conventional cam controller type. An electrically power/brake cam controller (G.E. type SCM II) responds to signals from the master controller, and selects one of four basic types of traction motor current control, together with a series of switchable resistor banks. The four control configurations are two series connections, series/parallel connection of pairs of traction motors, and series/parallel connection plus two stages of field weakening. The purpose of these four controller positions, known as P1 through P4, is described briefly in Table 2-2.

TABLE 2-2. CONTROLLER POWER POSITIONS.

Controller Position	Purpose	Nominal Maximum Speed (mi/h)
P1	Minimum Acceleration Switching	10
P2	Intermediate Acceleration - Operations	25
P3	Maximum Acceleration - Operations	45
P4	Maximum Acceleration (minimum field) - Operations	65

Logic circuits in the propulsion and control system respond to a load weigh transducer in the air spring supply line to the front truck, and compensate for vehicle weight to provide constant acceleration and deceleration levels regardless of passenger load. These circuits also provide jerk (rate-of-change of acceleration) limit protection.

The propulsion and control system is essentially the same as that of the Blue Line cars, with the exception that the Orange Line cars are provided with a spin/slide wheel protection system. The system monitors axle speeds and responds to differences greater than 6 mi/h, or axle accelerations or de-

terations in excess of 8 mi/h/s. Upon detection of a spin during acceleration, power is removed from the affected car until the spin is corrected. Power is then reapplied automatically under jerk-limited control. Upon detection of a slide during braking, the dynamic braking is reduced to zero on the affected car for the duration of the brake application. Braking control then reverts automatically to the friction brakes, but is reduced to zero on the affected truck until the slide is corrected. Braking is then reapplied to the commanded level on a jerk-limited basis. The wheel slide protection system is functional for all braking commands except emergency braking.

TRACTION MOTORS AND GEAR UNITS

The traction motors are 4-pole d.c., series-wound units; each pair of motors on a truck is connected in series so that each motor operates on 300 V d.c. The motors are self-ventilated. Each motor is suspended from rubber cushioned hangers on the truck, and is resiliently mounted to a parallel-double reduction gear box with an overall reduction ratio of 6.13:1. Misalignment between motor and gear box is accommodated by a gear-type coupling.

BRAKING SYSTEM

Friction braking is provided by Westinghouse Air Brake Company (WABCO) RT-2 tread brake units, one unit for each wheel. Under normal operation, the major braking effort is provided by the dynamic braking capability of the vehicle propulsion system, with the friction brakes taking over at low speeds to compensate for the drop-out of dynamic braking. The friction braking system is capable of providing full service braking deceleration levels in the event that dynamic braking fails, and provides all braking effort in the emergency mode. Control of both dynamic and friction braking is provided by an EP system with a SAP system providing control redundancy in the event of a failure of the EP system.

The term 'blended braking' is commonly used to define continuous blending of dynamic and friction braking effort to achieve a constant commanded deceleration rate. In the case of the Orange Line car, the normal service braking could be more accurately described as 'switched' braking, since the propulsion system switches from friction to dynamic braking at 120 A (or, similarly, from dynamic to friction braking at braking currents as high as 400 A. The only true blending occurs at the transition from one braking mode to the other. However, a considerable amount of detail development has been carried out on this relatively simple system to allow the smooth blending of tractive efforts.

3 Description of Facilities

The following paragraphs describe the Transit Test Track (TTT), including details of construction, elevation and grades, and artificial perturbations. A brief description of the climatic conditions prevalent at Pueblo is also given.

TRANSIT TEST TRACK

The Performance, Ride Quality, and Noise tests were conducted on the TTT, a 9.1-mi oval incorporating six typical types of transit track construction. The TTT includes a perturbed section, typical grade crossings and switches, and a 4,000-ft level tangent section that is used for all performance testing, and for instrumentation calibration prior to each day's testing.

Track orientation and plan are shown in Figure 3-1, and track profile is shown in Figure 3-2. Table 3-1 shows the characteristics of each of the six track sections. The perturbed section of the TTT is located between stations 11.8 and 14.0. The perturbations were made only to the outer rail in profile and alignment; wavelength varied between 14 and 56 ft. Table 3-2 details the amplitude and waveforms of the perturbations. The level tangent section of track between stations 30.0 and 34.0 was used for all Brake, Acceleration, and Train resistance tests.

The track is designed for sustained 80 mi/h vehicle operation with the exception of the perturbed track section, which is subject to a speed limit based on Ride Quality test requirements and safety considerations. For this program, the test speed limit for the perturbed section was 65 mi/h.

Power is provided to the TTT by conventional third rail and by a section of overhead catenary cable; the third rail was constructed to New York City Transit Authority (NYCTA) specifications. A special third rail shoe was supplied by Ohio Brass to make the Orange Line cars compatible with the TTT third rail configuration.

Two alternate sources of electrical power were employed:

- A mercury arc rectifier station purchased from the Chicago Transit Authority (CTA). Nominal no-load line voltage at the third rail shoe was 750 V d.c., with a current limit of 7,500 A for two hours. The rectifier station no-load line voltage can be preset from 610-780 V d.c.
- One of two newly-commissioned rectifier stations was also used. These are purpose-built to suit the test requirements of the TTC. The voltage can be varied infinitely

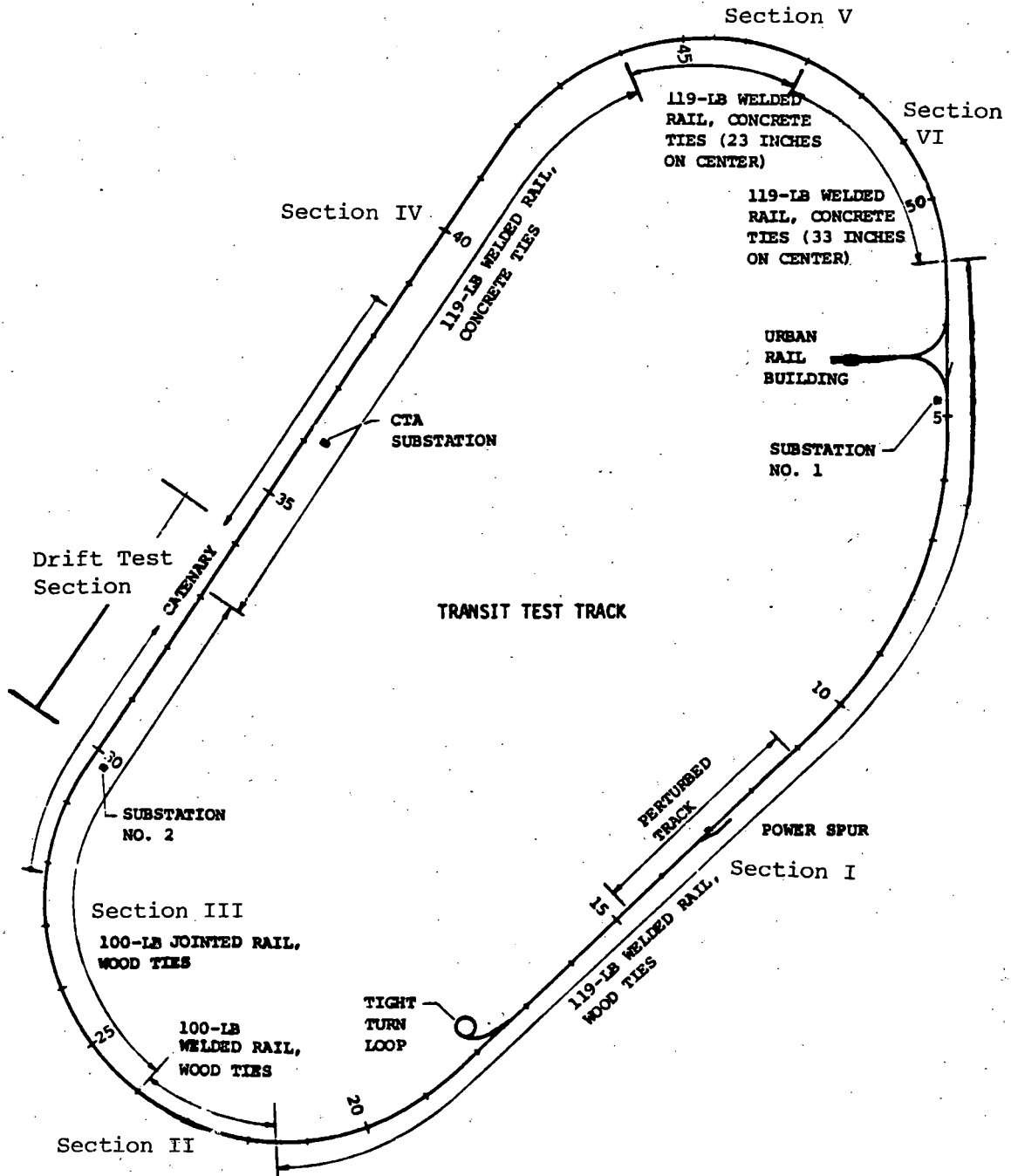
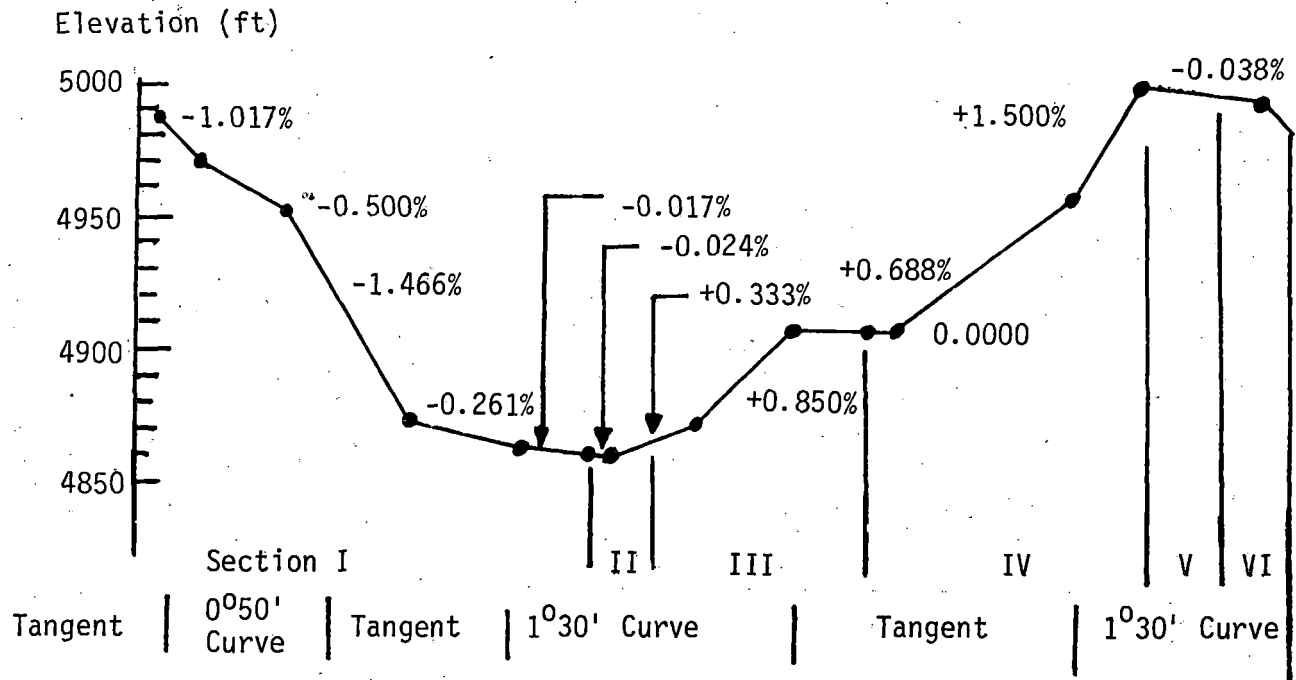


FIGURE 3-1 TRANSIT TEST TRACK.



NOTES:

Track Curvature:

Sta.	to	Sta.	Degree of Curve
55.3		10.3	0° 50'
18.9		29.4	1° 30'
41.8		50.8	1° 30'

Curve Superelevation:

1°30' curves are superelevated a maximum of 4.5". The maximum superelevation on the 0°50' curve is 2".

Elevation:

Minimum - 4,863 ft. at Sta. 22.0.
 Maximum - 5,003 ft. at Sta. 46.0.

FIGURE 3-2 TRANSIT TEST TRACK PROFILE SHOWING GRADES.

TABLE 3-1. TTT CONSTRUCTION DETAILS.

Section	Location (Sta to Sta)	Alignment	Trackage	Fastener	Rail
I	51.0 - 17.4	Tangent and 0° 50' curve	Wooden ties 24" on center	Spike	119 lb/yd Welded
	17.4 - 21.5	1° 30' curve	Wooden ties 23" on center		
II	21.5 - 24.0	1° 30' curve	Wooden ties 23" on center	Spike	100 lb/yd Welded
III	24.0 - 29.0	1° 30' curve	Wooden ties 23" on center	Spike	100 lb/yd Jointed
	29.0 - 33.0	Tangent	Wooden ties 24" on center		
IV	33.0 - 40.5	Tangent	Concrete ties 30" on center	Spring Clip	119 lb/yd Welded
	40.5 - 44.0	1° 30'	Concrete ties 27" on center		
V	44.0 - 47.0	1° 30'	Concrete ties 23" on center	Spring Clip	119 lb/yd Welded
VI	47.0 - 51.0	1° 30'	Concrete ties 33" on center	Spring Clip	119 lb/yd Welded

TABLE 3-2. AMPLITUDE AND WAVEFORMS OF TTT PERTURBATIONS, DESIGN SPECIFICATIONS.

Sta 11.8	Profile				Alignment			
	Sta 12.0	Sta 12.2	Sta 12.4	Sta. 12.6	Sta. 13.6	Sta 13.8	Sta 14.0	
1.5"	0.38"	0.38"	0.75"	1.5"	0.75"	0.38"	0.75"	
1.48" ± 1 tie	0.30" ± 1 tie	0.36" ± 1 tie	0.71" ± 1 tie	1.43" ± 1 tie	0.74" ± 1 tie	0.30" ± 1 tie	0.71" ± 1 tie	
1.42" ± 2 ties	0.15" ± 2 ties	0.30" ± 2 ties	0.61" ± 2 ties	1.22" ± 2 ties	0.71" ± 2 ties	0.15" ± 2 ties	0.61" ± 2 ties	
1.34" ± 3 ties	0.02" ± 3 ties	0.23" ± 3 ties	0.46" ± 3 ties	0.92" ± 3 ties	0.67" ± 3 ties	0.02" ± 3 ties	0.46" ± 3 ties	
1.22" ± 4 ties	0" ± 4 ties	0.15" ± 4 ties	0.29" ± 4 ties	0.58" ± 4 ties	0.61" ± 4 ties	0" ± 4 ties	0.29" ± 4 ties	
1.70" ± 5 ties		0.07" ± 5 ties	0.14" ± 5 ties	0.28" ± 5 ties	0.54" ± 5 ties		0.14" ± 5 ties	
0.92" ± 6 ties		0.02" ± 6 ties	0.04" ± 6 ties	0.07" ± 6 ties	0.46" ± 6 ties		0.04" ± 6 ties	
0.75" ± 7 ties		0" ± 7 ties	0" ± 7 ties	0" ± 7 ties	0.38" ± 7 ties		0" ± 7 ties	
0.58" ± 8 ties					0.29" ± 8 ties			
0.42" ± 9 ties					0.21" ± 9 ties			
0.28" ± 10 ties					0.14" ± 10 ties			
0.16" ± 11 ties					0.08" ± 11 ties			
0.07" ± 12 ties					0.04" ± 12 ties			
0.02" ± 13 ties					0.01" ± 13 ties			
0" ± 14 ties					0" ± 14 ties			
Wave Length	56'	14'	28'	28'	28'	56'	14'	28'

- Notes:
1. Only outer rail is perturbed.
 2. Alignment accomplished by perturbing rail towards outside of oval.
 3. Perturbations are symmetrical around station number; distance from station number is indicated in number of ties.

infinitely from 400 to 1000 V d.c. with a current limit of 11,000 A. The stations each feed from one bus to all of the TTT and are designed to operate in several alternate modes, including computer control. Voltage can be controlled at a constant level at the substation, or sensed at the position of the vehicle, and held to a constant value at the vehicle regardless of demand or voltage drop through the rails; in alternate modes of operation the test vehicle can be subjected to a voltage profile or a voltage step as might occur in revenue service at the transition between one substation and another. For the Orange Line test program the substation was manually controlled and the voltage was regulated to maintain a nominal no-load level at the substation.

CLIMATIC CONDITIONS

The TTC is located on semiarid rangeland, subject to large daily temperature variations, bright sunlight, and low humidity. Average daily temperatures range between a minimum of 15° F in January and a maximum of 92° F in July. The lowest temperature on record is -31° F and the highest is 105° F. Freezing temperatures occur during 152 days of the year. Annual precipitation averages 12". The sun shines about 73 percent of the daylight hours. At ground level, there is typically 25 to 75 percent more solar radiant energy in this region than along the northeast coastal regions of the United States.

In general, the dry and sandy conditions with minimal industrial pollution result in high wheel rail adhesion. The elevation (4,950 ft) gives a lower air density than is usual at most transit properties. Average barometric pressure is 25.2" of mercury.

INSTRUMENTATION, DATA ACQUISITION, AND DATA PROCESSING

A detailed discussion of the data acquisition process, a description of the instrumentation used, and the data processing methodology and equipment is included in Appendix A. Pertinent aspects of data acquisition, instrumentation, and data processing for each test are included in the following sections to provide a detailed supplement to the abstracts in the appendix.

4 Performance Characteristics

The following section describes and discusses the results of a series of tests designed to evaluate the cars' performance characteristics. For each performance topic, the discussion is divided into a statement of the objectives, including vehicle design specification criteria where appropriate, a description of the test methods, and a presentation of the test results. The following topics are discussed:

- Acceleration Performance. The effect of vehicle weight, master controller position, line voltage, and direction of travel/lead car on that performance is presented.
- Braking Performance - blended, friction-only, and emergency modes of operation. The effect of control mode (EP or SAP), vehicle weight, and alternate methods of emergency brake initiation are discussed.
- Spin/Slide Efficiency. The effectiveness of the vehicles' spin/slide protection system is presented in terms of the percentage of the available adhesion that the vehicles are able to use in a wheel spin or slide situation.
- Train Resistance. The results of a series of drift tests, which defined the resistance force acting on the vehicles as a function of speed, are presented. The results are compared with train resistance values calculated from the empirical Davis formula, which defines resistance to motion as a combination of rolling resistance, wheel flange effects, and aerodynamic drag.
- Energy Consumption. The energy consumption of a two-car train is presented, for a simulation of the revenue service route for the MBTA Orange Line.
- Duty Cycle. Time history data of brake shoe temperatures for each wheelset of a car are presented for friction-only braking operation, over a simulated service route representing a round trip on the MBTA Orange Line.

ACCELERATION

Objectives

The objectives of the acceleration performance tests were to evaluate the acceleration characteristics of the two-car train, and to determine the effects of vehicle weight, master controller position, line voltage and direction of travel on those characteristics. A secondary objective was to determine whether the vehicles met the requirements of the vehicle design specifications with regard to acceleration performance. The

criteria are quoted below:

- "With half-worn wheels, on tangent track the maximum average acceleration rate shall be 2.5 mi/h/s. Means shall be provided to maintain constant accelerating and braking rates at the above value independent of car loading up to 22,400 lbs passenger load (AW3).
- The constant rate of acceleration shall be carried to approximately 20 mi/h with a rush hour passenger load (AW3).
- A two-car train with a rush hour passenger load shall be able to attain an operating speed of 40 mi/h in not more than 25 seconds and 65 mi/h in not more than 170 seconds.
- All control equipment shall be designed to provide smooth power operation and be adjusted to limit the rate of change of acceleration to a maximum of 2.0 mi/h/s² under all operating conditions. Sufficient steps shall be provided in the controller to limit the variation of the rate during steps of acceleration to a maximum 0.6 mi/h/s."

Test Method

Acceleration tests were carried out from a standing start on level, tangent track. Where the total speed range could not be accomplished in one pass, overlapping test runs were made, entering the test section at a speed just below the exit speed of the previous run. In this way, the entire acceleration was accomplished on level, tangent track. The test variables included vehicle weights of AWO, AW3, and AW4; master controller positions P1 through P4; line voltages of 550, 575, and 610 V d.c., and the effect of direction of travel and lead car (car 01208 leading counterclockwise around the track and 01209 leading clockwise).

Results

The vehicles' full service acceleration characteristics at vehicle weights of AWO, AW3, and AW4, and the corresponding speed/time and distance/time relationships for these weights, are shown in Figures 4-1 and 4-2. For clarity, the Y-axis origins of the acceleration plots have been staggered vertically: the 2.5 indices at the left hand side of each plot represent a 2.5 mi/h/s acceleration level for each respective plot with a vertical scale as indicated. The plots show that the initial acceleration levels were 0.1 to 0.5 mi/h/s better than the specification requirement of 2.5 mi/h/s at vehicle weights up to AW3, and that the vehicles still met the 2.5 mi/h/s rate at AW4 weight. This initial acceleration was maintained up to approximately 25 mi/h at all weights, meeting the specification requirement that it be sustained up to 20 mi/h at AW3 vehicle weight. Figure 4-2 shows that the distance and speed relationships with elapsed time were independent of vehicle weight.

The recorded times to 40 and 65 mi/h are shown in Table 4-1 compared to the specification requirements. The 65 mi/h times were compiled from three test runs with overlapping speed ranges. The table shows that the cars met the time-to-speed requirements at all weights, including AW4.

TABLE 4-1 VEHICLE TIME-TO-SPEED DATA COMPARED TO SPECIFICATION REQUIREMENT.

Car Weight	Time to Speed (Seconds)			
	Speed 40 mi/h		Speed 65 mi/h	
	Veh. spec.	Test Data	Veh. Spec.	Test
AW0	25	20.6	170	102.0
AW3	25	21.5	170	130.4
AW4	None	22.4	None	116.5

Note:
P4 Master Controller
Line Voltage 575 V d.c.

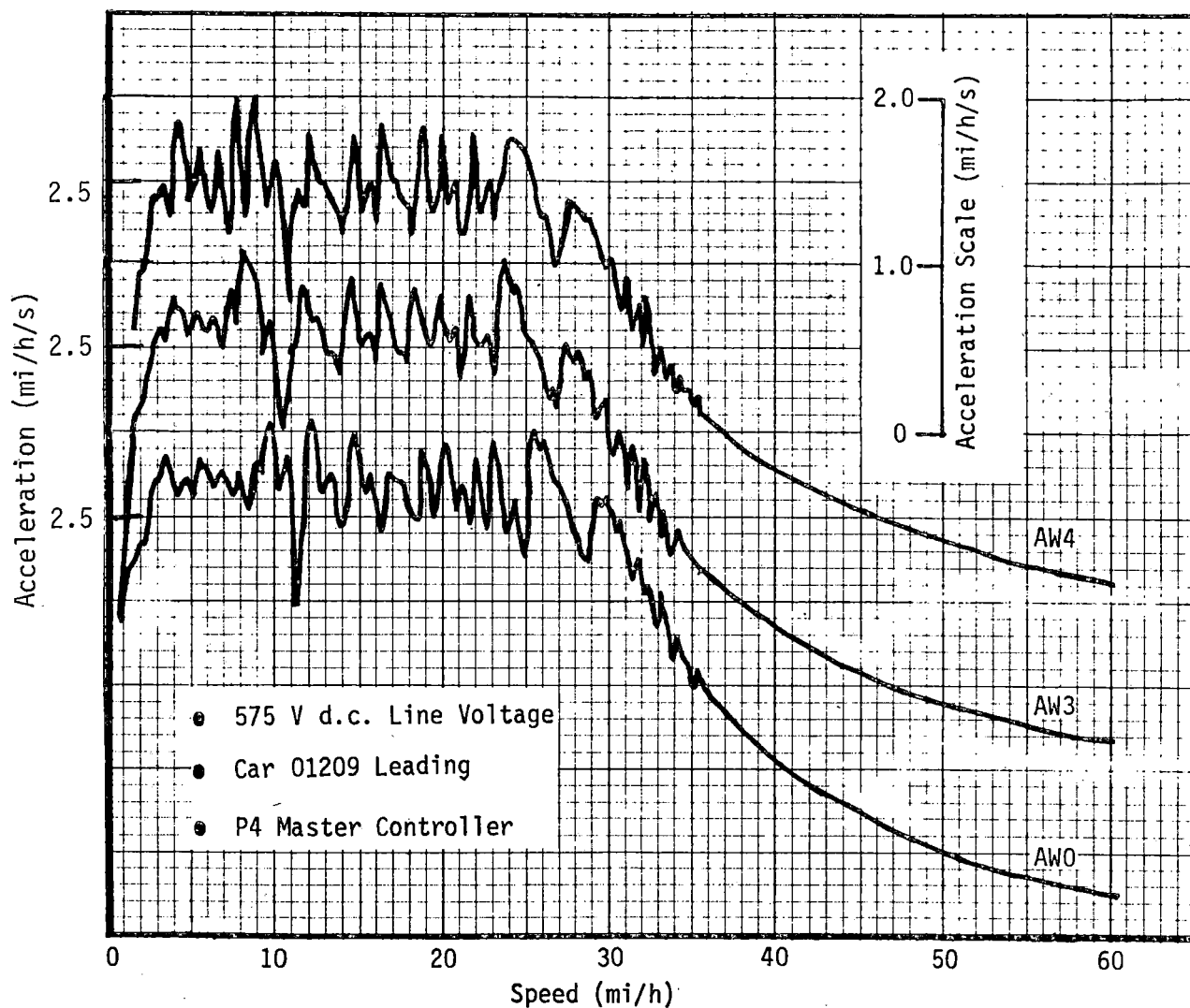


FIGURE 4-1 EFFECT OF VEHICLE WEIGHT ON ACCELERATION CHARACTERISTICS.

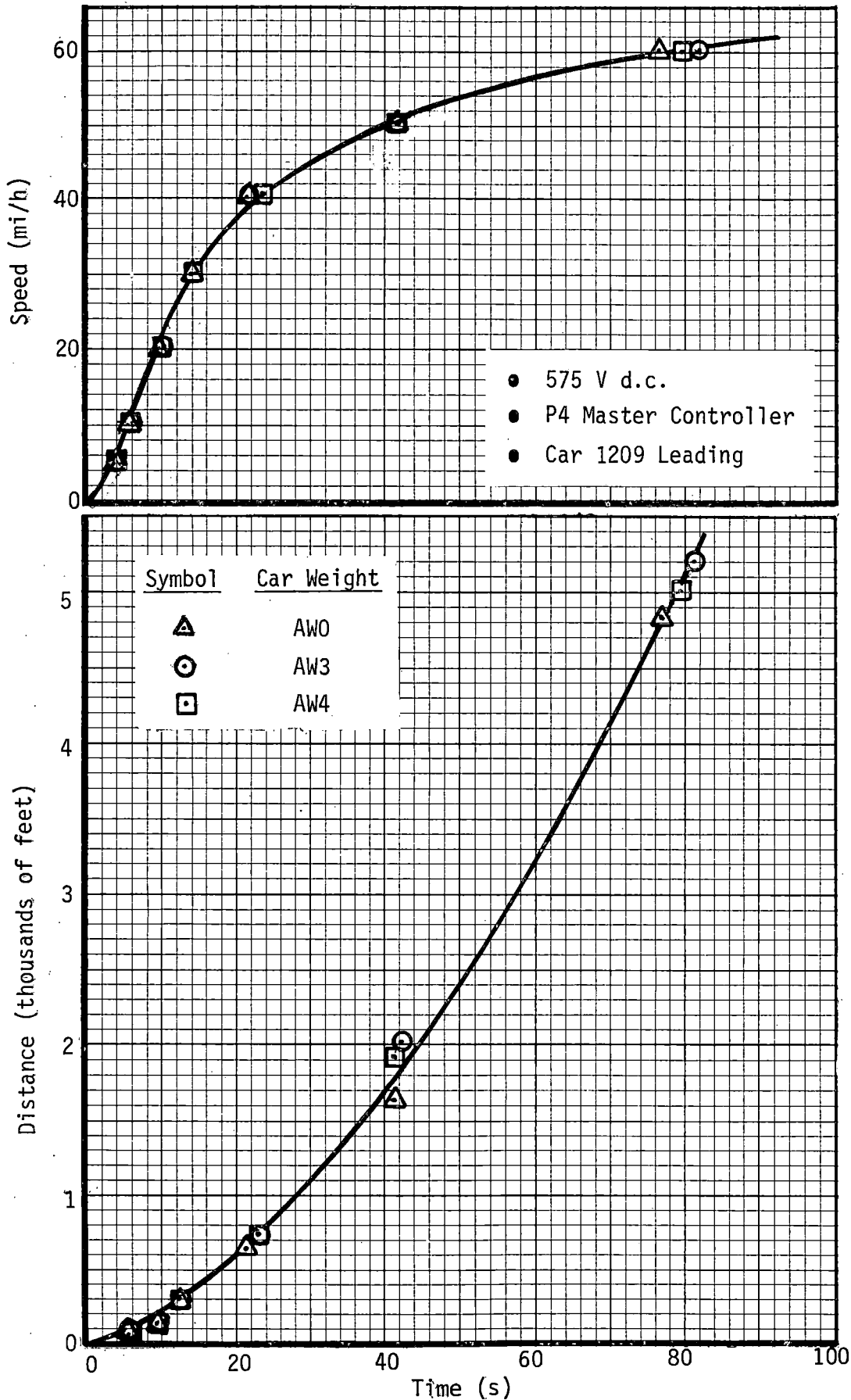


FIGURE 4-2 EFFECT OF VEHICLE WEIGHT ON TIME/DISTANCE AND TIME/SPEED RELATIONSHIPS.

The variation of acceleration due to cam controller steps was generally in the range ± 0.3 mi/h/s, thus meeting the requirement for a maximum variation of 0.6 mi/h/s, but one notable exception occurred at approximately 11 mi/h, where the variation was up to ± 0.5 mi/h/s. This variation occurred at the transition from series to series-parallel connection of the traction motors; the magnitude of the variation is thought to be due in part to the 'soft' nature of the line voltage at TTC.

Acceleration characteristics due to power settings P1 through P4 are illustrated in Figure 4-3, with the corresponding time/distance and time/speed plots shown in Figure 4-4. Initial accelerations of 0.9, 1.6, and 2.6 mi/h/s were achieved for controller settings P1, P2, and P3; note that the initial acceleration at the P3 position is identical to the P4 position up to 23 mi/h, where two additional steps of motor field weakening are applied in P4 to sustain the acceleration above motor base speed.

The variations of acceleration performance with line voltage are shown in Figures 4-5 and 4-6 where data from runs at 550, 575, and 610 V d.c. nominal line voltage are presented. Initial acceleration up to 25 mi/h was little affected by line voltage variations, and initial acceleration performance exceeded the specification requirement of 2.5 mi/h/s throughout the voltage range tested. At speeds over 25 mi/h performance was marginally affected by line voltage, as might be expected. However, effects were minor, with speed and distance increments of approximately 5 mi/h and 300 feet, 60 seconds after starting, between the extremes of the voltage range. The effects of direction of travel or operating from the alternate vehicle were evaluated by comparing test data taken with car 01209 leading, traveling clockwise around the TTT, to data obtained in a counterclockwise direction of travel with car 01208 leading. No discernible differences in performance could be detected due to direction of travel or lead car; the data are presented in Figures 4-7 and 4-8.

Control response time and jerk rates were evaluated for accelerations from a standing start for master controller positions P1 through P4 at AW3 vehicle weight, and for AWO, AW3, and AW4 vehicle weights at the P4 setting. Control response time was defined as the time from first motion of the motorman's master controller to the initiation of vehicle motion. Jerk rate (the initial rate of change of acceleration) was defined from the initial slope of the acceleration trace. The control response and jerk rate data are presented in Table 4-2. Control response times were in the range 0.70 to 1.00 seconds with no significant trends due to master controller position or vehicle weight. There is no specification requirement for response time. Jerk rates generally met the vehicle specification requirement for a maximum of 2.0 mi/h/s², with values in the range 1.00 to 1.46, with the exception of the P1 master controller acceleration at AW3 weight with a value of 2.25 mi/h/s². Since the P1 controller position is not included in the jerk limiting circuitry, the jerk rate for this position can be considered to be outside the scope of the specification criterion.

TABLE 4-2 CONTROL RESPONSE TIMES AND JERK RATES UNDER ACCELERATION, FROM A STANDING START.

Vehicle Weight Code	Master Controller Position	Response Time (Seconds)	Jerk Rate (mi/h/s)
AW3	P1	0.80	2.25
AW3	P2	0.70	1.46
AW3	P3	0.95	1.06
AW3	P4	1.00	1.00
AW4	P4	0.85	1.08
AW0	P4	0.95	1.27

Note:

Car 01209 Leading
Line Voltage 575 V d.c.

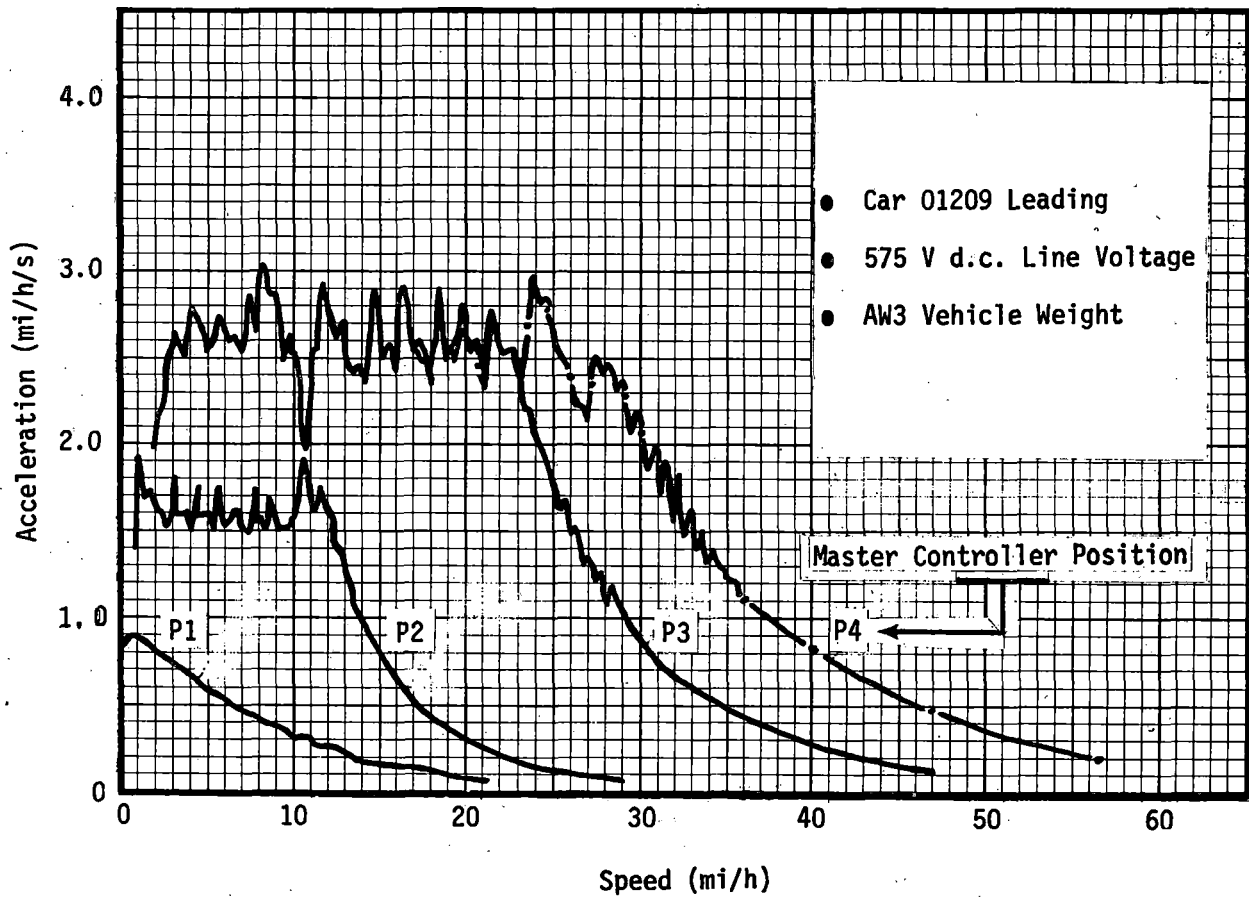


FIGURE 4-3 EFFECT OF MASTER CONTROLLER POSITION ON ACCELERATION CHARACTERISTICS.

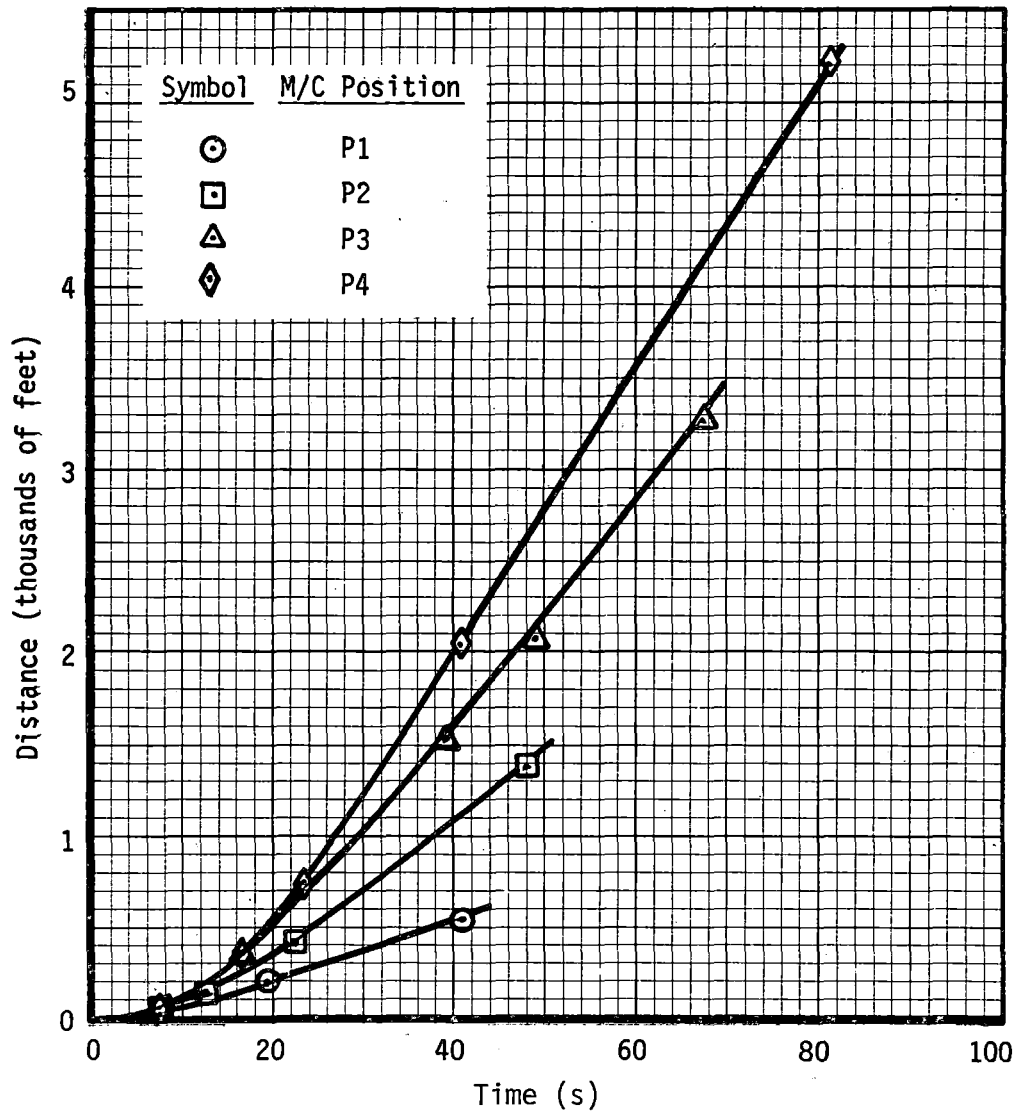
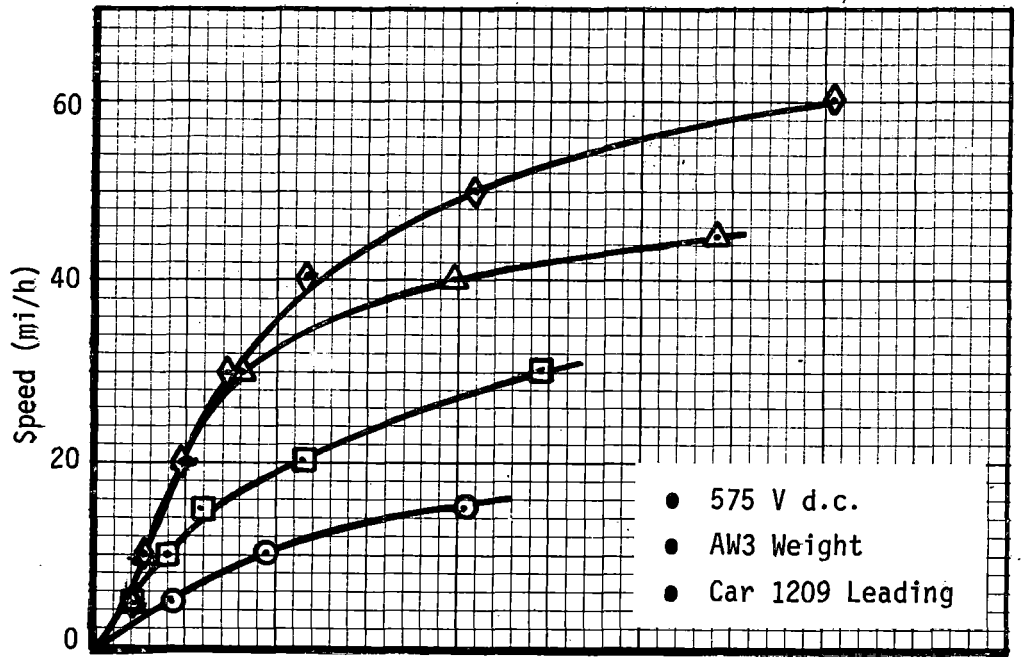


FIGURE 4-4 EFFECT OF MASTER CONTROLLER POSITION ON TIME/DISTANCE AND TIME/SPEED RELATIONSHIPS.

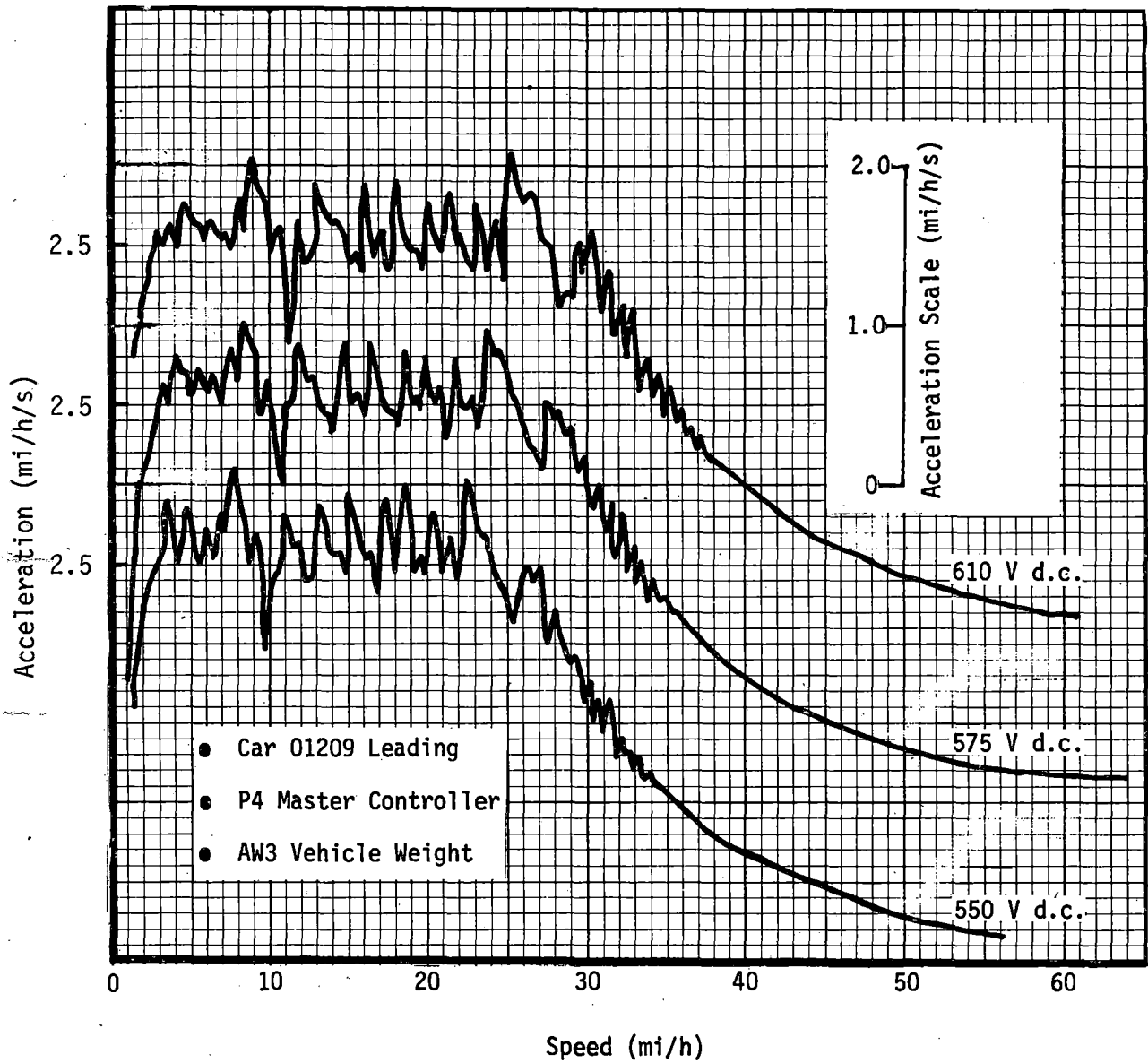


FIGURE 4-5 EFFECT OF LINE VOLTAGE ON ACCELERATION CHARACTERISTICS.

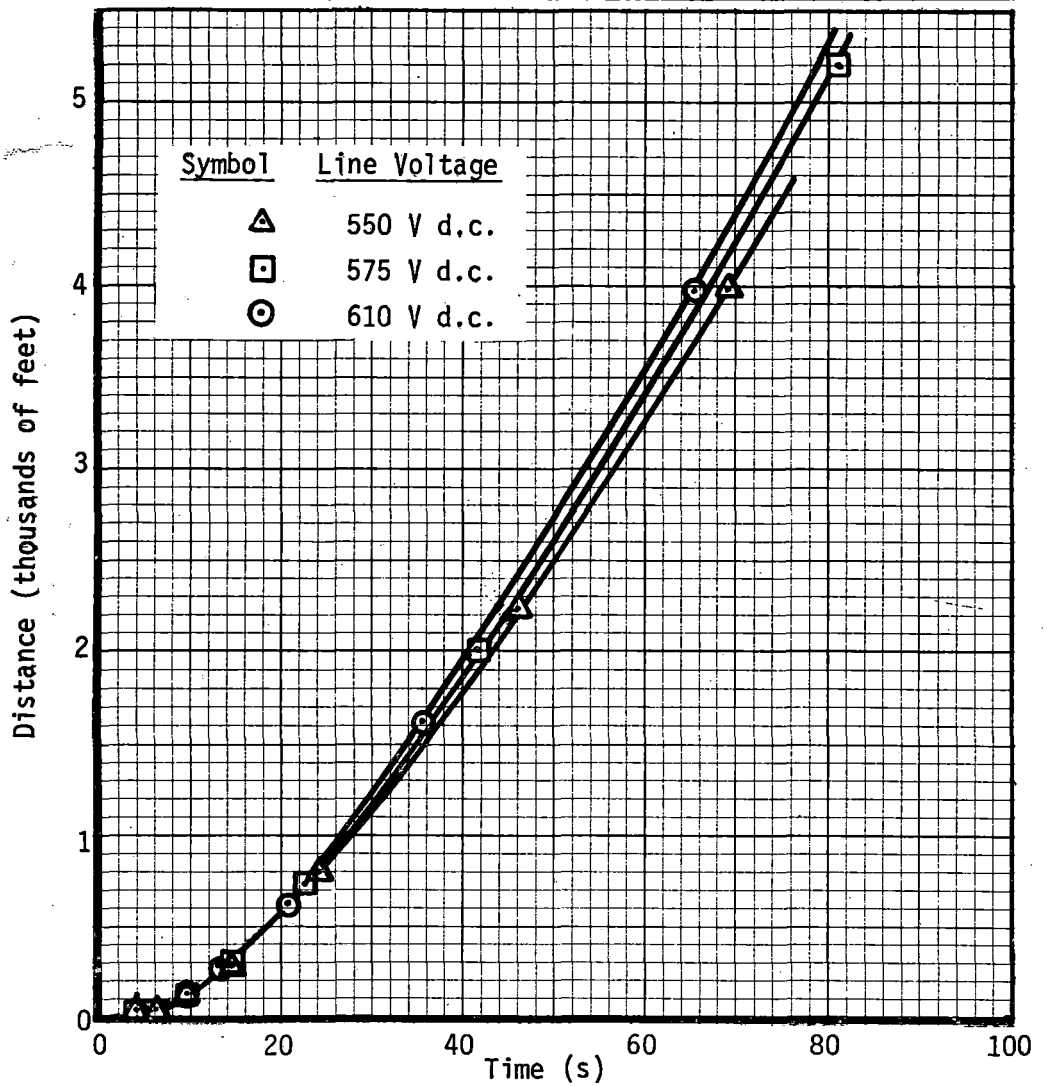
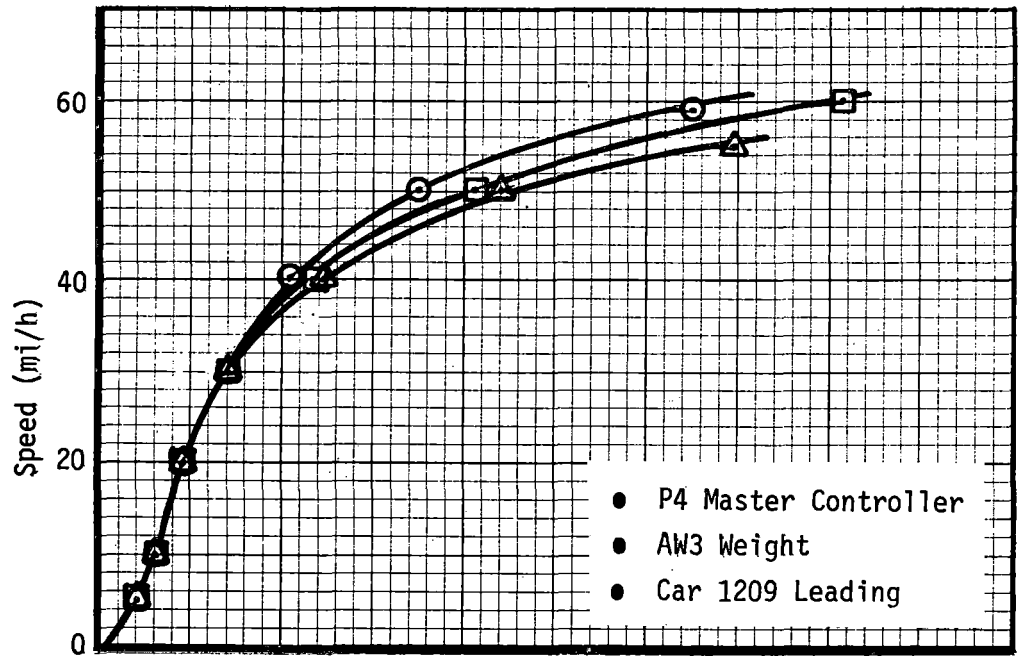


FIGURE 4-6 EFFECT OF LINE VOLTAGE ON TIME/DISTANCE AND TIME/SPEED RELATIONSHIPS.

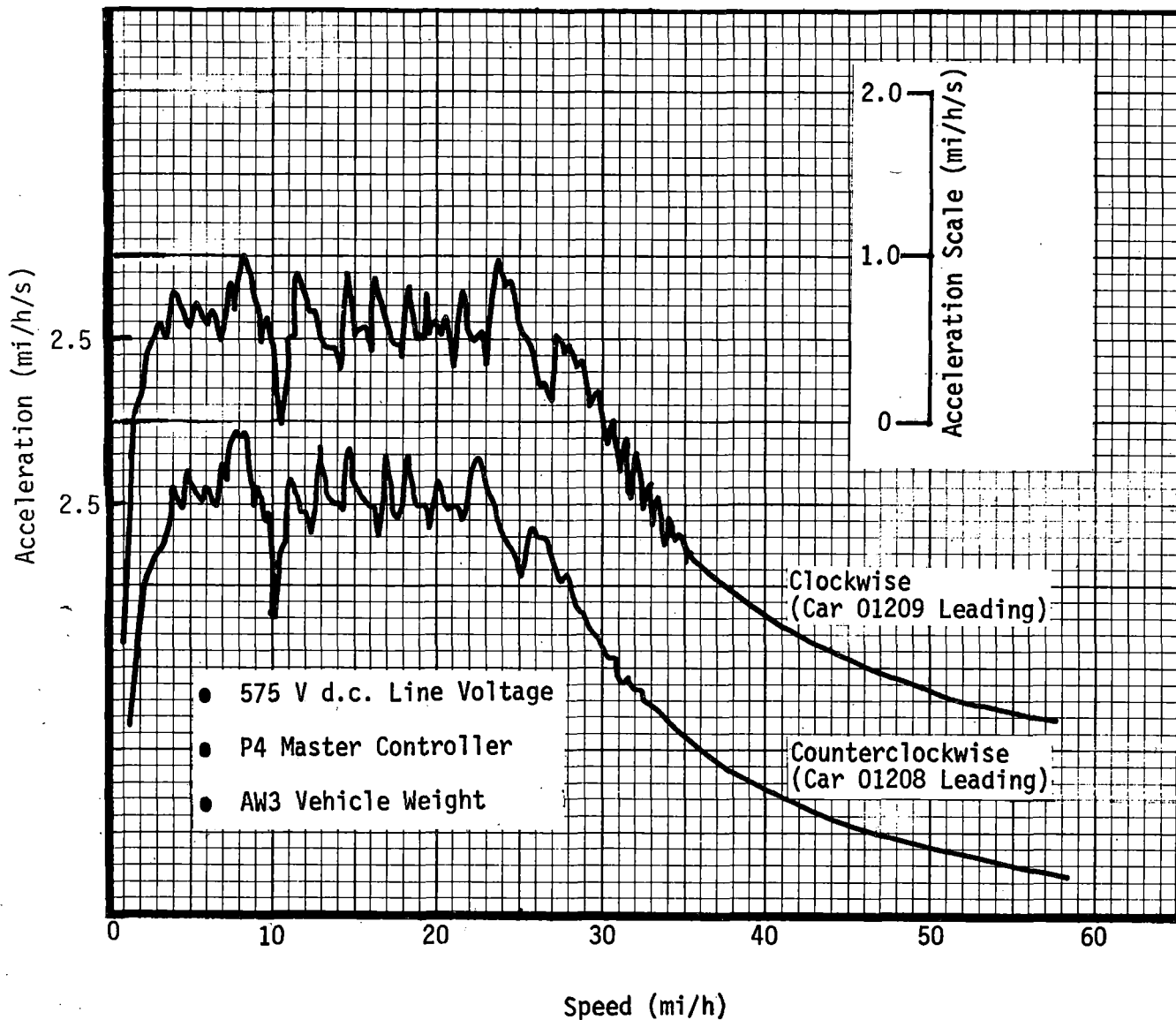


FIGURE 4-7 EFFECT OF DIRECTION OF TRAVEL/LEAD CAR ON ACCELERATION CHARACTERISTICS.

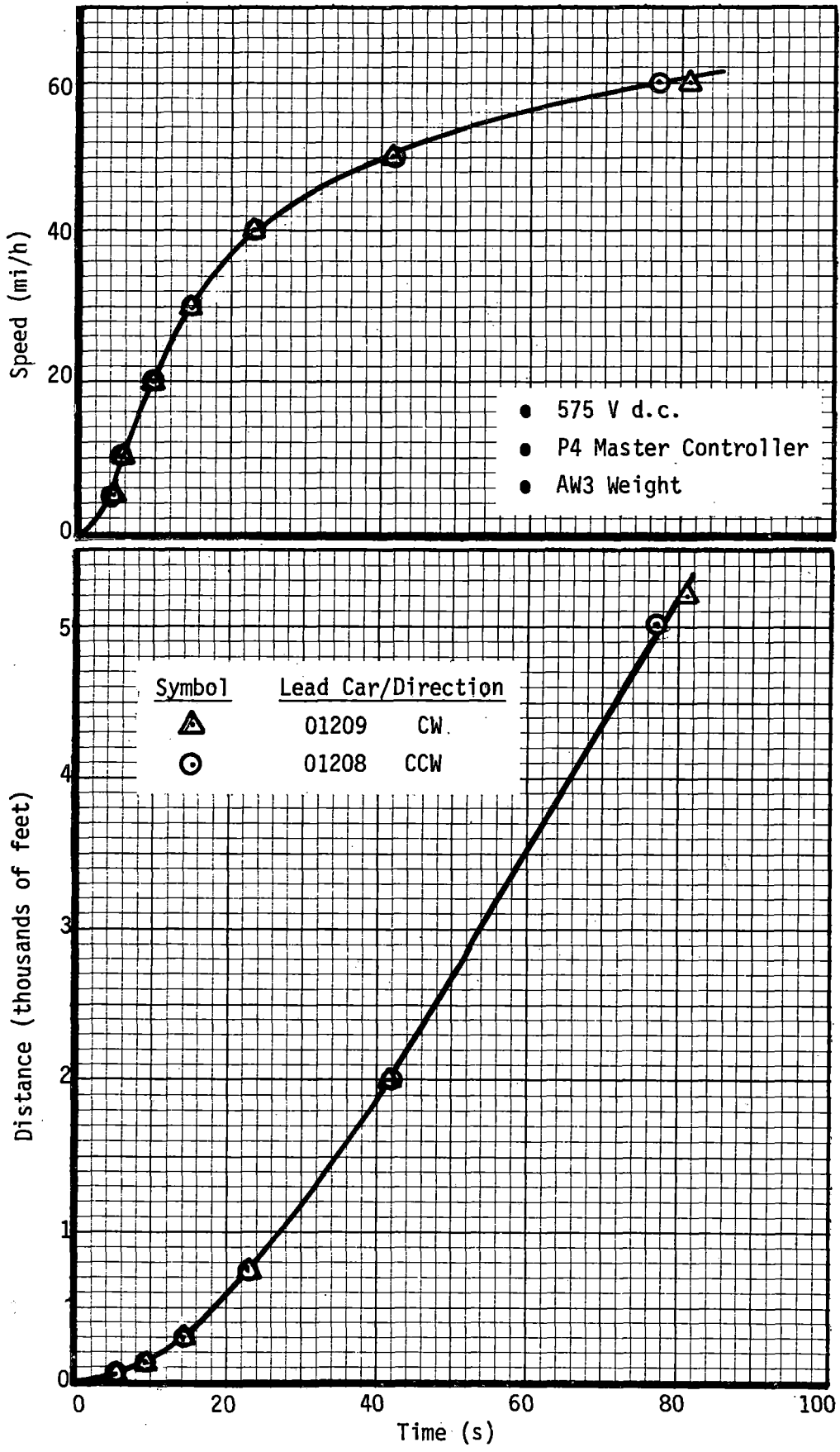


FIGURE 4-8 EFFECT OF DIRECTION OF TRAVEL/LEAD CAR ON TIME/DISTANCE AND TIME/SPEED RELATIONSHIPS.

BRAKING

Objectives

The objectives of the tests were to evaluate the braking characteristics of the vehicles in all modes of brake operation, and to delineate the effects of vehicle weight, car direction, and controller position on those characteristics. The performance was compared to the vehicle specification requirements which are quoted below:

- "The maximum average braking rate shall be 1.5 mi/h/s at 65 mi/h tapered uniformly to 2.75 mi/h/s at 50 mi/h, and maintained at this level to a stop.
- The braking rates shall be independent of vehicle weight up to 22,400 lbs passenger load (AW3 vehicle weight).
- The dynamic brakes shall be fully effective down to vehicle speeds of approximately 15 mi/h. When the dynamic braking effort fades, the friction brakes must apply automatically and complete the stop without noticeable change in braking rate.
- The friction brakes shall be capable of maintaining the maximum deceleration rate of 2.75 mi/h/s with a rush hour passenger load (AW3), and shall provide an emergency braking rate of 3.25 mi/h/s.
- Control equipment shall be designed to provide smooth brake application and be adjusted to limit the rate of change of deceleration to maximum of 2.0 mi/h/s², except for emergency brake application.
- Sufficient steps shall be provided in the control system to limit the variation of deceleration to a maximum of 0.6 mi/h/s.
- Emergency brake application shall be obtained from the emergency position of the master controller, the 'deadman' handle, the emergency valve, the wayside trip valve, or by any rapid reduction of brake pipe pressure at any point in the train."

Test Method

Braking tests were carried out on level, tangent track. The effect of the following variables was evaluated:

- Vehicle weight. All other variables were evaluated at vehicle weights of AWO and AW3.
- Braking mode. The test program evaluated blended and friction-only modes of operation using the EP and SAP systems, and emergency friction braking initiated by the master controller, the 'deadman', the emergency brake valve, and the external tripcock.

- Braking Entry Speed. Initial speeds of 65, 50, 40, 30, 20, and 10 mi/h were examined for each brake operation mode and vehicle weight.
- Master Controller Position. The majority of test runs were carried out for the maximum, full service master controller position. A limited number of minimum braking application test runs was also made.
- Direction. Test runs were made in a clockwise direction of travel from station 30.0 towards station 34.0, with car 01209 leading. A limited number of check runs was made in a counterclockwise direction with car 01208 leading.

Before testing (vehicle stationary and unaffected by weight transfer effects) brake cylinder pressures were set to values which, according to L.T. Klauder & Associates, had given acceptable performance levels during braking tests on the MBTA property in Boston. For a true AWO weight car (85 psig air bag pressure) brake cylinder pressures were set to 35 psig, full service application; corresponding emergency pressures were 39 psig. Brake cylinder pressures at AW3 weight averaged 48 psig (full service application) and 56 psig (emergency).

Results

Blended Braking. Braking deceleration characteristics for blended full service braking in the EP mode at AWO and AW3 weight are shown in Figures 4-9 and 4-10. For clarity, the Y-axis origins have been staggered vertically for each initial speed. Braking deceleration characteristics are plotted for each brake entry speed; the 3.0 indices at the left hand side of each plot represent the 3.0 mi/h/s level for each respective entry speed. A vertical scale is indicated.

The figures show that the vehicles met the specification requirement for a full service braking deceleration rate of 2.75 mi/h/s in the EP mode of operation with average deceleration levels of approximately 3.0 mi/h/s. The levels were independent of vehicle weight up to AW3. The requirement for a high speed taper, from 1.5 mi/h/s at 65 mi/h to 2.75 mi/h/s at 50 mi/h, was also met. Deceleration levels were independent of initial speed, the 3.0 mi/h/s average being attained at all brake entry speeds. Variation of deceleration level about a mean value due to control resistor steps was estimated from the plots to be a maximum of ± 0.4 mi/h/s. The vehicle specification is somewhat vague on this limit, it not being clear if the stated allowable variation of 0.6 mi/h/s is a peak-to-peak or a half-amplitude allowable tolerance; subjectively, the ± 0.4 mi/h/s variation is not at all objectionable to the passenger. For the purposes of the braking performance discussion, the variation is assumed to be a peak-to-peak value. Transition from dynamic braking to friction braking can be seen to occur marginally below 15 mi/h throughout the brake entry speed range, with the average braking rate increasing to a level approximately 0.5 mi/h/s higher than the 3.0 mi/h/s dynamic rate at 10 to 12 mi/h, due to friction brake application. The

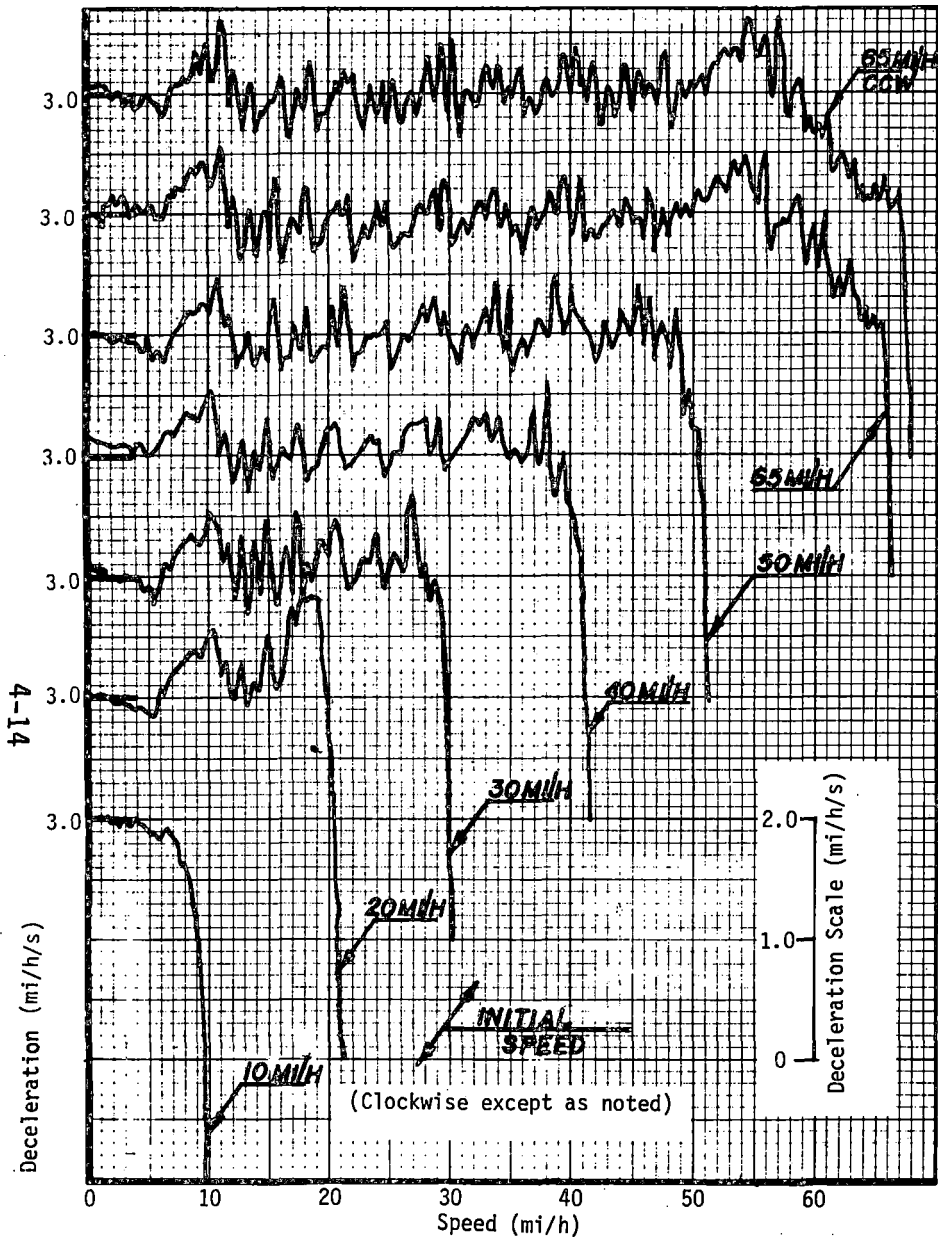


FIGURE 4-9 FULL SERVICE EP BLENDED BRAKING CHARACTERISTICS, AWO WEIGHT.

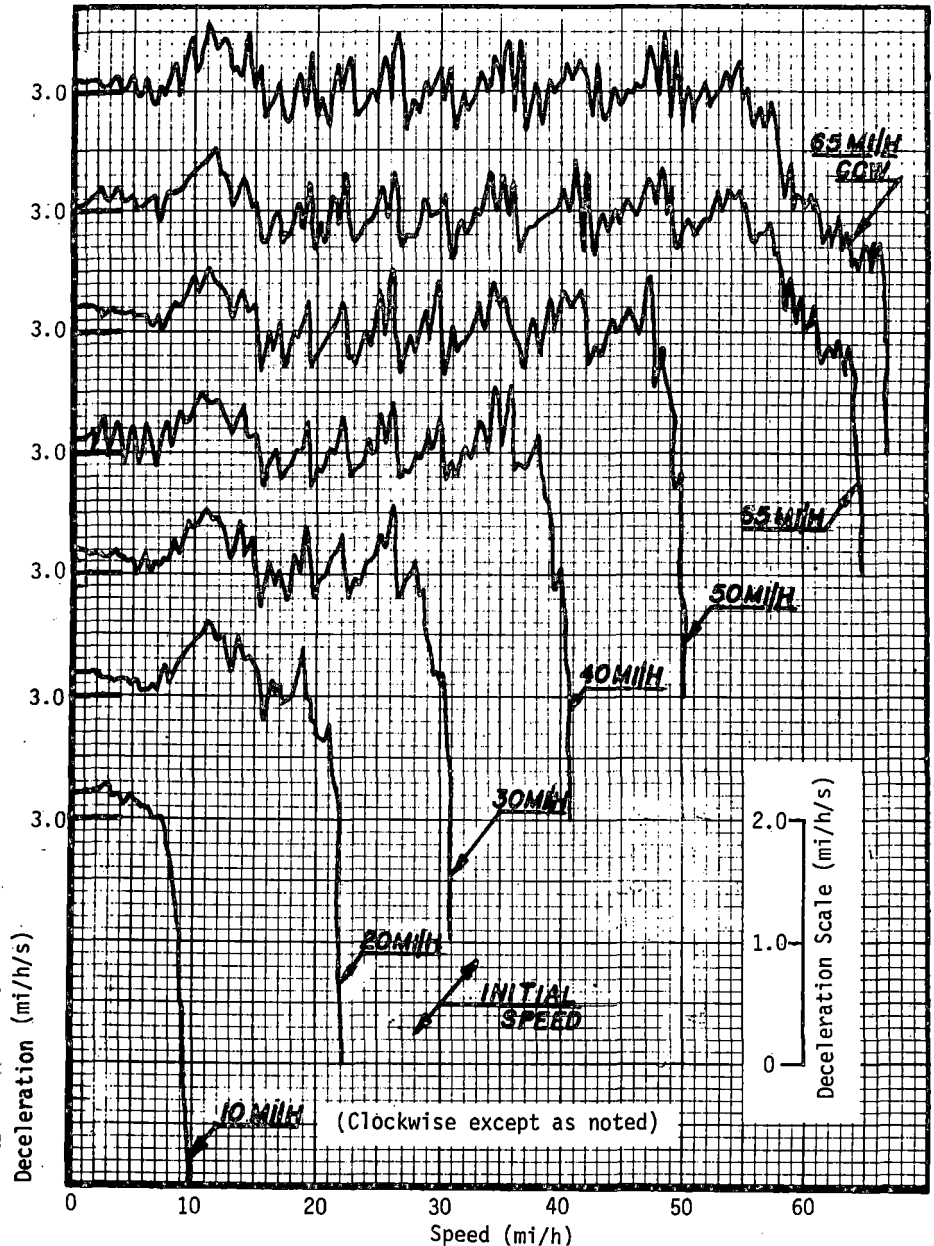


FIGURE 4-10 FULL SERVICE EP BLENDED BRAKING CHARACTERISTICS, AW3 WEIGHT.

vehicle speed at which the transition from dynamic to friction braking occurs was defined by the oscillograph traces of brake cylinder pressure. The requirement for the dynamic braking to be effective down to 15 mi/h or less was generally met.

In the SAP mode of blended braking, the deceleration characteristics, illustrated in Figures 4-11 and 4-12, show that deceleration levels were typically 0.1 to 0.2 mi/h/s lower than for the EP mode of operation. Average deceleration values were typically 2.8 to 2.9 mi/h/s throughout the brake entry speed range, meeting the 2.75 mi/h/s specification requirement, with no apparent effects due to vehicle weight between the AWO and AW3 cases. Variation effects due to controller steps were similar to the values obtained for EP braking, and an effective speed taper can be observed from 65 to 50 mi/h. Operation in the opposite track direction from the cab of car 01208 had negligible effects on deceleration levels for either EP or SAP modes of operation.

Stopping distance and time-to-stop data for EP and SAP modes of blended braking at AWO and AW3 vehicle weight are presented in Figures 4-13 and 4-14, for each initial speed tested. Time and distance counters were triggered at first motion of the master controller; therefore, the data include control response effects. Typically, the times required to stop in the SAP mode were increased by 1 to 2 seconds over those for the EP mode. This is to be expected, and is a function of the increased time required to stabilize the brake command from the train brake pipe system in the SAP mode, as compared to electronic sensing in the EP mode. As a result, stopping distances for the SAP mode were increased in proportion to the initial speed, compared to stopping distances for the EP mode. Typically, 100 to 150 ft more distance was required to stop when using SAP braking at speeds above 50 mi/h. Overlaying the AWO and AW3 time and distance plots showed that there were no significant effects on stopping distance or the time required to stop due to vehicle weight, over the AWO-AW3 range.

In general, the vehicles met the specification criteria for full service braking in the blended mode with both EP and SAP control. They demonstrated excellent compensation for passenger load, and showed no significant differences in performance due to direction of travel or operation from either cab.

Friction Braking. Braking deceleration characteristics for full service friction braking in the EP mode at AWO and AW3 vehicle weights are shown in Figures 4-15 and 4-16, with corresponding plots for the SAP braking mode in Figures 4-17 and 4-18. As for the blended braking cases, data are presented for brake entry speeds from 65 to 10 mi/h, with the Y-axis deceleration origins for each initial speed staggered vertically for clarity.

The plots show deceleration trends which are typical of friction-only braking. At initial speeds greater than 30 mi/h each stop is characterized by an initial braking rate of

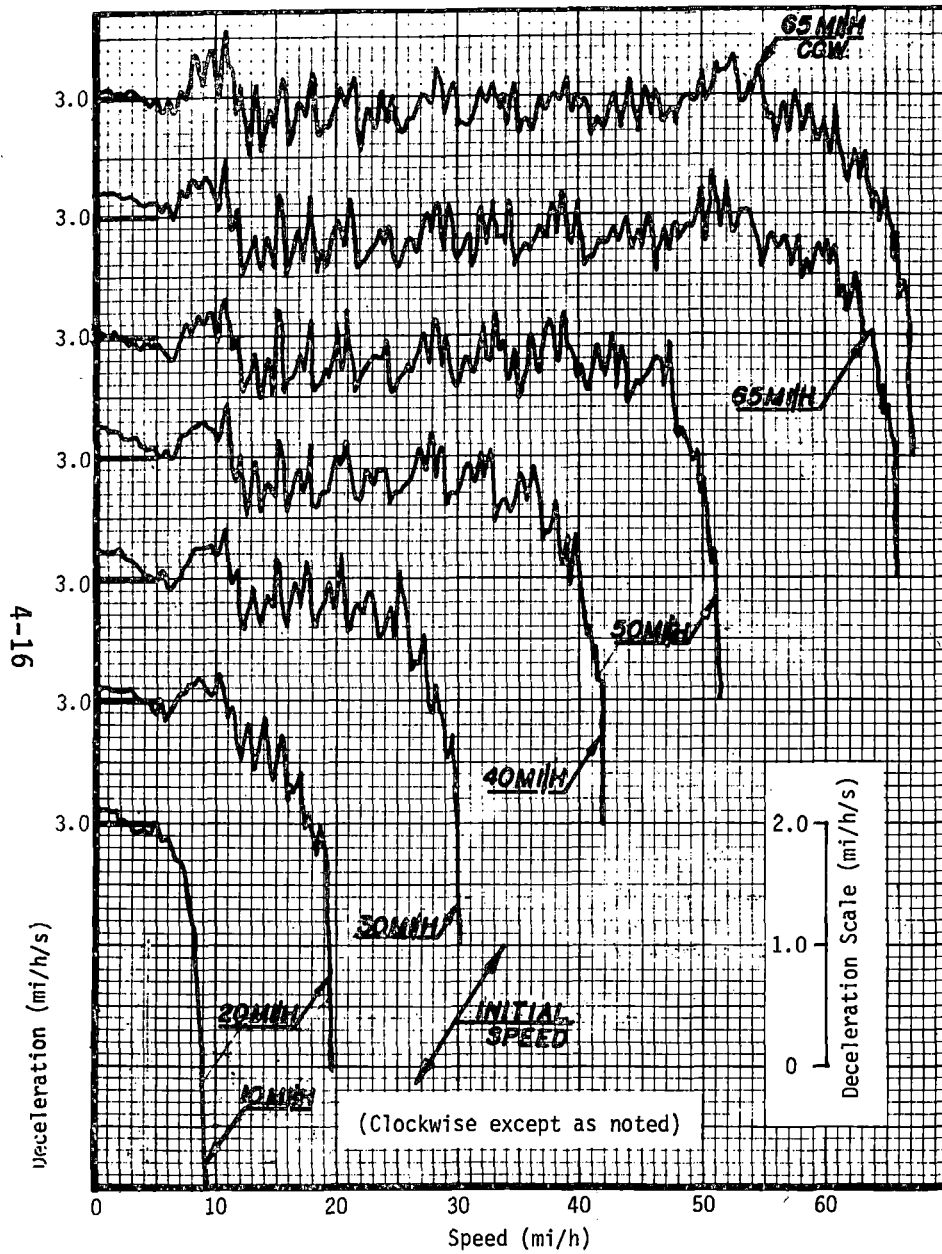


FIGURE 4-11 FULL SERVICE SAP BLENDED BRAKING CHARACTERISTICS, AWO WEIGHT.

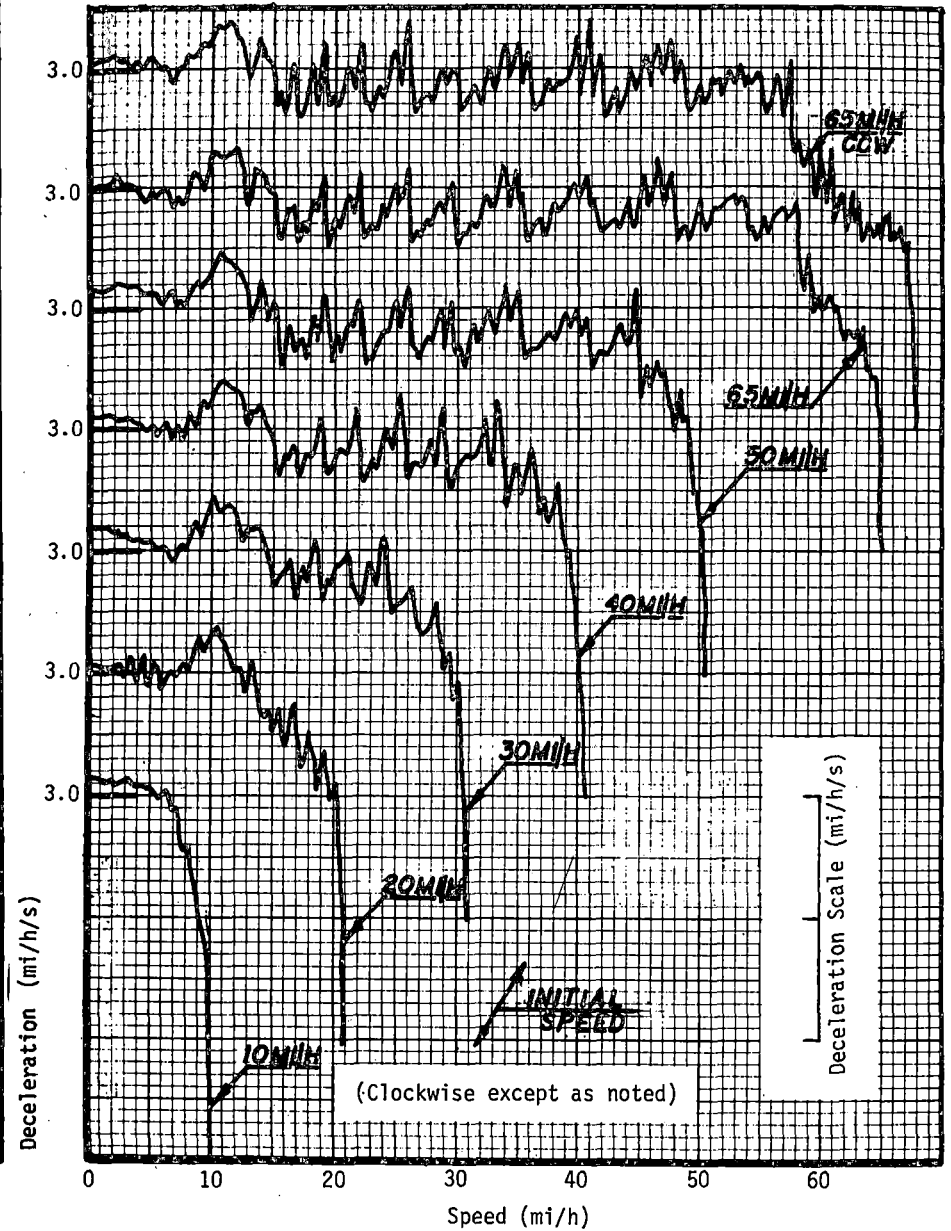


FIGURE 4-12 FULL SERVICE SAP BLENDED BRAKING CHARACTERISTICS, AW3 WEIGHT.

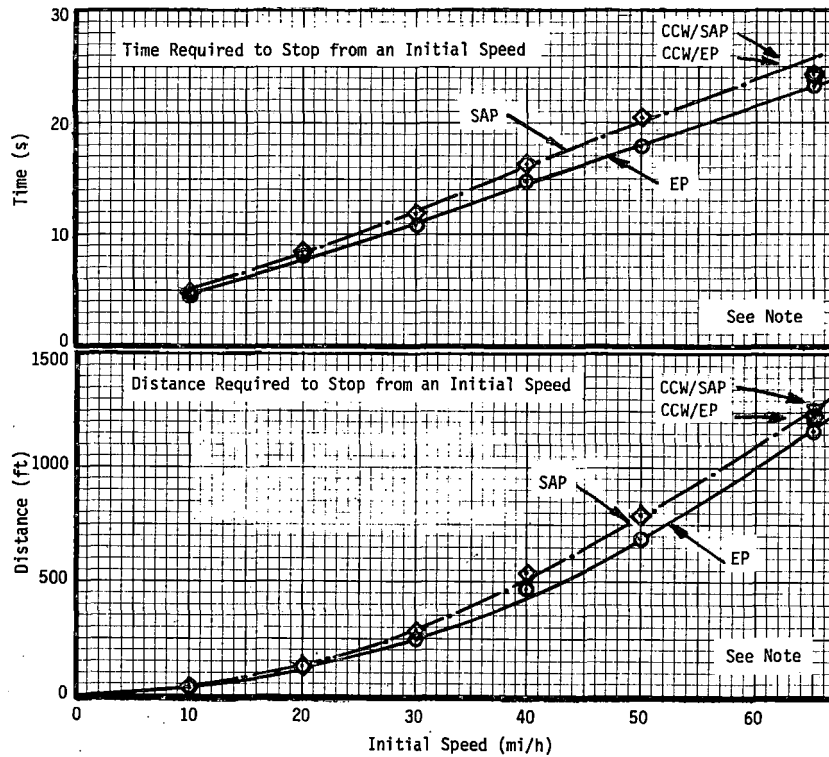


FIGURE 4-13 TIME AND DISTANCE REQUIRED TO STOP, BLENDED BRAKING, AWO WEIGHT.

NOTE:

- EP/SAP Mode Comparison
- Data from First Motion of Master Control, Includes Control Response Time.
- Full Service Braking

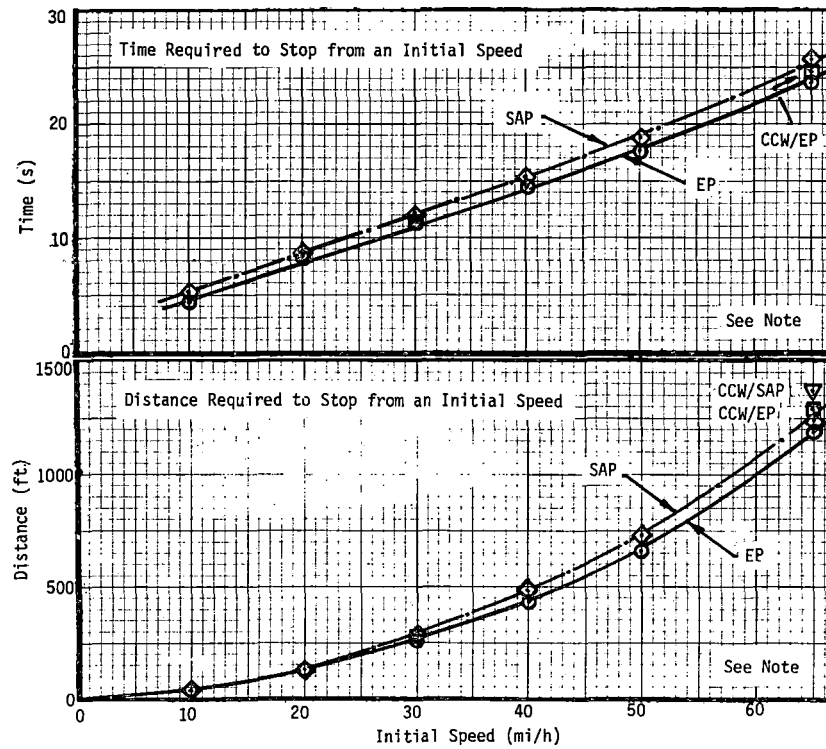


FIGURE 4-14 TIME AND DISTANCE REQUIRED TO STOP, BLENDED BRAKING, AW3 WEIGHT.

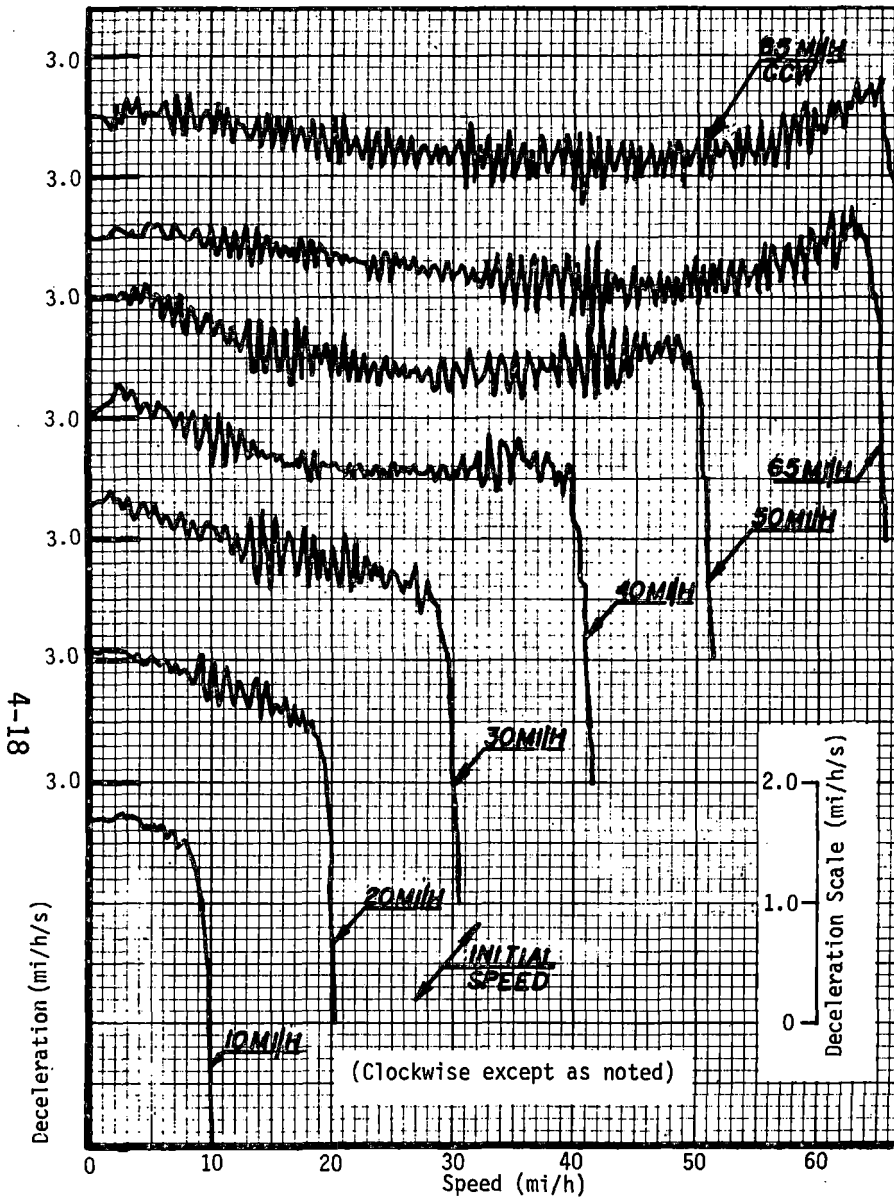


FIGURE 4-15 FULL SERVICE EP FRICTION BRAKING CHARACTERISTICS, AWO WEIGHT.

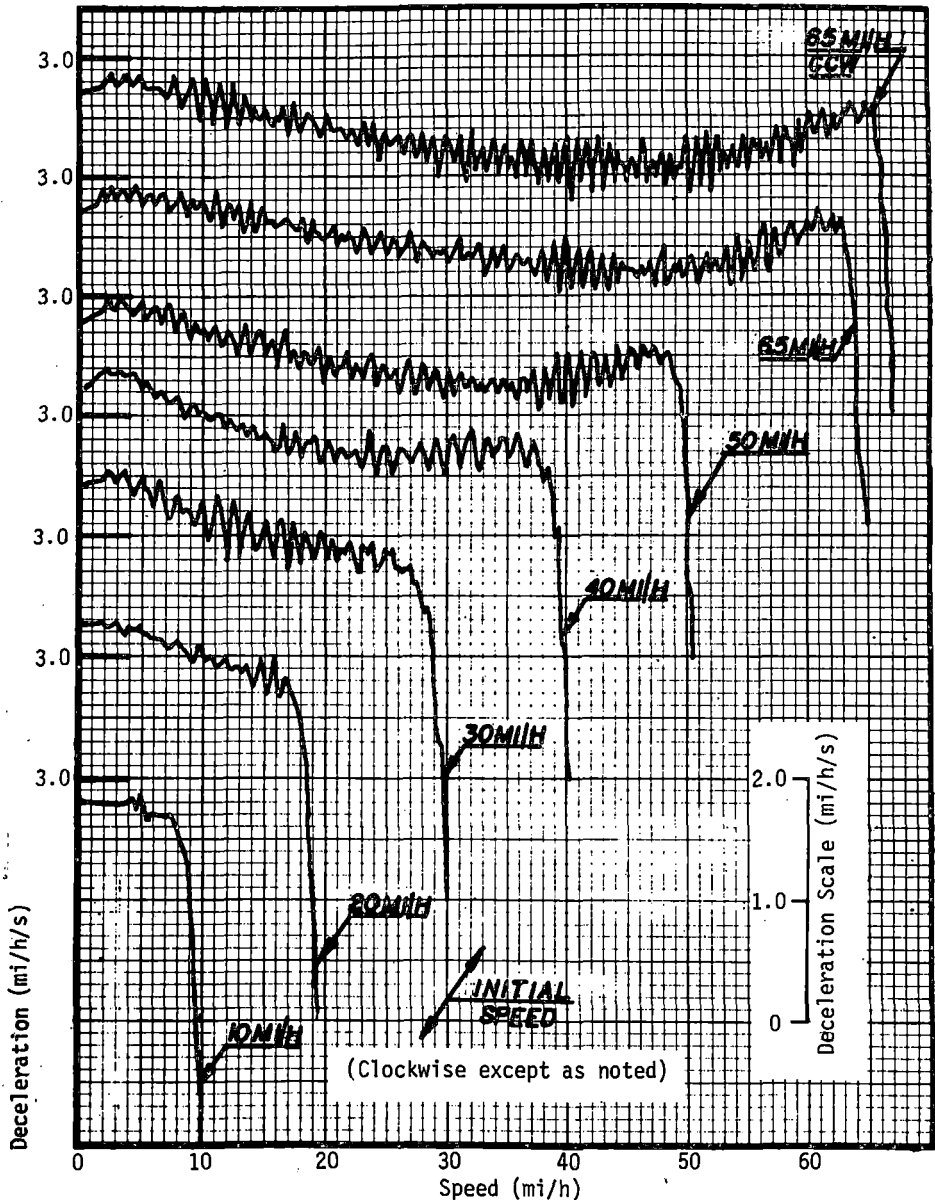


FIGURE 4-16 FULL SERVICE EP FRICTION BRAKING CHARACTERISTICS, AW3 WEIGHT.

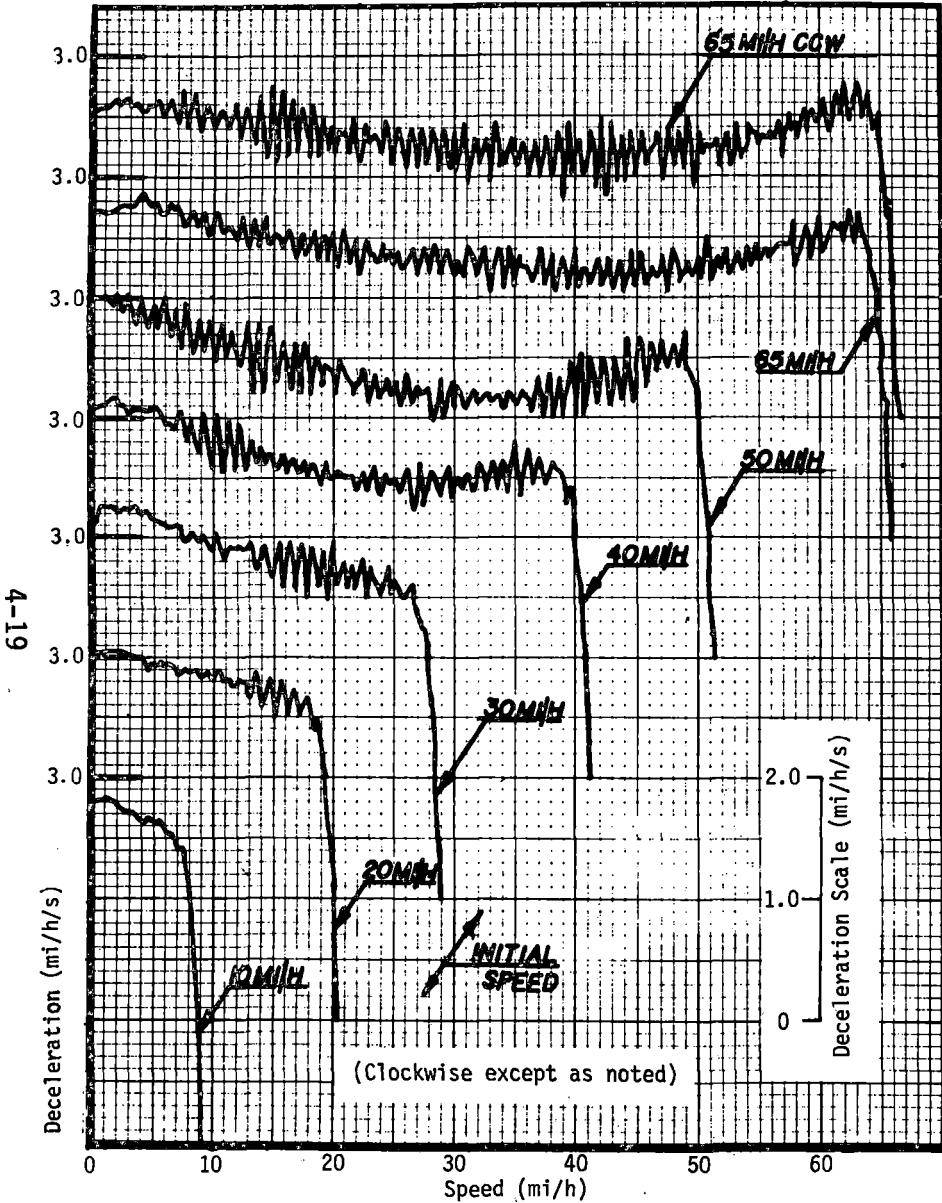


FIGURE 4-17 FULL SERVICE SAP FRICTION BRAKING CHARACTERISTICS, AWO WEIGHT.

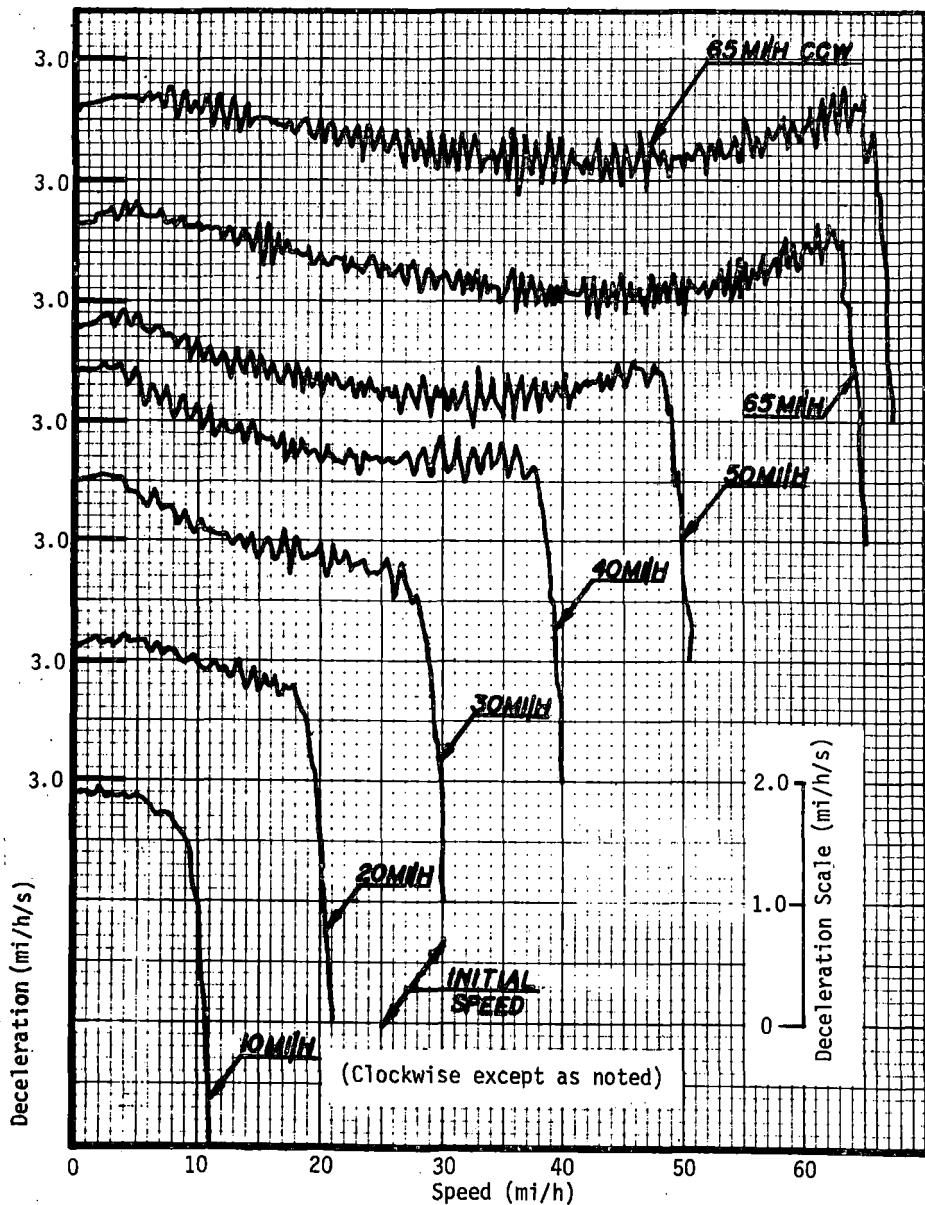


FIGURE 4-18 FULL SERVICE SAP FRICTION BRAKING CHARACTERISTICS, AW3 WEIGHT.

approximately 2.5 mi/h/s, followed by some deterioration in braking rate to the midpoint of the speed range for the stop; deceleration level then increases up to a peak at less than 5 mi/h, immediately before the vehicles come to a stop. At AWO vehicle weight, for initial speeds greater than 30 mi/h, and similarly at initial speeds greater than 40 mi/h at AW3 vehicle weight, deceleration levels fell below the 2.75 mi/h/s specification criterion at some point during the run. Variation of deceleration about the average value was reduced for the friction braking cases compared to blended braking, due to the absence of cam controller/brake resistor switching steps in the friction braking mode; typical variations for friction braking were ± 0.3 mi/h/s for initial speeds above 50 mi/h.

Average decelerations were also computed from stopping distance and time-to-stop data for each case. This was done in order to gain an understanding of overall deceleration levels, which are otherwise obscured by the variation of deceleration with speed throughout the stop. The average computed values are presented in Figure 4-19 plotted versus initial brake entry speeds, for AWO and AW3 vehicle weights, with EP and SAP modes of operation. The times and distances used to calculate the average deceleration values include increments caused by control response time, since they were measured from first motion of the master controller.

Figure 4-19 shows that, based on deceleration levels averaged over the entire stop, the vehicles meet the requirements of the specification for initial speeds up to 40 mi/h. Above this speed, average deceleration levels deteriorate significantly; at 50 mi/h initial speeds, they are in the range 2.4 to 2.5 mi/h/s.

In general, differences in the deceleration levels between EP or SAP modes of operation are insignificant, and can be ignored; full service braking levels were marginally higher for AWO than for AW3 vehicle weight, in particular for the 30 mi/h initial speed case (0.2 to 0.3 mi/h/s).

Time and distance required to stop versus initial speed plots are presented in Figures 4-20 and 4-21 for AWO and AW3 vehicle weights, respectively, with EP and SAP modes of operation. Again, no significant trends were observed with vehicle weight; the SAP mode of operation gives marginally worse stopping distance and time-to-stop performance because of increased control response times.

Emergency Braking. Emergency braking deceleration characteristics are presented in Figures 4-22 and 4-23 for vehicle weights of AWO and AW3, respectively. Corresponding stopping distance and time-to-stop plots are shown in Figures 4-24 and 4-25. These plots are for emergency stops initiated by releasing the motorman's 'deadman' handle on the master controller. Comparing the characteristics for the two vehicle weights, the performance was better at AW3 than at AWO; deceleration levels were 0.2 to 0.3 mi/h/s higher throughout the range of initial brake entry speeds at AW3. The emergency

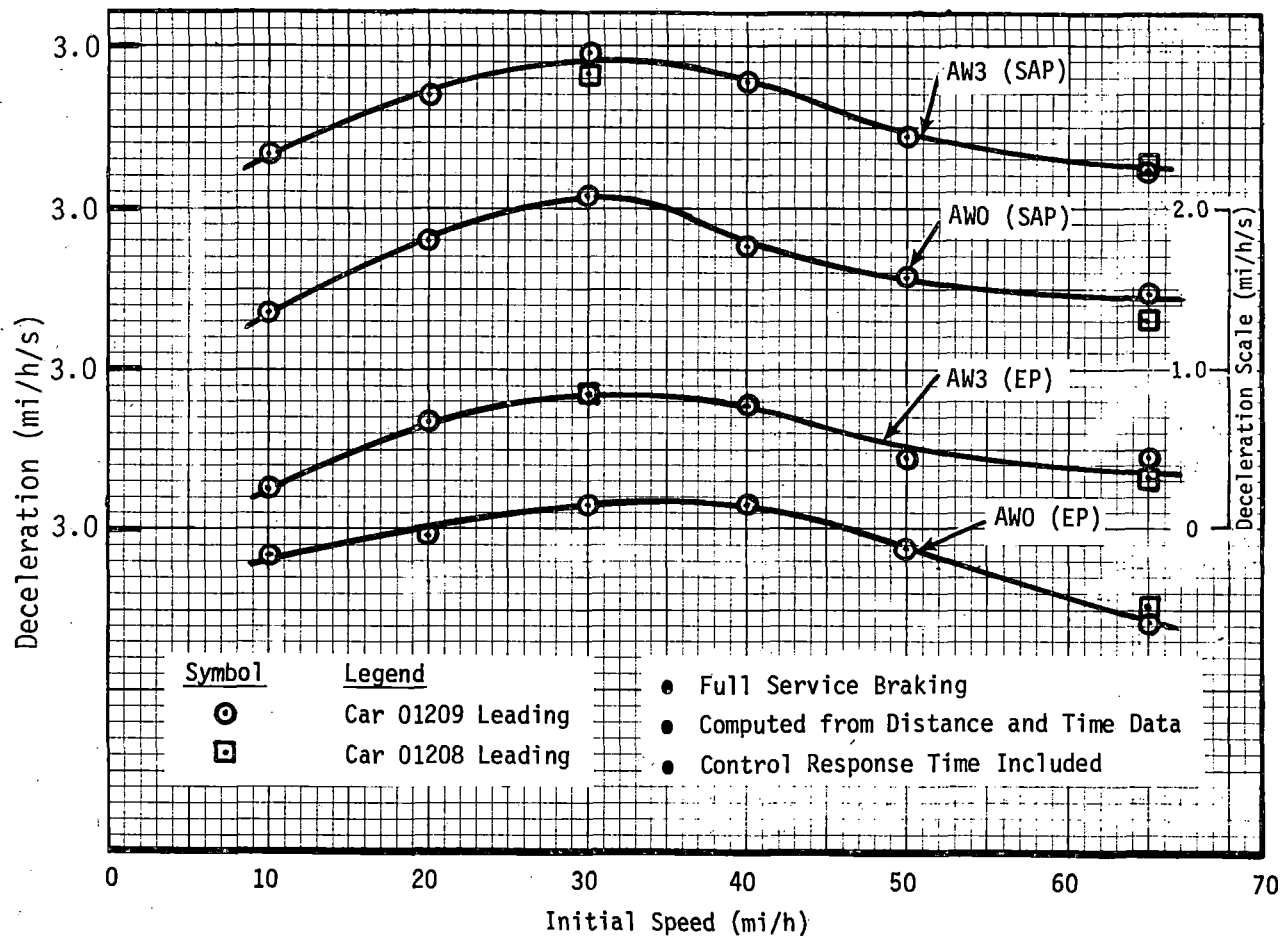


FIGURE 4-19 AVERAGE BRAKING DECELERATION CHARACTERISTICS, FRICTION BRAKING.

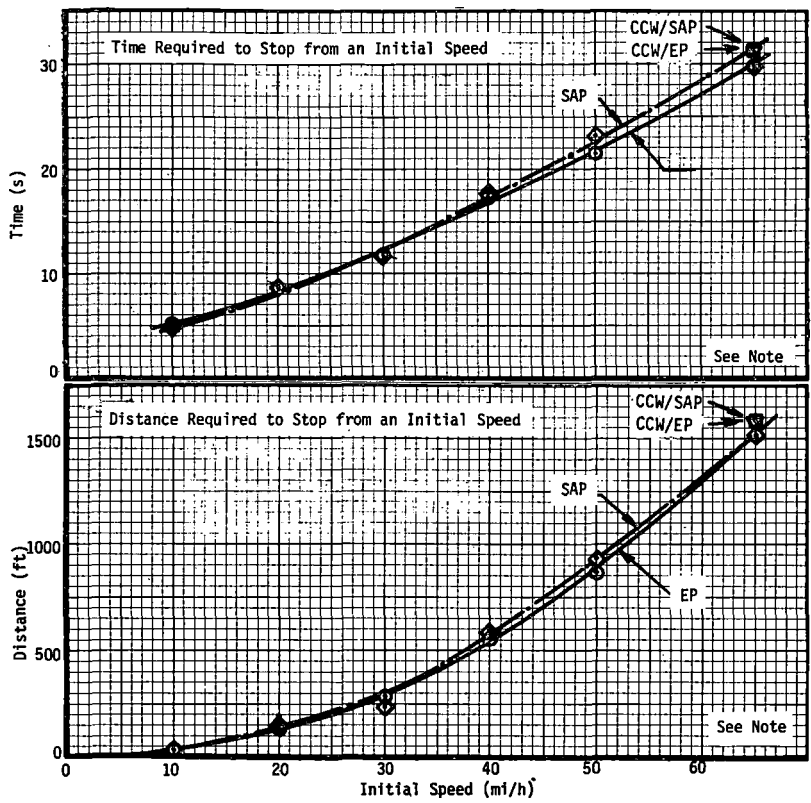


FIGURE 4-20 TIME AND DISTANCE REQUIRED TO STOP, FRICTION BRAKING, AWO WEIGHT.

- NOTE:
- EP/SAP Mode Comparison
 - Data from First Motion of Master Control, Includes Control Response Time,
 - Full Service Braking

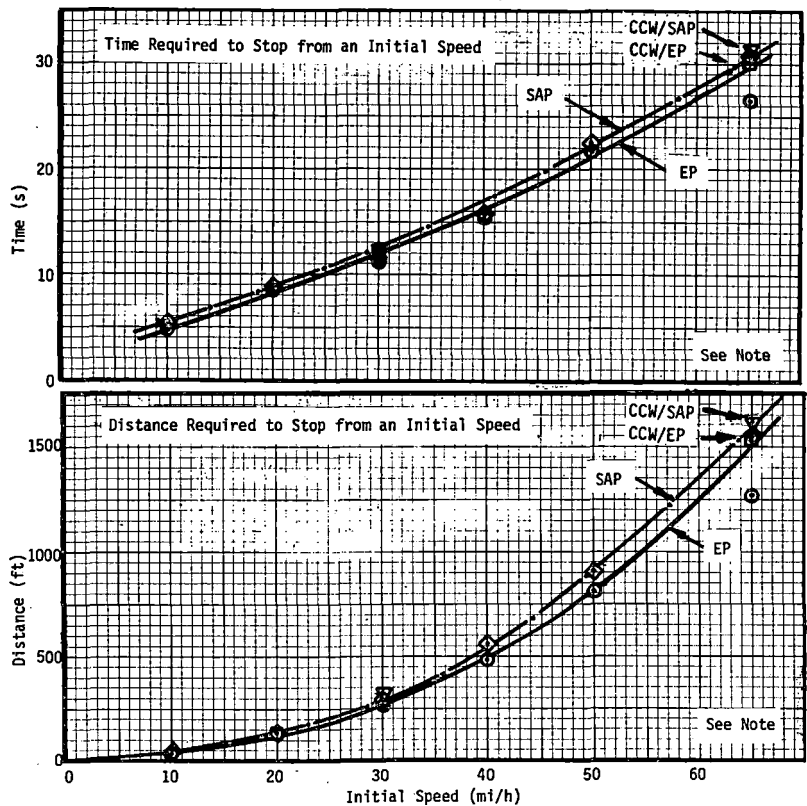


FIGURE 4-21 TIME AND DISTANCE REQUIRED TO STOP, FRICTION BRAKING, AW3 WEIGHT.

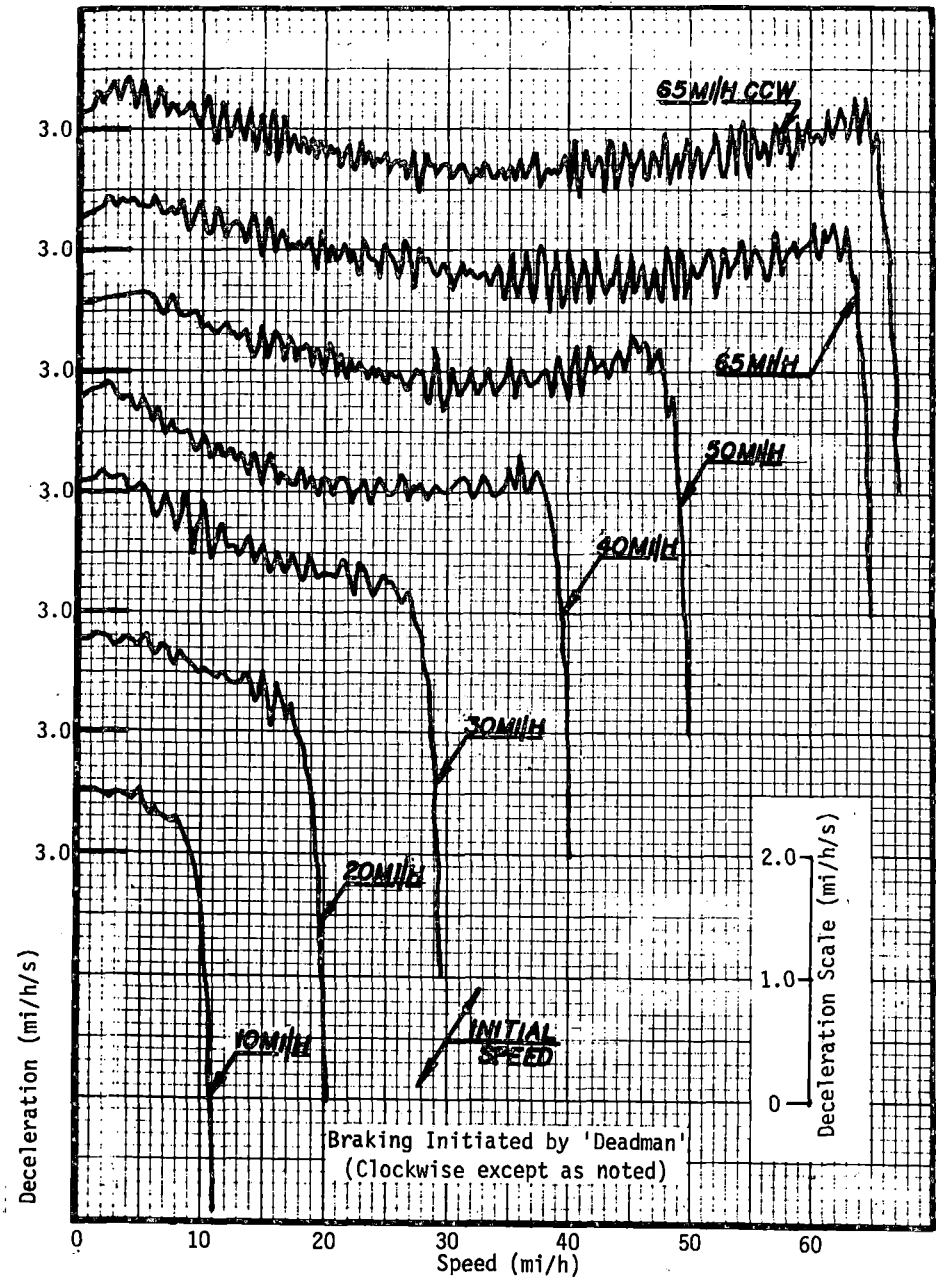
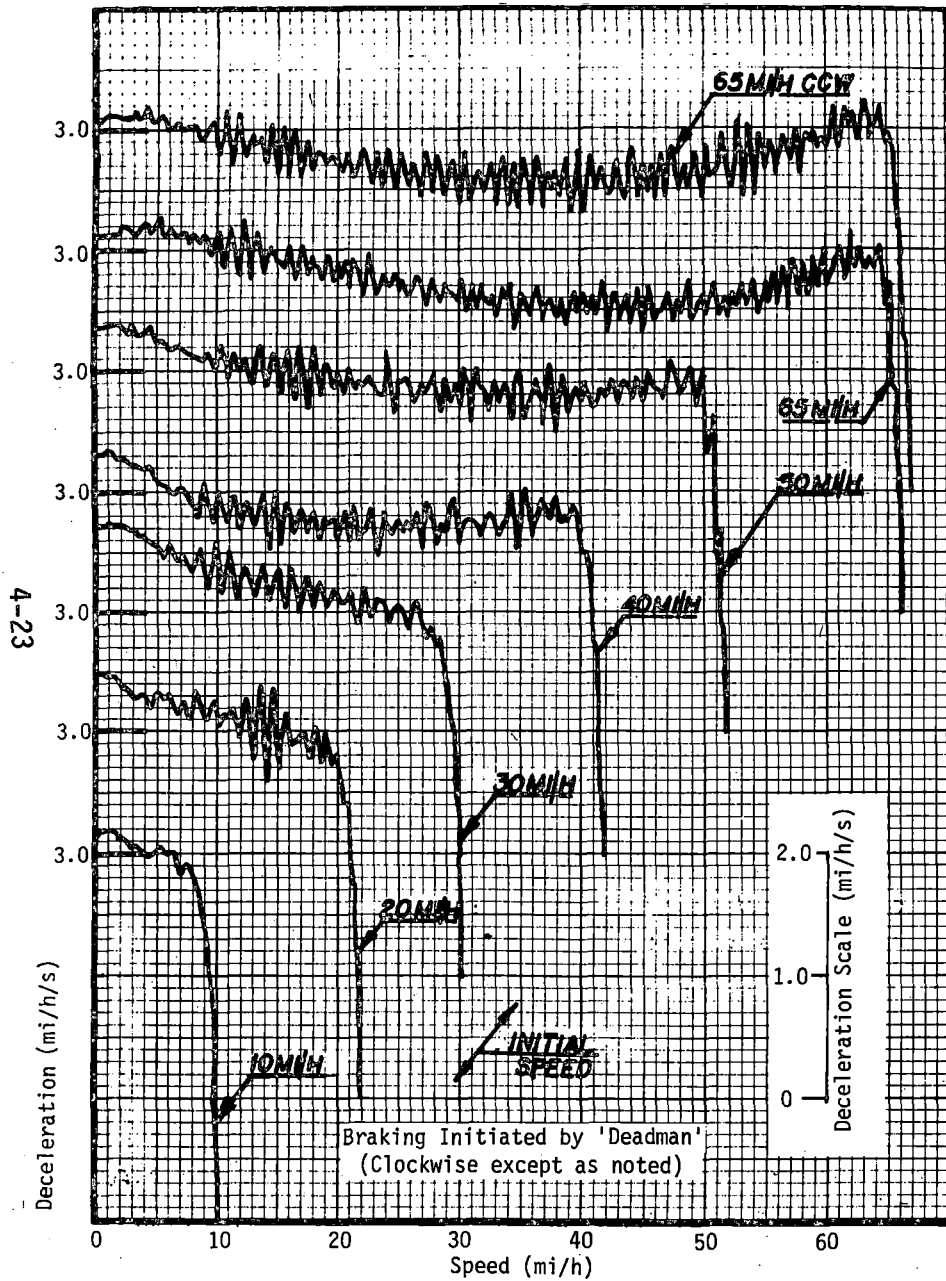


FIGURE 4-22 EMERGENCY BRAKING CHARACTERISTICS, AWO WEIGHT. FIGURE 4-23 EMERGENCY BRAKING CHARACTERISTICS, AW3 WEIGHT.

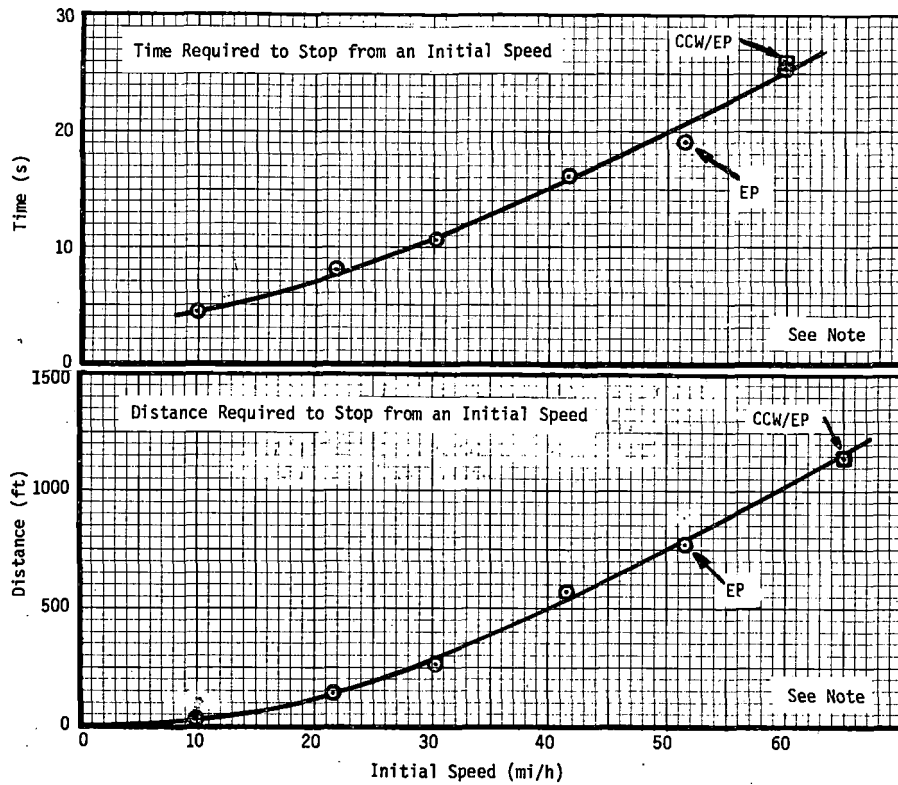


FIGURE 4-24 TIME AND DISTANCE REQUIRED TO STOP, EMERGENCY BRAKING, AWO WEIGHT.

NOTE:

- Emergency Braking Initiated by 'Deadman'
- Data from First Motion of Master Control, Includes System Response

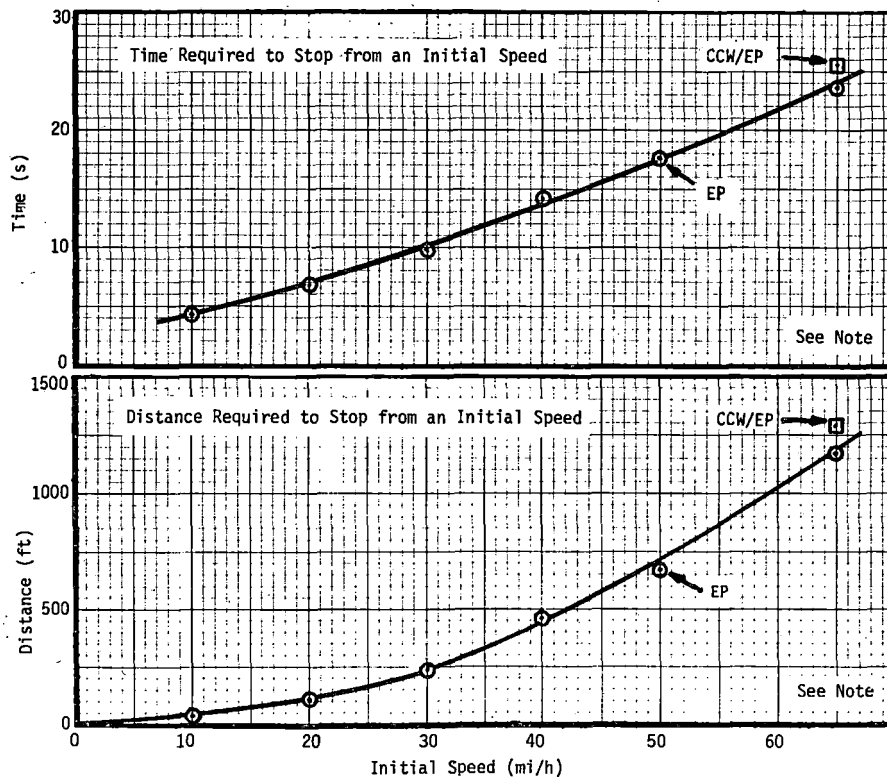


FIGURE 4-25 TIME AND DISTANCE REQUIRED TO STOP, EMERGENCY BRAKING, AW3 WEIGHT.

braking runs showed large changes in deceleration across the speed range, making an evaluation of overall deceleration level and verification of specification compliance difficult. Typically, for the 65 mi/h initial speed case at AW3 vehicle weight, the initial deceleration peaked at 3.1 mi/h/s at 63 mi/h, then fell steadily to 2.75 mi/h/s at 40 mi/h; thereafter the rate of deceleration increased linearly to a 3.4 mi/h/s rate at 3 mi/h immediately prior to coming to a complete stop. In order to establish how close the vehicles met the intent of the 3.25 mi/h/s (vehicle specification) deceleration rate for emergency braking, average deceleration rates were computed from stopping distance and time-to-stop data. These calculated average values are tabulated in Tables 4-3 and 4-4 for all modes of emergency brake initiation; i.e., master controller, external wayside tripcock, emergency brake valve, and deadman. The average values for deadman brake initiation are plotted (Figure 4-26) versus initial speed for AWO and AW3 weights. The calculated values were compared to average deceleration values obtained by numerical integration of the deceleration characteristics as a cross-check, and showed correlation in the majority of cases within 0.1 mi/h/s, thereby validating the approach. The stopping distances and times used in the calculations are from first motion of the master controller oscillograph trace. The average deceleration plots confirm that emergency braking performance was better at AW3 vehicle weight than at AWO, by approximately 0.2 to 0.3 mi/h/s; they also show that the vehicles did not meet the emergency braking deceleration criteria on an average basis, except for 18-30 mi/h initial braking speeds at AW3 weight. Variation of deceleration about an instantaneous mean was limited to ± 0.3 mi/h/s, with the worst cases occurring for initial speeds of 50 and 65 mi/h. This meets the specification requirement for a maximum variation of deceleration of 0.6 mi/h/s.

Jerk Rate. Jerk rates were examined for full service brake applications at each of the initial braking speeds tested. Data from EP and SAP modes of braking and vehicle weights of AWO and AW3 were analyzed. The method of analysis is illustrated in Figure 4-27, which shows a typical deceleration time history; the case presented is for a 30 mi/h initial speed at AWO vehicle weight, using SAP control. The jerk rate is represented by the initial slope of the deceleration time history, as shown in the figure. Data analysis was conducted from the oscillograph chart records, and the jerk values obtained from this analysis are presented in Figure 4-28. It can be seen that the data follow a general trend, the highest jerk rates occurring at 20 mi/h, with considerably lower values at both lower and higher initial speeds. Jerk rates of up to 6.5 mi/h/s² were experienced at 20 mi/h initial speed for the AWO weight/SAP mode case, with typical values in the range 4.2 to 4.9 mi/h/s². The highest jerk rates over the initial speed range were recorded for the AWO vehicle weight case. The vehicles generally met the jerk limit requirement of 2.0 mi/h/s² at initial speeds of 40 mi/h and higher, with the exception of the AWO weight/EP mode case, where jerk rates in the range 3.1 to 3.6 mi/h/s² were experienced.

TABLE 4-3 SUMMARY OF EMERGENCY BRAKING DATA, AW3 WEIGHT.

Initial Speed mi/h	Lead Car/ Direction	Brake Mode	Time to * Stop (Seconds)	Distance to Stop (ft)	Average ** Deceleration (mi/h/s)
65	01209CW	Master Controller	26.1	1328.3	2.65
65	01209CW	Master Controller	25.6	1298.3	2.69
65	01209CW	Tripcock	25.9	1275.9	2.59
65	01208CCW	Tripcock	25.7	1291.4	2.66
65	01209CW	Emergency Brake Valve	25.7	1285.7	2.65
65	01208CCW	Emergency Brake Valve	25.4	1277.4	2.69
65	01209CW	Deadman	25.4	1289.2	2.72
65	01208CCW	Deadman	25.9	1296.8	2.63
50	01209CW	Deadman	19.1	774.4	2.89
40	01209CW	Deadman	16.2	514.2	2.66
30	01209CW	Deadman	10.7	259.7	3.08
20	01209CW	Deadman	8.0	141.3	3.00
10	01209CW	Deadman	4.3	36.3	2.67

* Includes Control Response Time

** Computed from Time and Distance to Stop Data

TABLE 4-4 SUMMARY OF EMERGENCY BRAKING DATA, AWO WEIGHT.

Initial Speed mi/h	Lead Car/ Direction	Brake Mode	Time to * Stop (Seconds)	Distance to Stop (ft)	Average ** Deceleration (mi/h/s)
65	01209CW	Master Controller	25.0	1240.5	2.70
65	01208CCW	Master Controller	25.6	1284.4	2.66
65	01209CW	Tripcock	23.6	1166.4	2.85
65	01208CCW	Tripcock	25.1	1280.6	2.76
65	01209CW	Emergency Brake Valve	24.5	1191.0	2.70
65	01208CCW	Emergency Brake Valve	24.6	1250.1	2.81
65	01209CW	Deadman	23.7	1174.3	2.84
65	01208CCW	Deadman	25.7	1297.9	2.67
50	01209CW	Deadman	17.5	670.4	2.98
40	01209CW	Deadman	14.1	452.7	3.10
30	01209CW	Deadman	9.9	228.7	3.17
20	01209CW	Deadman	6.8	112.6	3.31
10	01209CW	Deadman	4.3	38.8	2.85

* Includes Control Response Time

** Computed from Time and Distance to Stop Data

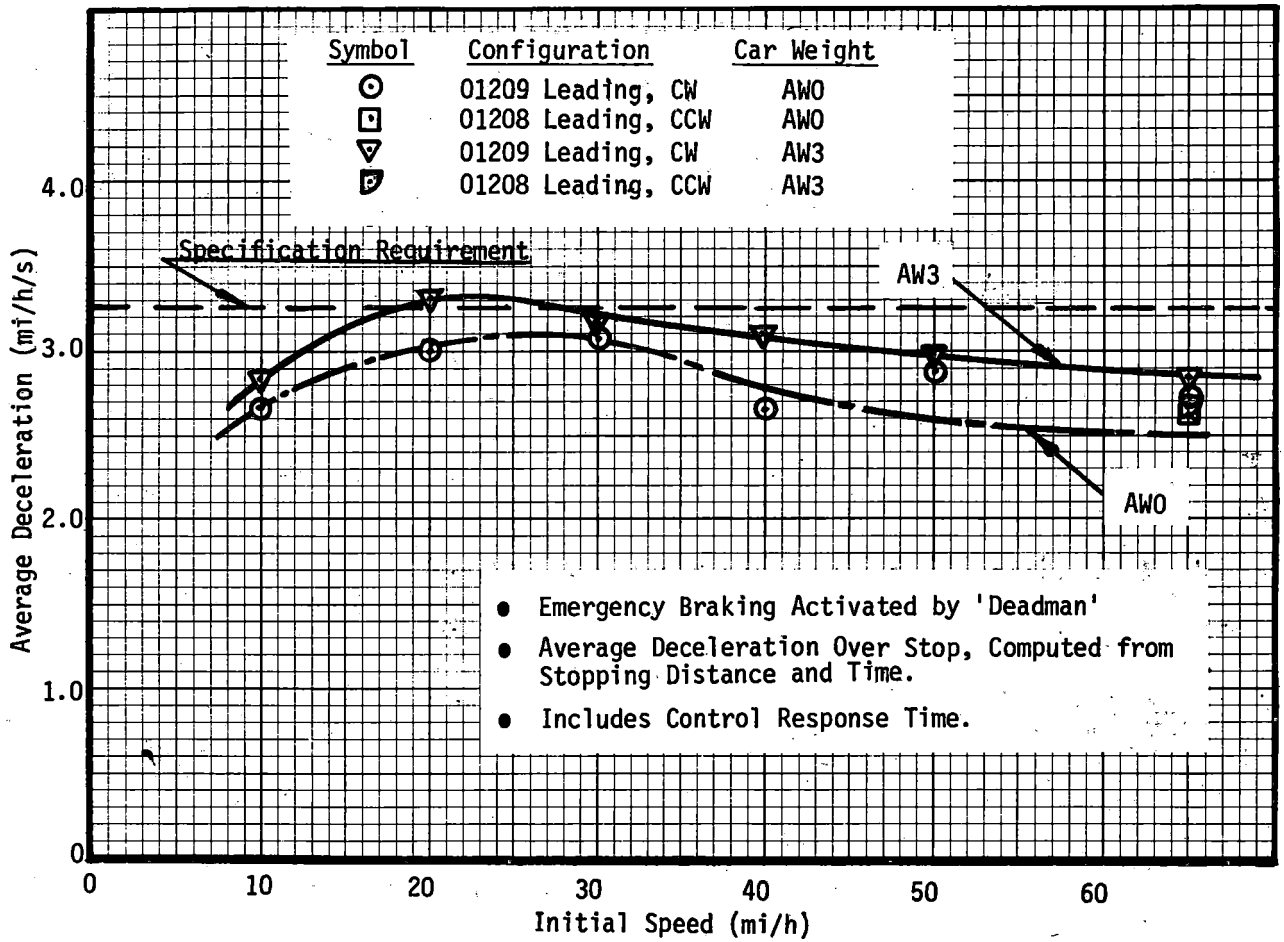


FIGURE 4-26 AVERAGE DECELERATION CHARACTERISTICS, EMERGENCY BRAKING.

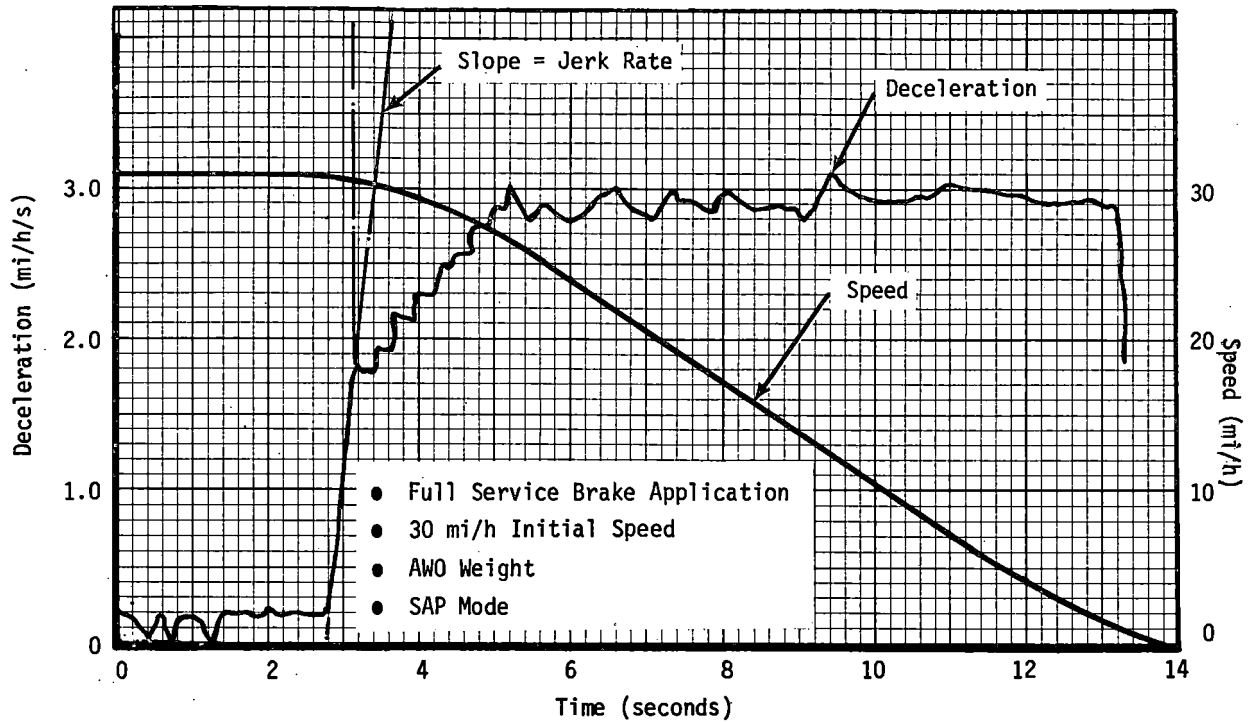


FIGURE 4-27 JERK RATE DETERMINATION FOR A TYPICAL BRAKE APPLICATION.

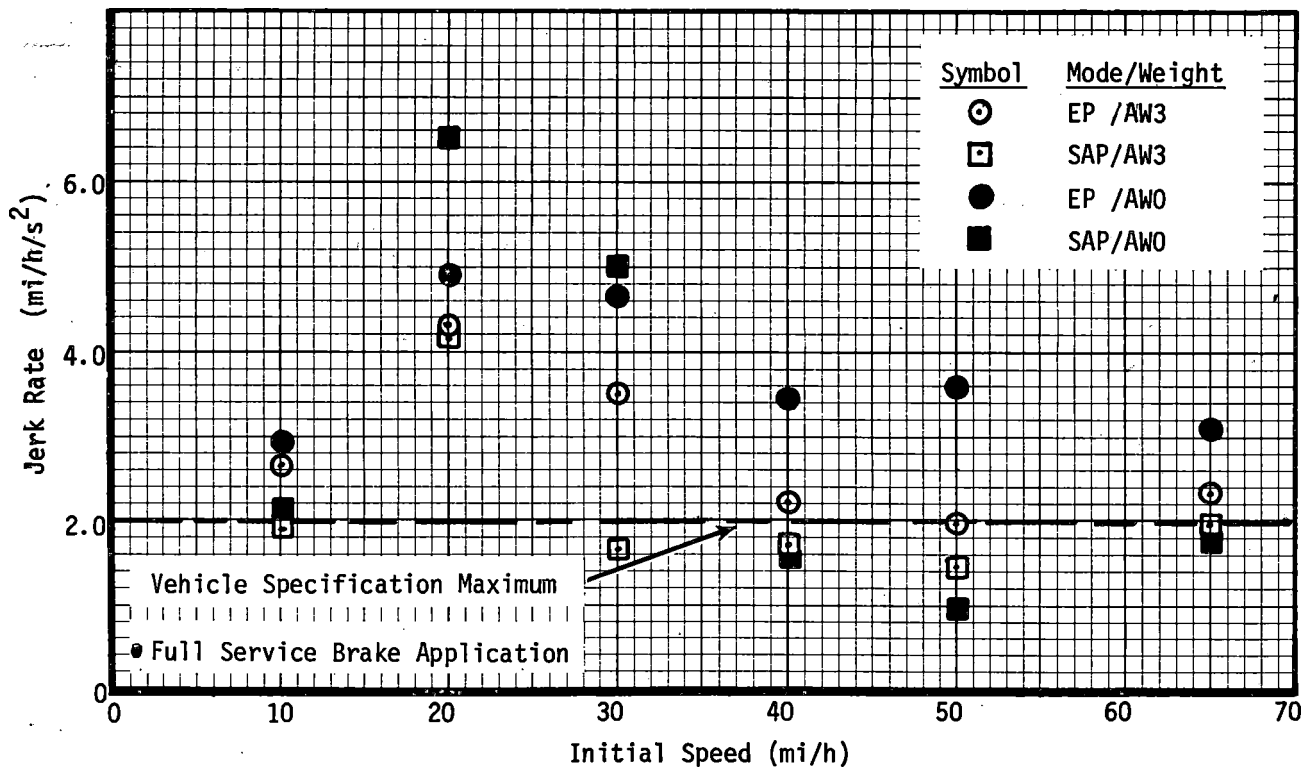


FIGURE 4-28 EFFECT OF WEIGHT AND CONTROL MODE ON JERK RATE.

Summarizing, the vehicles had high rates of change of acceleration due to the initial brake application at speeds up to 40 mi/h, with some improvement over this initial speed. Jerk rates were improved at higher passenger loads and the vehicles meet the specification jerk limit criterion at speeds over 40 mi/h and AW3 vehicle weight. The AW0 weight/EP mode case exceeds the criterion at all speeds.

Control Response. Control response times, from first motion of the master controller to the initiation of a deceleration, were evaluated for all of the full service braking runs. The control response data is presented in Figure 4-29. The data show that control response times are independent of vehicle weight and control mode, there being a 0.25-second spread in the data at any one initial speed. A trend with initial brake entry speed is evident, however, the response times falling from the 1.0- to 1.25-second range at 10 mi/h to a 0.6- to 0.8-second range at 65 mi/h. This may be the result of the psychological effect of speed on the vehicle operator, affecting the speed with which he moves the master controller, as no logical explanation for the trend can be found in the vehicle system. There are no vehicle specification criteria for response time.

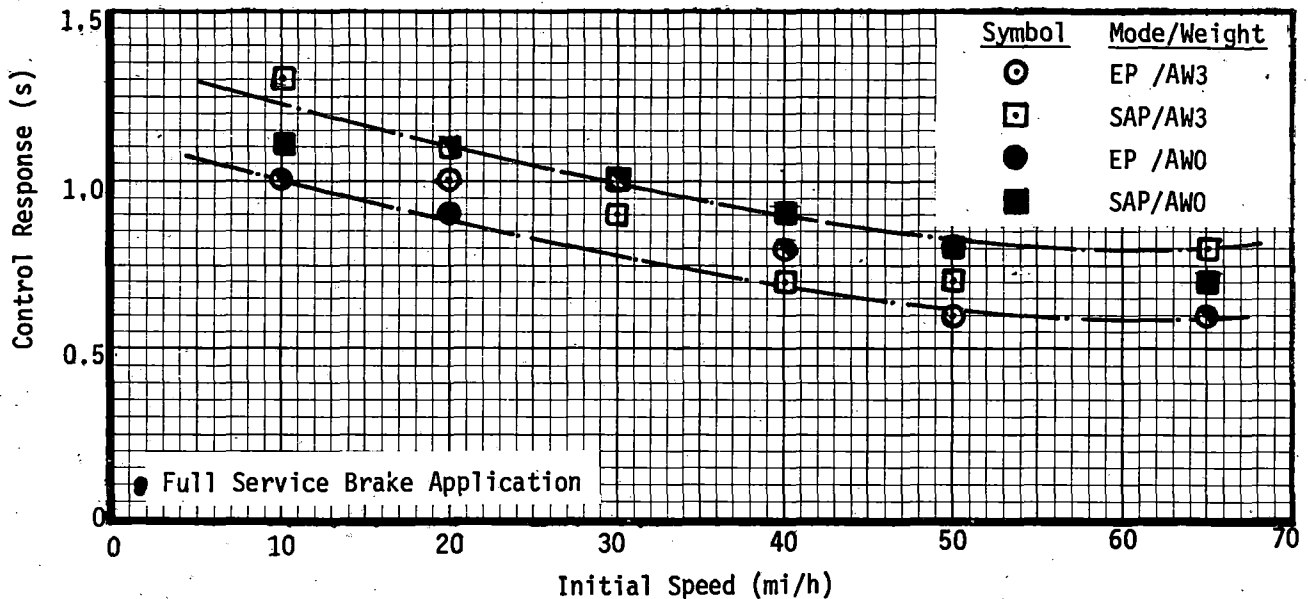


FIGURE 4-29 EFFECT OF WEIGHT AND CONTROL MODE ON CONTROL RESPONSE.

SPIN/SLIDE PROTECTION SYSTEM EFFICIENCY

Objective

The objective of the test was to determine the efficiency of the vehicles' spin/slide protection system; i.e., its ability to provide optimal tractive effort during periods of reduced reduced rail adhesion under acceleration and braking. The test results were compared to the vehicle specification which states:

"The efficiency of the wheel spin/slide protection system shall be at least 70 percent during wheel spins in acceleration and slides in braking over the entire speed range of the cars. The efficiency is defined as being equal to the actual change in speed, expressed as a percentage of the maximum change in speed dictated by the limit of adhesion, during any continuous sequence of the wheel spin/slide protection system."

Test Method

The vehicles were equipped with spray nozzles arranged to spray a mixture of water and soap solution directly into the wheel/rail interface of every wheelset in the train. The soap solution reduced the wheel/rail adhesion to the point where it would not sustain the tractive effort demands of the vehicles and continuous spin or slide activity was induced, thereby activating the vehicles spin/slide protection system. The soap solution was made by adding approximately 16 fluid ounces of liquid soap and eight ounces of mineral oil to 40 gallons of water.

The spray nozzles were fabricated by drilling a standard pipe union blank with a No. 60 drill (0.040" diameter); the resulting flow rate when spraying was approximately 1 gallon/minute per car. The nozzles were connected (by means of 1/4" I.D. flexible plastic tubing) to a 40-gallon tank containing the soap solution; the tank was pressurized to approximately 100 psig from the trainline air supply.

Prior to the test runs, a 3,000-ft section of track was conditioned by making a series of slow passes through it, spraying soap solution on the rail. Test runs were then made on the preconditioned rail, with the spray nozzles operating. Full power accelerations were made from a standing start with data collection being terminated when wheel spin activity ceased at approximately 30 mi/h. Braking runs were made from an initial speed of 65 mi/h, the spray nozzles being activated when the test section was reached, followed by the sustained application of full service braking. In the braking mode, wheel slides were sustained over the entire speed range from 65 mi/h to a full stop.

Results

The test results discussion has been divided into three subsections describing the operation of the spin/slide protection system, the data analysis methods, and a presentation of the test data. It is hoped that this will provide the reader with an understanding of the rationale for the tests and the difficulty of obtaining a true evaluation of the spin/slide protection system's efficiency.

The Spin/Slide Protection System. A wheel slip occurs, by definition, whenever the tangential speed of a wheel differs from the linear speed of the vehicle; the slip is defined as a 'spin' whenever the tangential speed of the wheel exceeds the speed of the vehicle, and as a 'slide' whenever it is less.

The spin/slide protection system is designed to detect spins or slides whether they are random or synchronous; a slip is detected by the system when any wheelset exceeds a 6 mi/h speed difference from other axles on the car, or a rate of change of axle rpm equivalent to 8 mi/h/s. Detection of slips is determined on a per-axle basis.

Upon detection of a wheel spin during acceleration, power is removed from the affected car until the spin is corrected (the cam controller cycles back to a P1 position and the line breaker opens). Power is then reapplied automatically and the cam controller sequences back to its commanded position. The release and reapplication of power is jerk-limit controlled. Upon detection of a slide during braking, the dynamic braking is removed from the affected car for the duration of that brake application and can only be reset by a transfer to the power mode. Friction braking is simultaneously removed from the affected truck until the slide is corrected. Following slide correction, friction braking is automatically reapplied to the truck under jerk-limited control. The wheel spin/slide protection system is functional under all power and braking commands except for an emergency brake application.

Data Analysis Method. The vehicles' spin/slide protection system efficiencies were calculated on a 'per train' basis, using the longitudinal acceleration as an indicator of achieved tractive effort, since acceleration is proportional to tractive effort from the simple Force = Mass x Acceleration relationship. Numerical integration techniques were used on time history oscillograph chart records of vehicle longitudinal acceleration, to derive achieved average acceleration and maximum average acceleration (as limited by adhesion) values for each test run. A line faired through the acceleration peaks was used to represent the acceleration available at maximum tractive effort, as limited by wheel/rail adhesion.

$$\text{Spin/Slide System Efficiency} = \frac{\text{Achieved Average Acceleration}}{\text{Maximum Average Acceleration at Limit of Adhesion}}$$

The test run records were reviewed for wheel slips by examining the oscillograph records of individual axle speeds; runs most suitable for analysis were selected on the basis of having exhibited the highest number of simultaneous wheel slips throughout the train during the test period. Numerical integration was carried out on the longitudinal acceleration trace of the oscillograph records, using one-second time elements from the first detected slip to the resumption of full traction; the reduction in car line current and the removal of truck brake pressure were used as indicators of the system response to spins or slides, respectively.

Test Data. Typical time history traces showing wheel spin and slide characteristics under acceleration and braking are shown in Figures 4-30 and 4-31. The two upper traces in Figure 4-30 show typical line current trends for each car as the propulsion systems apply and remove power in response to wheel

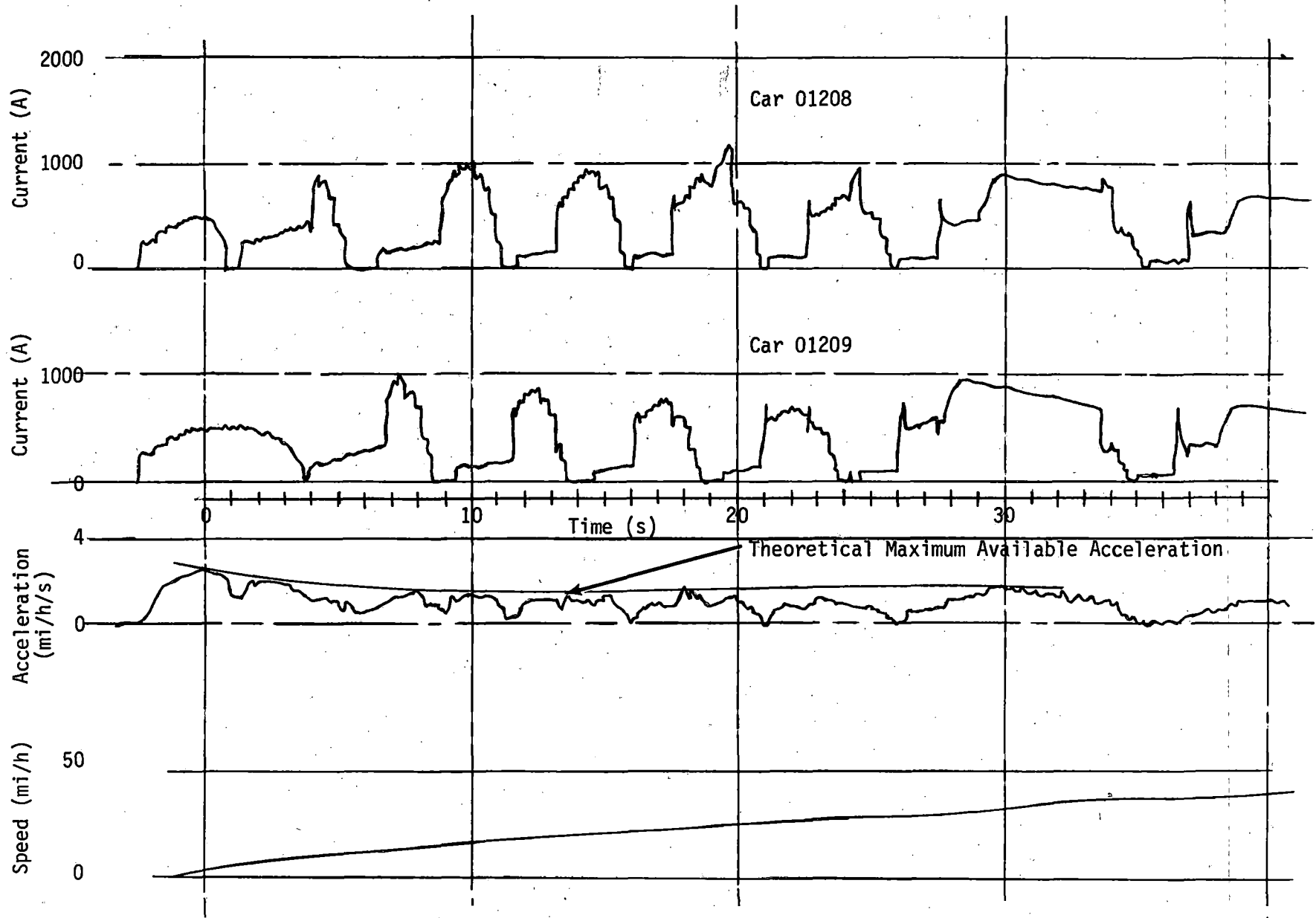


FIGURE 4-30 SPIN CHARACTERISTICS UNDER ACCELERATION.

4-33

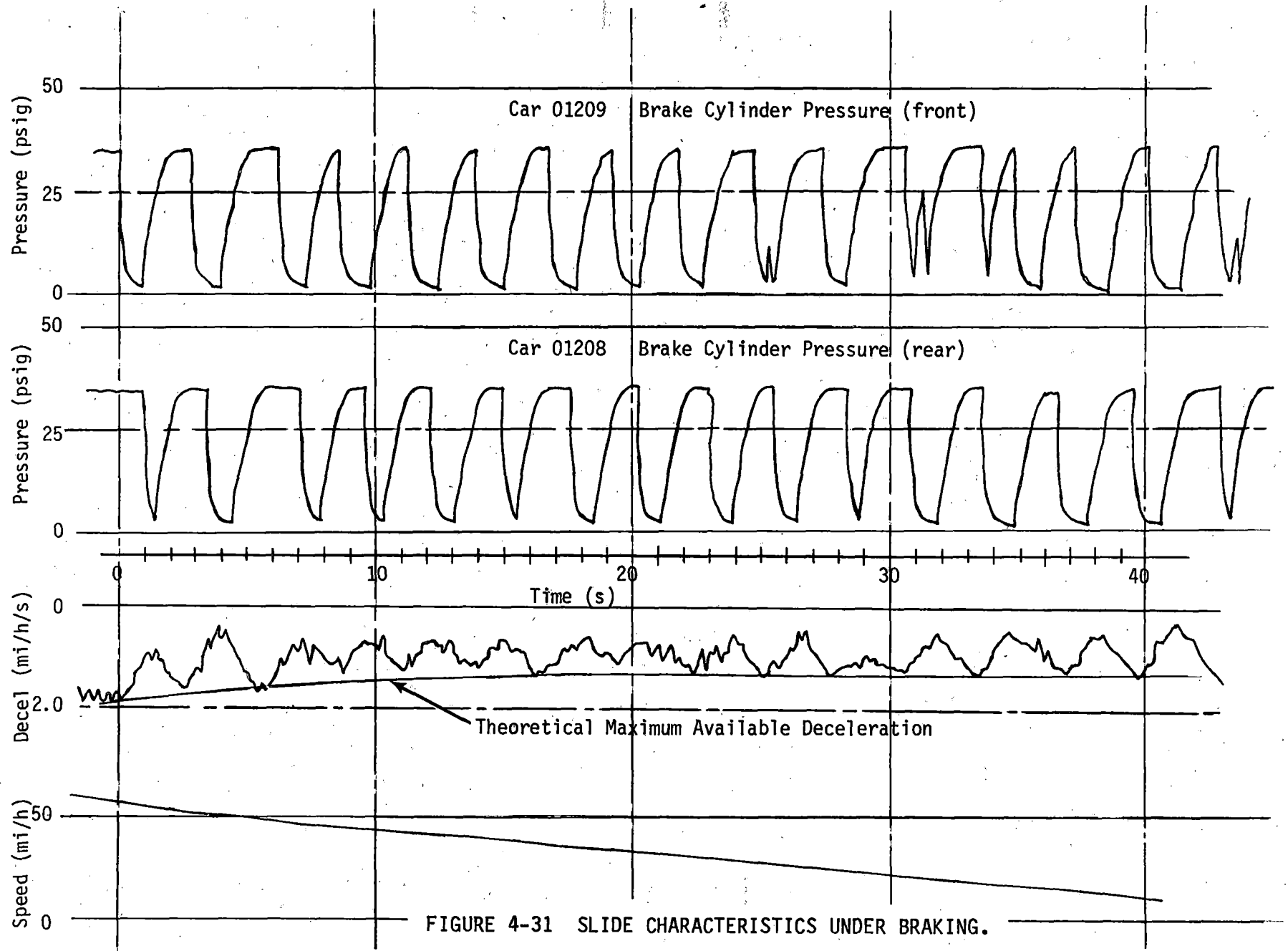


FIGURE 4-31 SLIDE CHARACTERISTICS UNDER BRAKING.

slips. Note that the time cycle between removal and reapplication of power to either car is approximately 5 seconds and that power applications are staggered between cars. When car 01208 is applying maximum tractive effort car 01209 is recovering from a tractive effort pause due to a wheel spin, and is applying a low level of power. Similarly, when car 01209 is applying maximum effort, car 01208 is operating at a low power level.

The third trace shows the characteristics of longitudinal acceleration, and the 'maximum available acceleration' line, faired through the acceleration peaks, which represents acceleration at the maximum available adhesion. The lower trace on Figure 4-30 is a time history of the ninth wheel signal which, since it is independent of the vehicle axles (and therefore free of spin effects), gives true vehicle speed. The time history characteristics for a typical full service brake application with sustained wheel slides are shown in Figure 4-31. The two upper traces show the brake cylinder pressures of the front and rear trucks of car 01208 as the friction braking is applied and removed on a 'per truck' basis, in response to wheel slides; brake cylinder pressure cycles were similar for car 01209. The traces show a full service pressure application of approximately 33 psig. which was cycled on and off at intervals of 2 1/2 seconds. Note that the phasing of brake application is random between trucks, so that momentary deceleration levels were achieved which were in the vicinity of the adhesion limits. The third trace is vehicle deceleration, with a curve drawn through the deceleration peaks representing the maximum deceleration at the available levels of adhesion. The lower trace is a time history of true vehicle speed.

Table 4-5 presents data analyzed from the spin/slide test program; three acceleration runs and one braking run were judged to be acceptable for analysis on the basis of having a sustained series of wheel slips. For the acceleration tests, spin/slide system efficiencies varied from 62 to 69 percent at wheel/rail adhesion coefficients between 0.064 and 0.075. System efficiency achieved was 70 percent for the braking test run examined, at a coefficient of adhesion of 0.077.

In reviewing the test results presented in this section, the reader should note and appreciate some of the difficulties involved in conducting a significant spin/slide test, obtaining valid data, and applying it to the 'real world' case. The test technique described herein relies on the use of the overall deceleration or accelerations levels recorded for the train to determine the levels that can be sustained by the rail, by fairing through the acceleration/deceleration peaks. The assumption here is that the acceleration peaks represent the maximum acceleration that can be achieved at the existing coefficient of adhesion. A review of the time history traces for the acceleration test run in Figure 4-30 shows that this is not necessarily valid. The line current traces show that the cars were applying tractive effort to the rail out of phase with each other; when one car was applying power and reaching the limit of adhesion, the other was recovering from a wheel

TABLE 4-5. SPIN/SLIDE TEST DATA.

Mode of Operation	Initial Velocity (mi/h)	Final Velocity (mi/h)	Distance Travelled (ft)	Time Taken (s)	Average Achieved Acceleration (mi/h/s)	Average Max. Available Acceleration (mi/h/s)	Spin/Slide System Efficiency (%)	Average Available Coefficient of Adhesion
Acceleration	3.5	28.5	705	26	1.02	1.64	62	.075
Acceleration	2.0	30.0	762	28	1.02	1.62	63	.074
Acceleration	0	35.0	1030	36	.98	1.42	69	.064
Braking	56.0	1.0	1965	48	1.19	1.70	70	.077

spin and at a low power output. It is likely that the peak accelerations would be higher if the vehicles' propulsion systems were operating in phase, and therefore the analysis technique underestimates the maximum available acceleration at the limit of adhesion. In the case of the braking data, the cycling of the brake applications on each truck is random so that at some points in time during the slide activity the brake applications are in phase. Here the deceleration peaks are true representations of the maximum deceleration at the limit of adhesion, and a 'maximum available deceleration' line can be joined through these points with confidence.

The analysis technique requires that all wheelsets in the train are slipping, in order that a true indication of system efficiency can be gained; any wheelset which does not slip will unduly influence the data and give rise to artificially high efficiency values. In order to achieve slips of all wheelsets, each is subjected to reduced adhesion levels by spraying soap solution ahead of the wheel/rail interface. In revenue service it is likely that each wheelset will provide a cleaning action for the wheelset following it, so that adhesion levels will improve progressively throughout the train from front to rear. If this is the case, it is unlikely that a train in revenue service will experience slips on all wheelsets in the manner induced by this test technique.

TRAIN RESISTANCE

Objectives

The objectives of this phase of the test program were to evaluate the open-air train resistance characteristics for a two-car train, and to compare the test data with train resistance values predicted by the empirical Davis formula. The resistance coefficients used in the Davis formula for this comparison were those defined in the vehicle design specification.

Test Method

The tests were carried out by allowing the vehicles to coast, from their maximum speed of 65 mi/h, through a section of level, tangent track. A series of successive runs was made such that each successive entry speed approximated the exit speed of the previous run, until the vehicles coasted to a full stop. Vehicle speed fell by approximately 6 mi/h for each pass. Tests were conducted in both clockwise and counterclockwise directions of travel on the track to minimize the effect of surface winds. The track section is constructed of 119 lb/yd welded rail and is maintained to FRA Class 6 standards. Speed, time, and distance parameters were recorded for each test run, and brake cylinder pressure and armature currents were monitored to ensure true coast conditions. Tests were conducted at AW0 and AW3 vehicle weights.

Results

Train resistance to motion is a combination of rolling resistance, wheel flange effects, and aerodynamic drag; it acts on the vehicles to slow them according to the simple Force = Mass x Acceleration relationship. This relationship is somewhat modified by the angular inertia of the rotating parts, and by second order losses due to motor windage, gearbox and bearing friction effects, etc. A 10 percent weight allowance is commonly added to the vehicle weight to accommodate these cumulative effects and has been used in this analysis. Thus, at any time during a drift run, the instantaneous train resistance is given by:

$$R = 1.1 \times \frac{WF}{g} \times \frac{88}{60} \quad (1)$$

where:

- R = Train Resistance (lbs)
- W = Weight of the Train (lbs)
- g = Acceleration due to gravity 32.2 ft/sec².
- F = Deceleration (mi/h/s).

The deceleration levels, as recorded by the vehicles' longitudinal accelerometer, which is normally used to evaluate acceleration and deceleration characteristics, are extremely small (0.05 to 0.20 mi/h/s) and subject to variation due to local irregularities in the track. The vehicles' ninth wheel speed signal was therefore used to compute the drift deceleration characteristics. The speed signal was low-pass filtered at 1.0 Hz to reduce noise and digitized at 32 samples per second. Time history plots of vehicle speed were made from the digital data for each test run. The local slopes of the speed time history plots were then calculated over 2-mi/h time intervals, to yield approximately 50 deceleration/speed data pairs for each drift run series. These values are plotted in Figures 4-32 and 4-33, which illustrate the drift deceleration characteristics for clockwise and counterclockwise directions of travel, at AWO and AW3 vehicle weights. From these plots the data were smoothed, and clockwise and counterclockwise data points were merged to cancel out wind effects. Train resistance values were then computed using equation (1). These are presented in Figure 4-34, plotted versus vehicle speed for AWO and AW3 vehicle weights. Superimposed on the plot are the train resistance measurements obtained from the 1979 test program conducted on the MBTA 'Blue Line' vehicles at the TTC. The Blue Line and Orange Line cars are similar in design, with the major exceptions of vehicle length (48 ft 10 in compared to 65 ft 2 in) and weight (60,160 lbs vs 66,330 lbs empty). The comparison, therefore, adds a further dimension to the train resistance measurements. The train resistance data obtained from the drift results were compared to theoretical values calculated from the empirical Davis formula.

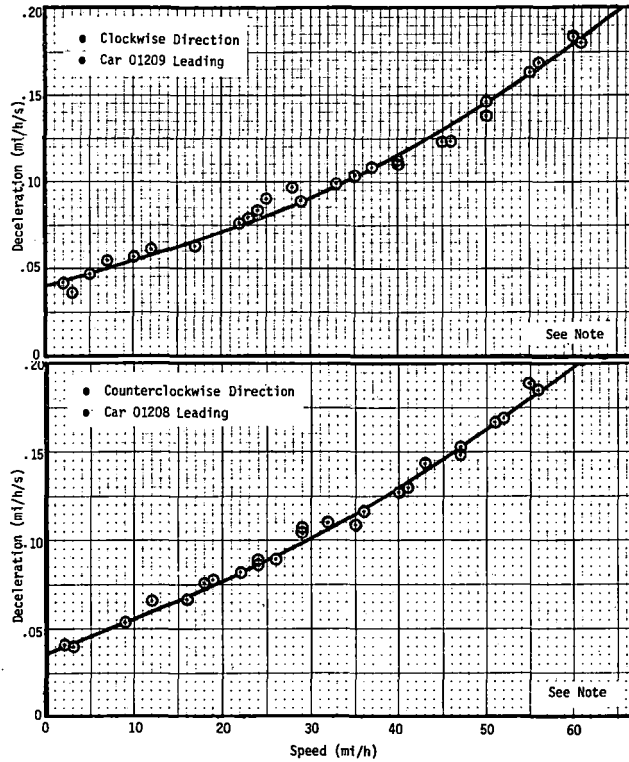


FIGURE 4-32 DRIFT DECELERATION CHARACTERISTICS, AWO WEIGHT.

NOTE:
 ● Level Tangent Track
 ● Welded Rail, FRA Class 6 Track

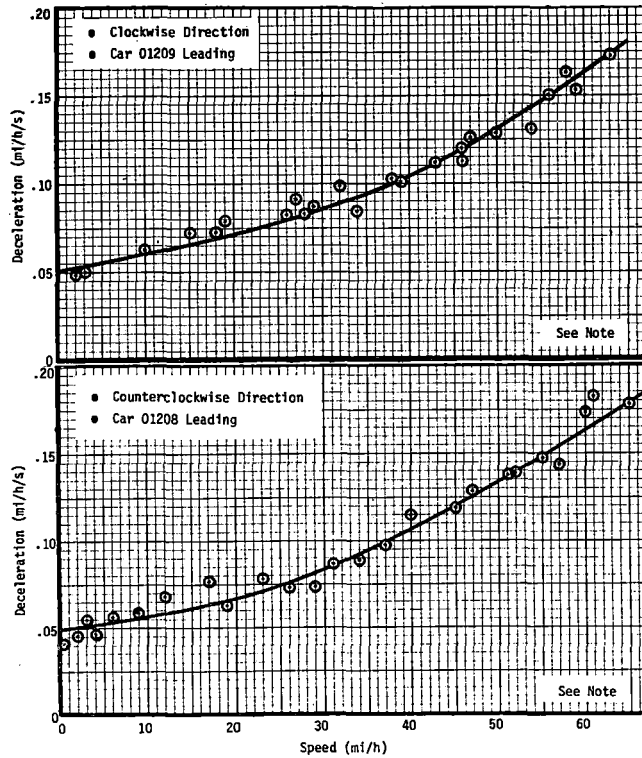


FIGURE 4-33 DRIFT DECELERATION CHARACTERISTICS, AW3 WEIGHT.

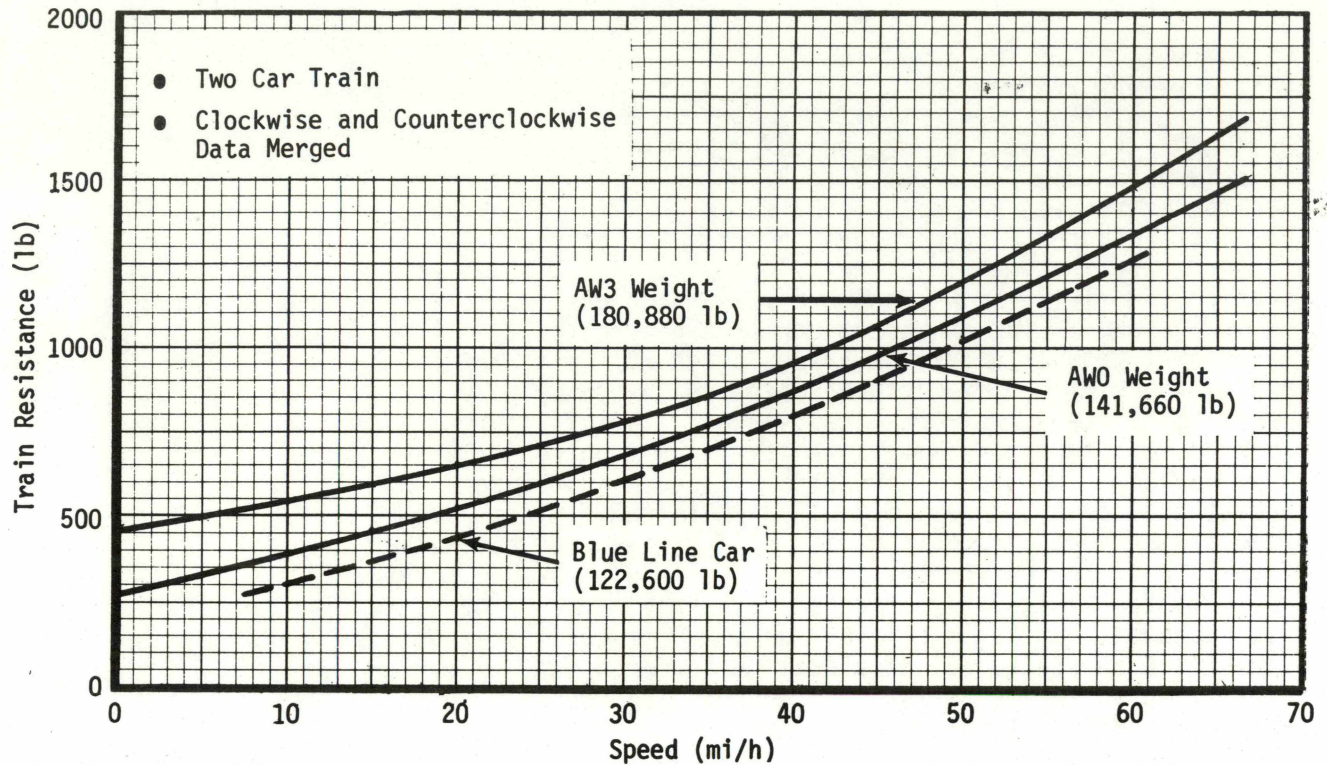


FIGURE 4-34 TRAIN RESISTANCE VARIATION WITH SPEED.

The modified Davis Formula for train resistance is:

$$TR = 1.3 + \frac{29}{W} + bV + \frac{cAV^2}{WN}$$

where:

TR = Train Resistance (lbs/ton),
 W = Weight per Axle (tons),
 b = Flanging Loss Coefficient,
 N = Number of Axles,
 V = Train Speed (mi/h),
 c = Air Resistance Coefficient, and
 A = Frontal Area of Train (ft²).

In this empirical formula, the first term represents rolling resistance; the second bearing and seal losses, the third flanging losses, and the fourth aerodynamic losses. Calculations of train resistance were made using the flanging and aerodynamic loss coefficients and frontal area quoted in the vehicle design specifications. These are:

Flanging Loss Coefficient	b = 0.045
Aerodynamic Loss Coefficient	c = 0.0024 (lead car)
Aerodynamic Loss Coefficient	c = 0.00034 (trailing car)
Frontal Area	A = 100 ft ²

The results of the comparison for a two-car train at AWO vehicle weight are presented in Figure 4-35. Train resistance values are plotted versus vehicle speed for the test data, and for the Davis formula calculated values at sea level, and the Davis formula values corrected to 5,000 ft altitude. The altitude correction was made simply by factoring the aerodynamic loss coefficient to account for the change in atmospheric pressure (25.2" of mercury locally, compared to 30.0" at sea level). The figure shows that the test data agree closely with the Davis formula values corrected for the effects of altitude. The uncorrected Davis formula values agree well with the test data up to 45 mi/h; beyond this speed they progressively overestimate the actual train resistance. This is to be expected, as the aerodynamic loss term is a function of velocity squared. The general trends illustrated in Figure 4-35 suggest that the uncorrected Davis formula coefficients provided in the vehicle specification will give a good estimation of vehicle train resistance in their sea level, revenue service environment. It is interesting to note, given the aerodynamic drag increment between sea level and 5,000 ft (22 lbs at 65 mi/h), that an additional deceleration increment of 0.03 mi/h/s is realized at sea level for this speed. This means that a vehicle operating at sea level, given the same braking tractive effort, can be expected to decelerate at a marginally higher rate down to 45 mi/h, than the same vehicle operating at 5,000 ft (i.e. at the TTC).

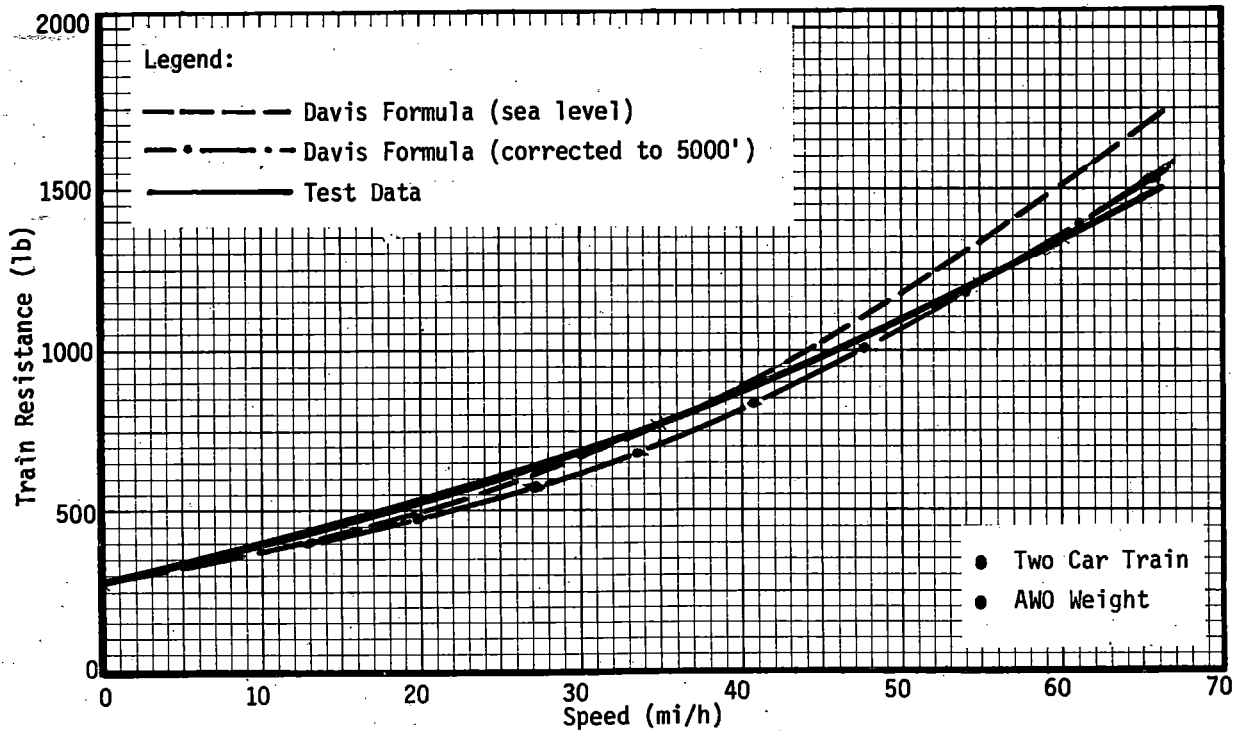


FIGURE 4-35 COMPARISON OF TRAIN RESISTANCE TEST DATA WITH DAVIS FORMULA CALCULATED VALUES.

ENERGY CONSUMPTION

Objectives

The objectives of the energy consumption tests were to measure the energy consumed by the vehicles while they operated over a simulated revenue service profile, with the propulsion system in (1), a standard configuration and (2), in one representing an energy-conserving mode of operation.

Test Method

The cars were operated over a profile representing operation on the MBTA Orange Line. The Orange Line simulation represents a round trip from Oak Grove to Forest Hills, and return to Oak Grove. The revenue service simulation is defined in terms of the distance between stations, the maximum section speeds, and the station dwell times; only the track gradients differed. It should be noted that the revenue service profile is a simulation only, used as a standardized base to obtain comparative energy consumption data. The profile is detailed in Appendix B.

The profile test runs were made at AW3 vehicle weight. Tests were conducted using full service acceleration and braking (P4 and 'Maximum' master controller positions, respectively) to accelerate to the required section speed and to brake for the stations; all minor speed adjustments were made using control inputs at the motorman's discretion. The Orange Line profile was also run with the accelerations restricted, by limiting the master controller position to a P3 setting. This represents a possible energy-conserving propulsion system configuration. The P3 position provides the same cam controller notching sequence and the same acceleration rate up to motor base speed as the P4 setting, but does not have two additional steps of field shunting above base speed. This is illustrated in the acceleration characteristics of Figure 4-3. The initial level of acceleration at P4 controller is maintained up to 25 mi/h, but falls off at 23 mi/h for the P3 position, and thereafter is substantially lower than the P4 level throughout the speed range.

Power was removed from floor/overhead heating systems, the air conditioning, and interior lights during all tests; however, all auxiliary systems, including the air compressor and motor-generator, were operating normally; their energy consumption is included in the data.

Onboard watt-hour meters were used to measure the energy consumed by each car. (Appendix A, "ENERGY CONSUMPTION WATT-HOUR METER", contains a brief description of these meters.) The data were tabulated at each station stop. In addition, line voltages and currents, motor currents, and speed, time, and brake pressure data were recorded on analog tape and are available for processing. The data presented here were recorded by the watt-hour meters. Third rail voltage was maintained at a nominal, no-load level of 610 V d.c. for all runs.

Results

The energy consumption test data are summarized in Table 4-6 and are presented as energy consumption totals for each car, averaged, and divided by mileage to present the data on a kilowatt-hour per car-mile basis. Time, distance, and average speed information is also presented for each run; the data are the average of three runs.

Comparing operation of the cars using maximum acceleration (P4 controller position) to that using a P3 setting (eliminating the two stages of motor field shunting) it can be seen that a savings of .3 kWh/car-mile was realized on the Orange Line profile. This represents an energy savings of 6 percent, for a penalty in round trip time of only 31 seconds. It should be noted that in a real-world situation energy consumption must be considered against a level of service, such as the number of round trips or the number of seat-miles provided in a day's operation. If an energy conservation measure significantly increases the round trip time for a route, then the need to add cars or trains to provide the same level of service may well cancel out the energy savings gained on a per-car basis.

TABLE 4-6. ENERGY CONSUMPTION SUMMARY.

Parameters	Profile	Orange Line (P3 Controller Position)	Orange Line (P4 Controller Position)	Blue Line 1st trip	Blue line 2nd trip
Car Type		-----Orange Line-----		-- Blue Line --	
Distance (mi)		21.83	21.81	9.96	9.96
Max. Speed (mi/h)		40	40	44	44
Trip Time (h:min:s)		1:04:23	1:03:52	--	--
Run Time (h:min:s)		0:52:53	0:52:22	--	--
Dwell Time (h:min:s)		0:11:30	0:11:30	--	--
Avg. Run Speed (mi/h)		24.8	25.0	--	--
Avg. Trip Speed (mi/h)		20.3	20.5	--	--
Average Consumption kWh	'A' Car	92.4	96.5	63.9	66.8
	'B' Car	103.4	112.2	53.9	54.8
	Total	195.8	208.7	117.8	121.6
	Avg.	97.9	104.4	58.9	60.8
kWh/Car Mile		4.5	4.8	5.9	6.1

Figure 4-36 illustrates the trends of energy consumption with distance traveled over the Orange Line route, and compares P4 and P3 master controller operation. This shows where the most gains are to be realized on the route when operation is restricted to the P3 controller position.

For general interest and because of the commonality of major systems used in the two car types, comparative energy consumption data for the MBTA Blue Line vehicles¹ are also

¹ FRA/TTC-80/05, op. cit.

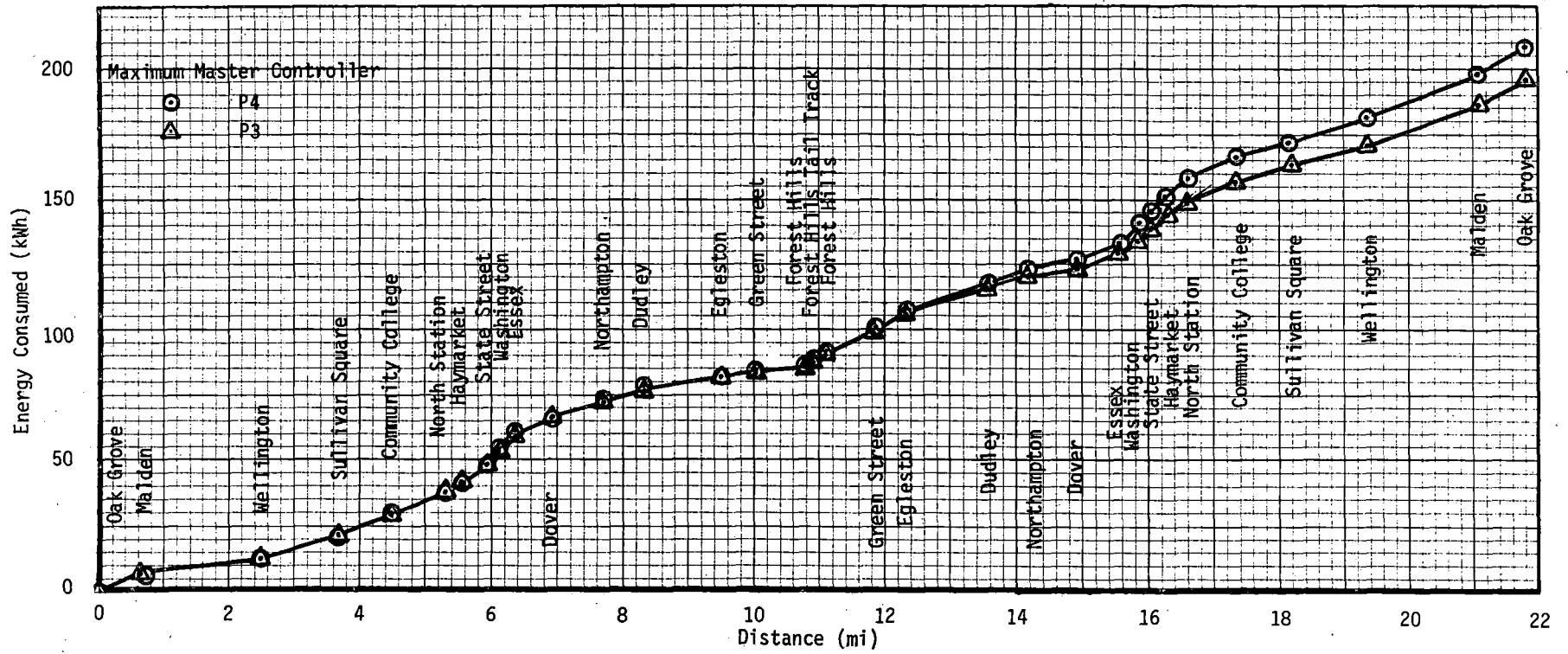


FIGURE 4-36 ENERGY CONSUMED BY A TWO-CAR TRAIN, ORANGE LINE ROUND TRIP SIMULATION.

presented in Table 4-6. The Blue Line cars were operated at a vehicle test weight of AW2; total train weight for the Blue Line energy consumption test runs was 139,180 lbs, compared to 180,880 lbs for the Orange Line cars.

Comparison of the operation of the cars on their own respective routes shows that the Blue Line operation uses more energy. Ignoring vehicle weight differences, the Blue Line simulation used 25 percent more energy on a kilowatt hour per car-mile basis than the Orange Line. Comparison of the two routes shows that the Blue Line route is more demanding; an average of 2.1 station stops per mile compared to 1.47 for the Orange Line could account for the Blue Line's higher energy needs.

DUTY CYCLE

Objective

The objective of the test was to determine the equilibrium temperatures of the vehicles' brake shoes when operated in a friction-only braking mode over a duty cycle simulating revenue service conditions.

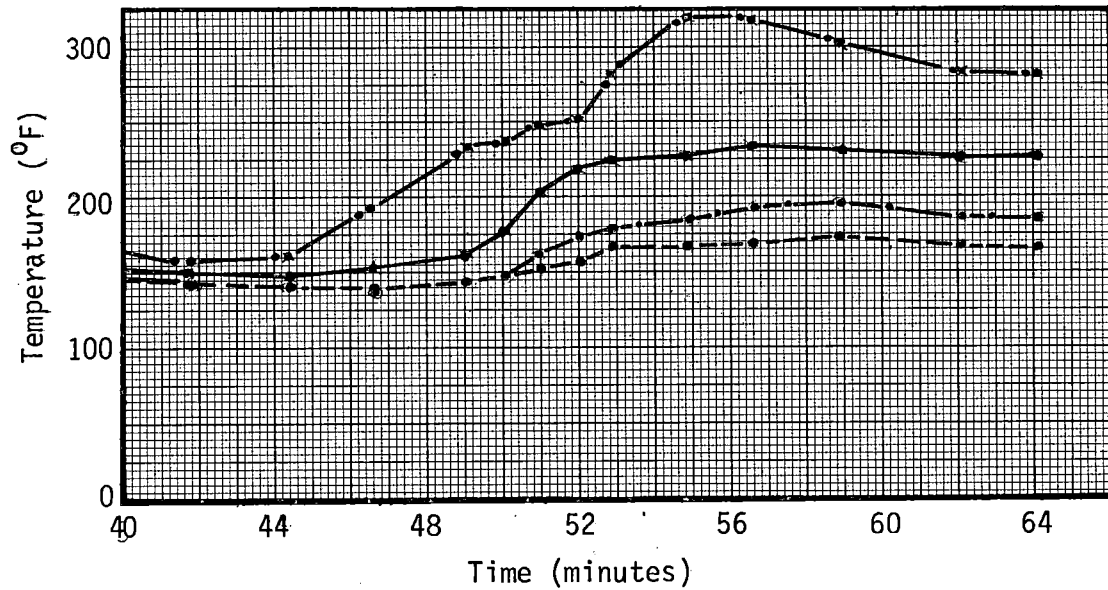
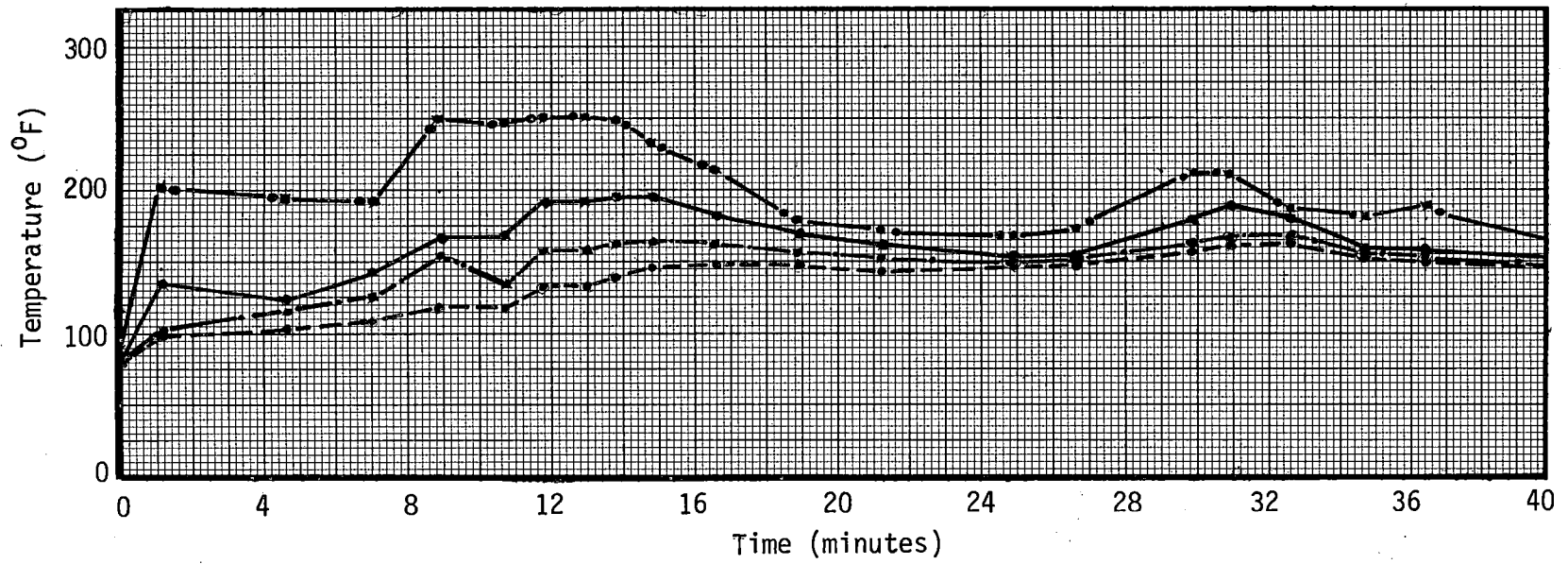
Test Method

Cars 01208 and 01209 were loaded to an AW4 vehicle weight and driven over a revenue service profile simulating a round trip on the MBTA Orange Line, from Oak Grove to Forest Hills and return. The details of the profile are to be found in Appendix B; the distances between station dwell times are identical with those of the Orange Line; the gradients differed, and were therefore not representative. The cars were operated using full power to accelerate to the required speeds and full service braking for the station stops; en route speed adjustments were made at the motorman's discretion to maintain the required maximum speed in any section. The cars were operated with their dynamic braking systems inoperative.

Each brake shoe on the left-hand side of car 01209 was instrumented with a Chromel-constantan thermocouple mounted in a hole drilled through the side of the shoe, so that it was positioned approximately 1/8" from the rubbing surface of the shoe. The outputs from the thermocouples were recorded using a data logger, which collected data immediately after each station stop. Elapsed time and cumulative distance measurements were also recorded from the ninth wheel instrumentation system.

Results

The temperature trends of the brake shoes on car 01209, with respect to elapsed time during operation over the revenue service profile, are shown in Figure 4-37. Corresponding distance data, together with the station stop names, are tabulated in Table 4-7. Correlation of the Figure 4-37 time history temperature data with Table 4-7 will allow the reader



Legend:

- Axle 1
- Axle 2
- Axle 3
- Axle 4

Notes:

- AW4 Weight
- Brake Shoes of Car 01209, Left Side
- Orange Line Revenue Profile Simulation (Round Trip)
- Friction-Only Braking

FIGURE 4-37 BRAKE SHOE TEMPERATURE TIME HISTORIES DURING ORANGE LINE DUTY CYCLE.

TABLE 4-7 THE ORANGE LINE ROUND TRIP, RECORDED TIMES AND DISTANCES.

Station Name	Cumulative Distance (ft)	Station/Station Distance (ft)	Cumulative Time (min)
Oak Grove	0	0	0
Malden	4,050	4,050	1.2 *
Wellington	13,180	9,130	4.6
Sullivan Sq.	19,500	6,320	7.05
Community Coll.	23,850	4,350	8.8
North Sta.	28,060	4,210	10.7
Haymarket	29,470	1,410	11.8
State	31,350	1,880	13.0
Washington	32,280	930	13.8
Essex	33,630	1,350	14.8
Dover	36,500	2,870	16.6
North Hampton	40,820	4,320	18.9
Dudley	43,950	3,130	21.2
Egleston	50,250	6,300	24.9
Green	53,060	2,810	26.6
Forrest Hills	57,000	3,940	29.0
Tail Track	57,570	570	29.9
Forrest Hills	58,340	770	32.6
Green	62,260	3,920	34.7
Egleston	65,090	2,830	36.4
Dudley	71,540	6,450	41.8
North Hampton	74,730	3,190	44.4
Dover	78,770	4,040	46.6
Essex	82,180	3,410	49.1
Washington	83,640	1,460	50.1
State	84,710	1,070	51.0
Haymarket	86,010	1,300	52.0
North Sta.	87,280	1,270	52.9
Community Coll.	91,620	4,340	54.9
Sullivan Sq.	95,980	4,360	56.6
Wellington	102,170	6,190	58.9
Malden	111,440	9,270	62.1
Oak Grove	115,150	3,710	64.1

MBTA No. 12 ORANGE LINE

* Times quoted are arrival times.

to assess the most arduous parts of the revenue service profile simulation. It can be seen from the temperature data that the thermocouple located on axle #3 indicated temperatures up to 100° F higher than those of any other axle. This thermocouple gave erratic temperature readings throughout the test program; the data for the axle #3 brake shoe are, therefore, suspect and have been discounted in the following test results discussion. An electrical checkout of the thermocouple and its data channel failed to locate the reasons for its erratic behavior and the higher-than-average temperature indications.

Brake shoe temperatures during the revenue service profile run stabilized in the 150° to 200° F range except for the last 12 minutes of the return trip, when the axle #1 brake shoe temperature increased and stabilized within the 225° to 235° F range. The reason for this increase is not readily apparent, particularly since axle #1 was lead axle for the initial, out-bound part of the profile and the trailing axle for the return trip. In this case, weight transfer effects could be expected to decrease the brake cylinder pressures slightly on axles #1 and #2 and correspondingly increase them on axles #3 and #4 during the return trip, producing the opposite trend. The general ranges of temperatures recorded, however, give no cause for concern when operating the vehicles over the Orange Line route in a friction-only braking mode, at the maximum speeds listed in the profile simulation. At the time of the test ambient temperature was 50° F, with 28 percent humidity and 10 mi/h wind speed.

5 Ride Quality Tests

The overall objective of the ride quality testing was to assess the quality of ride for a typical passenger. Vehicle vibration levels were compared to International Organization for Standardization (ISO) guidelines.² This publication gives provisional guidance for the acceptable human exposure to whole-body vibration, and suggests vibration limits for preserving comfort, working efficiency, and safety/health. In this instance the limits for preserving comfort were used, which are defined in the ISO guideline as the 'reduced comfort boundaries'. This standard defines and gives numerical values for limits of exposure to vibration levels transmitted from solid surfaces to the human body in the frequency range 1 to 80 Hz. In the transport situation, the reduced comfort boundary is related to difficulties of carrying out such operations as eating, reading, and writing.

For the analysis, the vibrations of the floor of the car were assumed to apply directly to the feet of a standing passenger, and because of the rigid nature of the seats, to the buttocks of a seated passenger. In this analysis angular vibrations have not been addressed. To compare the vibration signals with 'reduced comfort boundaries' the acceleration signals were processed into one-third octave bands; ISO 2631 addresses vibrations in the frequency range 1 to 80 Hz, based on acceleration intensities expressed as rms levels of the 20 one-third octave bands within that range. One-third octave analysis was also performed on frequencies below this range, in the area associated with motion sickness, or kinetosis (0.1 to 1.0 Hz).

One-third octave band vibration levels were synthesized from the data using the spectrum produced by the Fast Fourier Transform algorithm. The analysis was carried out using a spectrum analyzer, controlled by a desktop computer. By comparing the one-third octave band levels against the reduced comfort boundaries of the ISO 2631 standard, an exposure time for each band was produced. The band level which represents shortest exposure time gives the criterion for the reduced comfort level.

In addition, a single number characterization of the vibration level for a particular time segment was produced by frequency-weighting the signal with an analog filter network and computing the root mean square (rms) value. This has been termed the 'ride roughness' value and is addressed in ISO 2631 as a second method of considering ride quality. The weighted rms level of a signal was applied to a curve of ride roughness

² Guide for the Evaluation of Human Exposure to Whole-body Vibration,
ISO 2631-1974, International Organization for Standardization.

versus reduced comfort exposure time (Figure 5-1). Reduced comfort exposure times produced by this method are generally shorter than those obtained by the one-third octave band analysis. The method provides a convenient means of characterizing long sections of track, but provides no information on vibration frequency content. Detailed information of the data analysis is contained in Appendix A.

Vibration levels were recorded from eight servo accelerometers mounted on free standing bases. The bases rested on three sharp pins which provided solid contact with the floor of the car. They were located above the leading and rear trucks, and

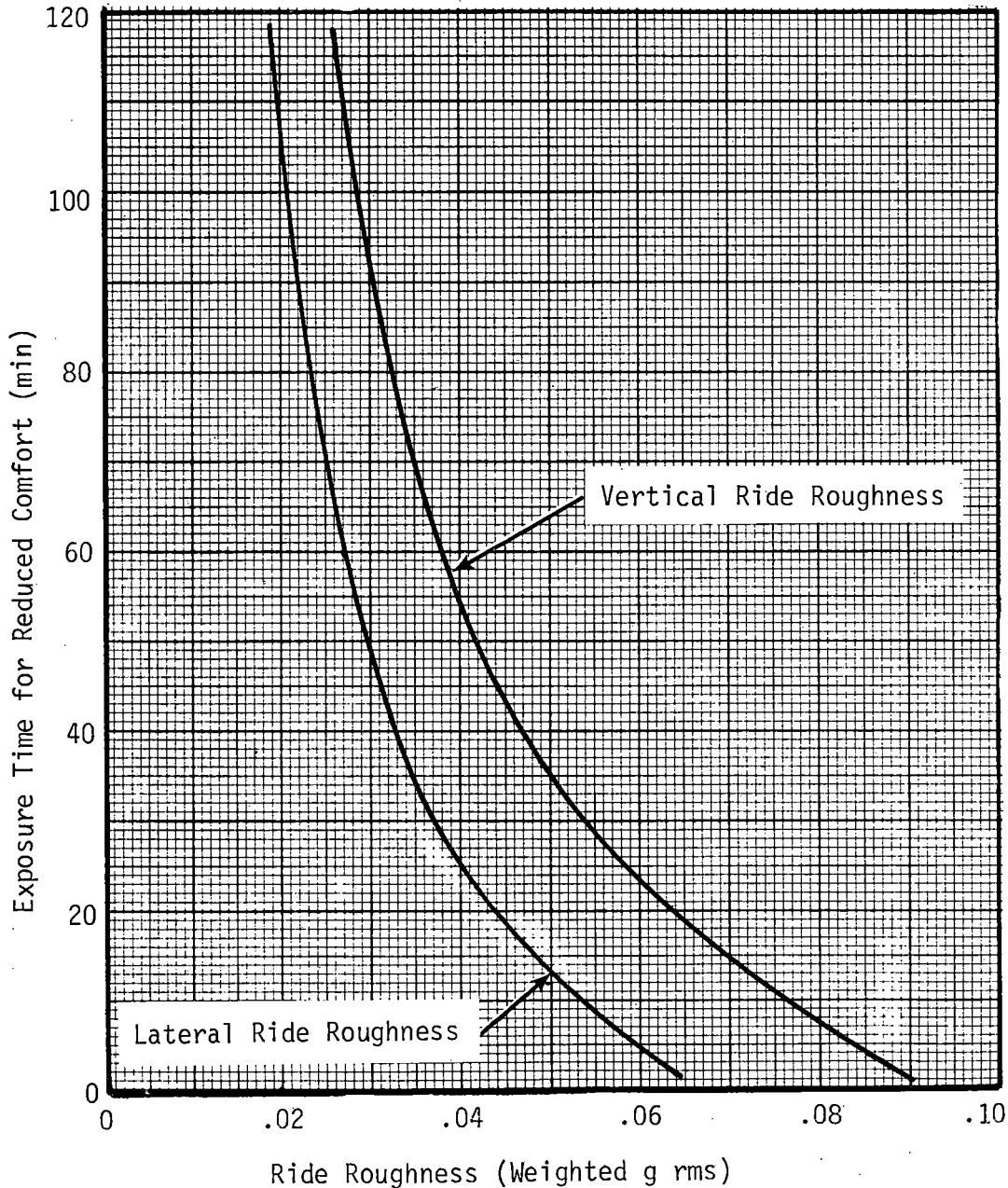
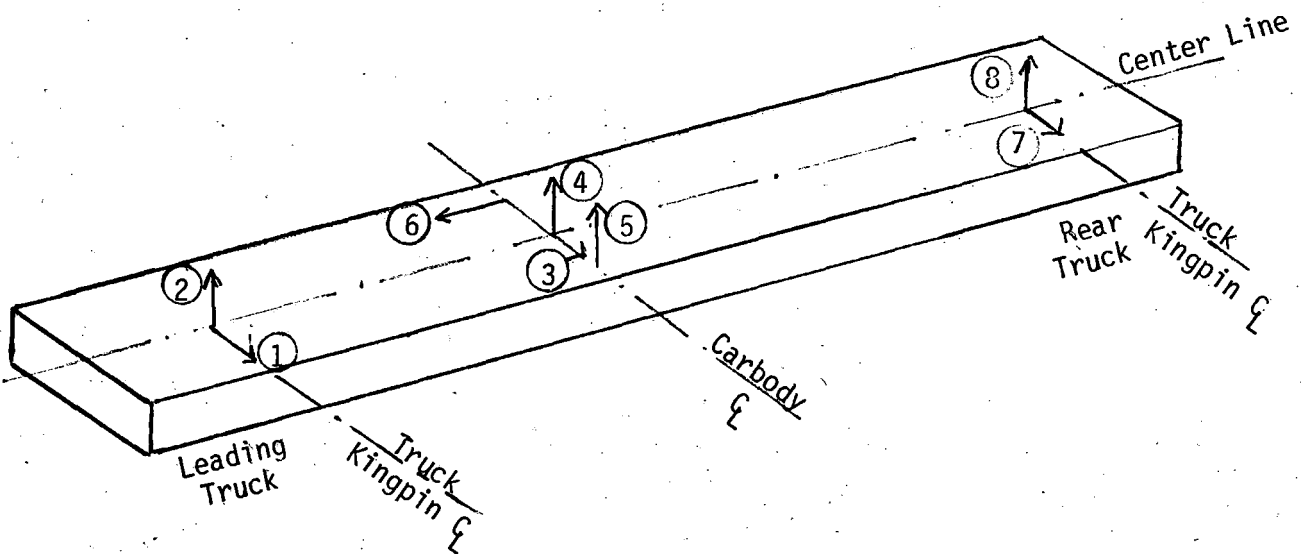


FIGURE 5-1 RIDE ROUGHNESS VS REDUCED COMFORT EXPOSURE TIME (ISO 2631).

in the center of car 01209 (Figure 5-2). The forward, mid, and rear positions each had vertical and lateral accelerometers on the vehicle centerline (longitudinal axis). In addition, the mid position had a vertical accelerometer on the left of the car and a longitudinal accelerometer on the right. The electrical output of each accelerometer was monitored on strip charts and FM-recorded on magnetic tape.



Legend:

- | | |
|---------------------------------|------------------------------|
| ① Forward, centerline, lateral | ⑤ Mid, left, vertical |
| ② Forward, centerline, vertical | ⑥ Mid, right, longitudinal |
| ③ Mid, centerline, lateral | ⑦ Rear, centerline, lateral |
| ④ Mid, centerline, vertical | ⑧ Rear, centerline, vertical |

FIGURE 5-2 CARBODY ACCELEROMETER LOCATIONS.

The ride quality was assessed in the following areas:

- Component-induced vibration.
- Comparison of ride quality to ISO 2631 reduced comfort boundaries.
- Effect of vehicle speed and weight.
- Effect of track section.
- Effect of acceleration and braking.
- Low frequency ride, associated with motion sickness.
- Comparison of the Orange and Blue Line vehicle ride quality.

A vehicle loading of AW3, representing a rush hour passenger load, was chosen as the main area of analysis. Lead weights

were distributed uniformly over the floor area to simulate the passenger load. The lead weights modified the behavior of the car somewhat; (actual passengers behave as damped sprung masses, and have a higher center of gravity). However, the general conclusions of the ride quality tests are still acceptable.

COMPONENT-INDUCED VIBRATION

Objective

To determine the carbody vibration levels arising from the operation of the auxiliary equipment.

Test Method

The vehicle was tested while stationary on level track. Five combinations of auxiliary equipment (motor generator set, air compressor, and evaporator fan) were tested and the accelerations of the floor were recorded on strip charts after low-pass filtering at 100 Hz. Also, all equipment was operated during door cycling for maximum component-induced vibration levels.

Results

Component-induced vibration levels were, at most, 0.002 g peak with the prime excitation occurring in the vertical direction. The Orange Line specifications state that for frequencies up to 60 Hz, lateral and vertical vibration should not exceed 0.04 g peak due to operation of the equipment or auxiliaries³. The levels due to undercar equipment were less than one-twentieth those specified; transients obtained during door cycling were also below the criterion, reaching a maximum of 0.02 g peak, or one-half the equipment specification level. Since the component-induced vibration levels were so low in comparison to the criterion, no further in-depth analysis was attempted.

COMPARISON OF RIDE QUALITY TO ISO 2631 REDUCED COMFORT BOUNDARIES

One-third octave band levels were compared against the ISO 2631 boundaries to evaluate the ride quality in relation to known exposure time limit criteria for reduced comfort. The data were taken from runs made on the tangent part of track section III to obtain values representative of general revenue operation.

The longitudinal and lateral ride of the vehicle, at the forward, mid, and rear of the car was excellent. In general, throughout the speed range, all one-third octave band levels

³ "Rapid Transit Car Procurement Technical Specifications", Massachusetts Bay Transportation Authority, (August 1976).

were lower than the 8-hour reduced comfort boundary. Figures 5-3 and 5-4 show the one-third octave band levels at 62 mi/h, AW3 weight, at the lateral and longitudinal accelerometer locations. Acceleration levels were a maximum of 0.01 g rms across the frequency bands.

The upper plot of Figure 5-5 shows the weighted and unweighted Fourier spectrum for the lateral direction at the forward location, and illustrates the effect of frequency-weighting the data to whole-body vibration criteria. The spectrum shows, in this case, that only the frequencies in the range 0 to 5 Hz are significant to passenger comfort.

The vertical ride of the car was characterized by a vibration, in the 10 Hz center frequency band, which dominated all other ride quality trends. The 10 Hz vibration was worse at the center of the car; for example, at 62 mi/h, Aw3 vehicle weight, the vibration level at that center frequency fell on the 25-minute reduced comfort boundary. This represents a vibration level of 0.1 g rms at the 10 Hz center frequency (see Figure 5-6). At 36 mi/h the 10 Hz level was much less severe, at 0.02 g rms (also Figure 5-6).

The vertical ride of the car over the trucks was somewhat improved compared to the center of the carbody. The 10 Hz frequency band predominated with levels approaching the 1-hour reduced comfort boundary at 62 mi/h, or a level of 0.04 g rms at that frequency. Figure 5-7 illustrates the frequency trends at 62 mi/h over the front and rear trucks.

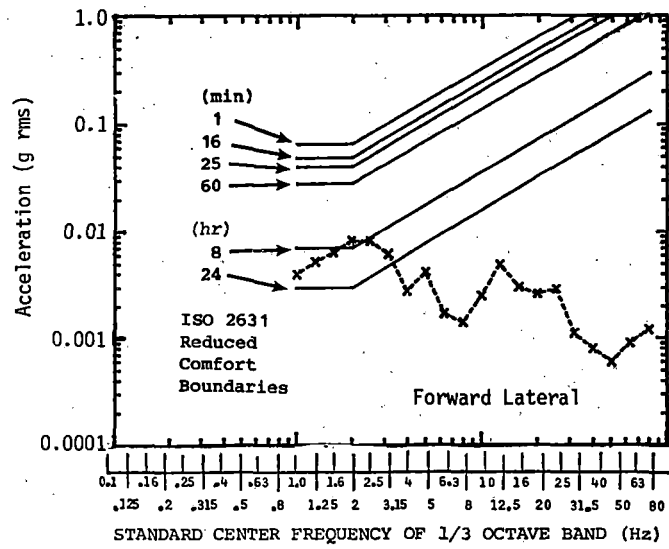
The lower plot of Figure 5-5 shows the weighted and unweighted Fourier spectrum for the vertical direction at the midcar location. The spectrum shows that in this case only the frequencies 0 to 15 Hz are significant in relation to passenger comfort.

Considering the data in weighted, time-history format, Figure 5-8 shows peaks with magnitudes ranging near 0.1 g rms for the vertical direction, midcar at 62 mi/h, AW3 weight. The data were processed using a 1-second rms averaging time. The time history shows a varying vertical acceleration level occurring over a 40-second period.

The high vertical vibration levels are most likely produced by forced harmonic vibration of a body bending mode. Should the excitation of this mode on the Orange Line track be greater than that at the TTT then the ride quality would be worse.

Comparison of the one-third octave band levels to the ISO guidelines shows the following:

- At all vehicle loadings and at speeds up to 60 mi/h, the lateral and longitudinal ride of the vehicle was excellent.



NOTE:
 ● 62 mi/h
 ● AW3 Weight

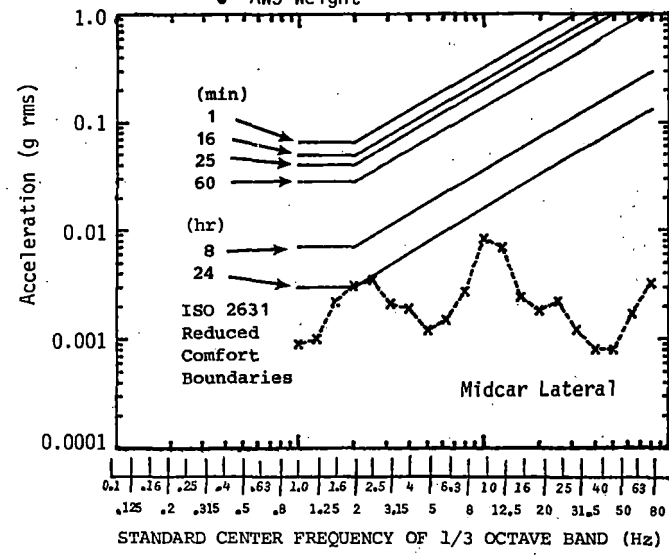
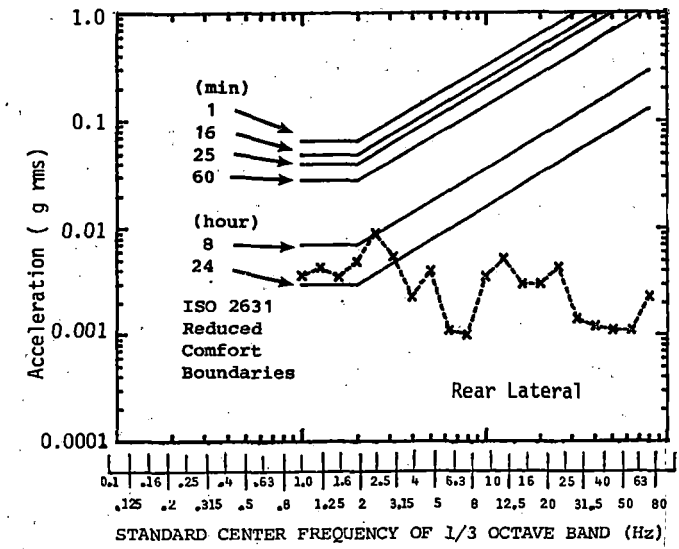


FIGURE 5-3



NOTE:
 ● 62 mi/h
 ● AW3 Weight

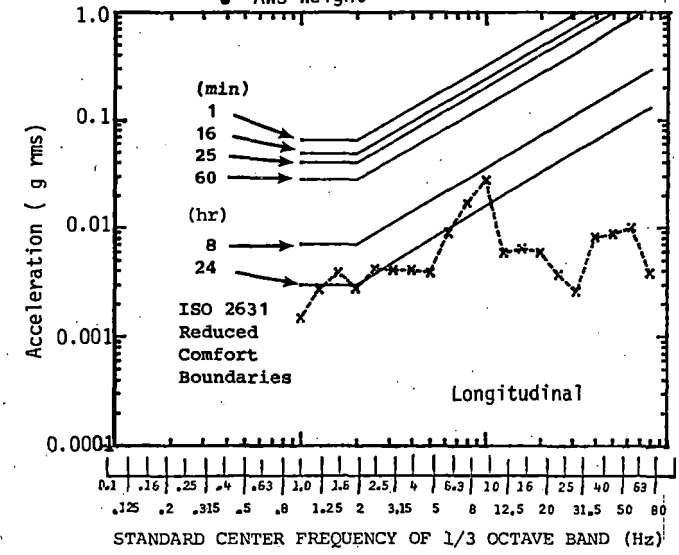


FIGURE 5-4

1/3 OCTAVE BAND VIBRATION LEVELS.

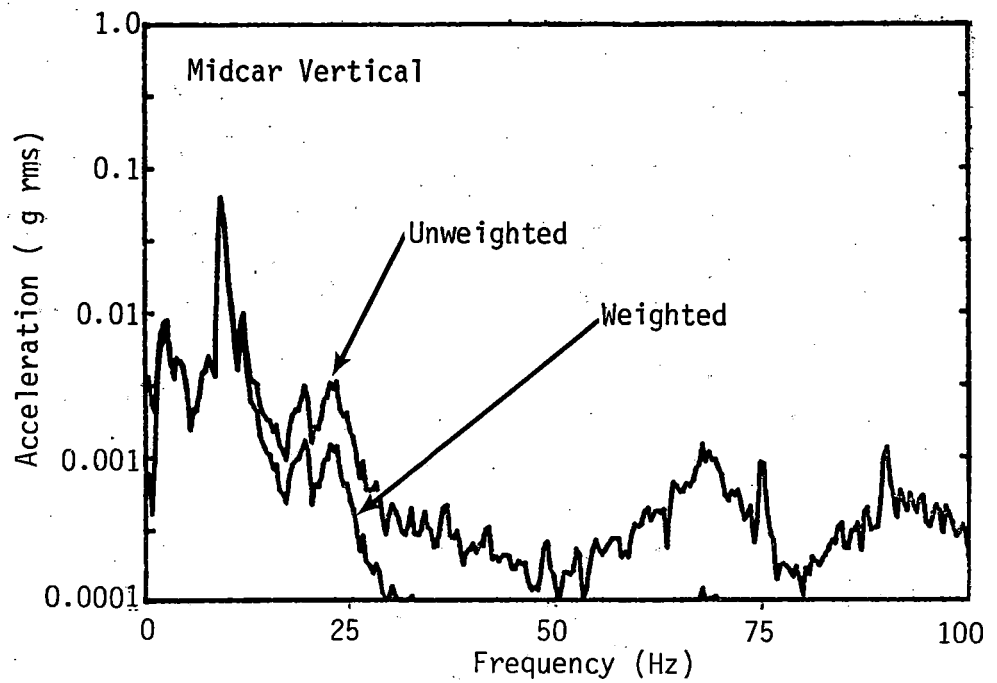
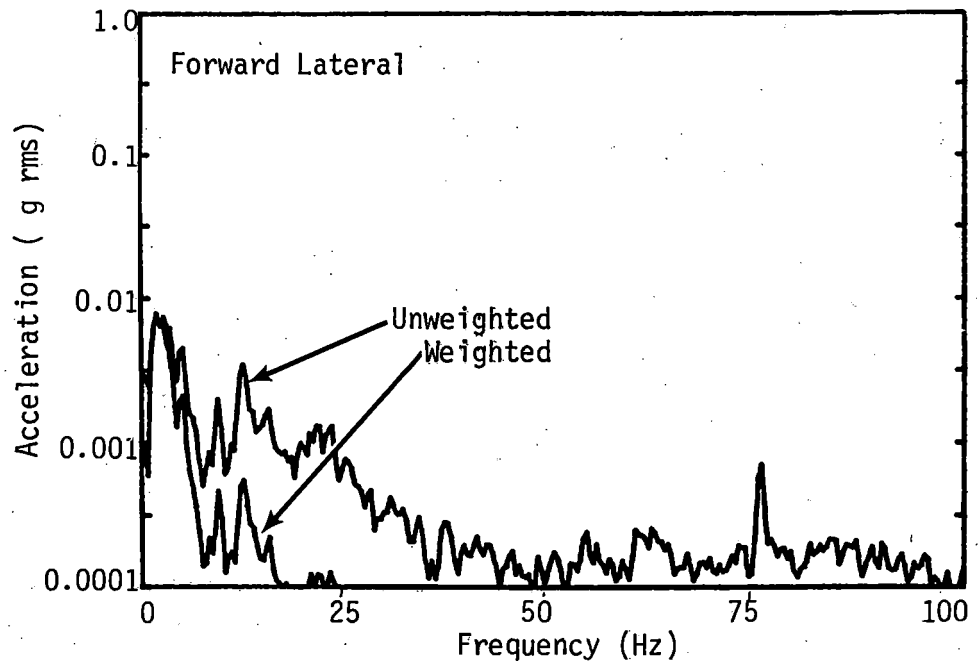
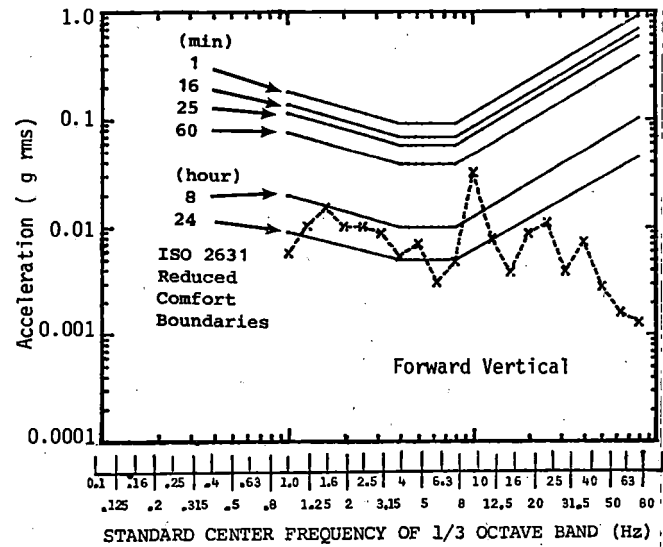
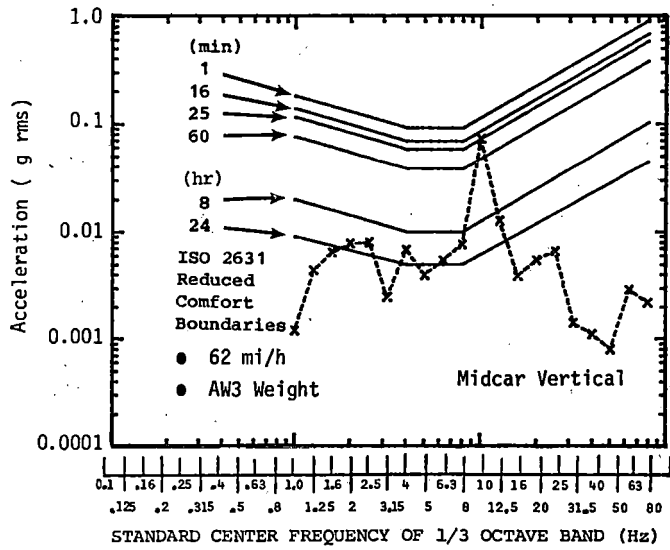


FIGURE 5-5 EFFECT OF ISO FREQUENCY-WEIGHTING APPLIED TO LATERAL AND VERTICAL SPECTRA.



8-9

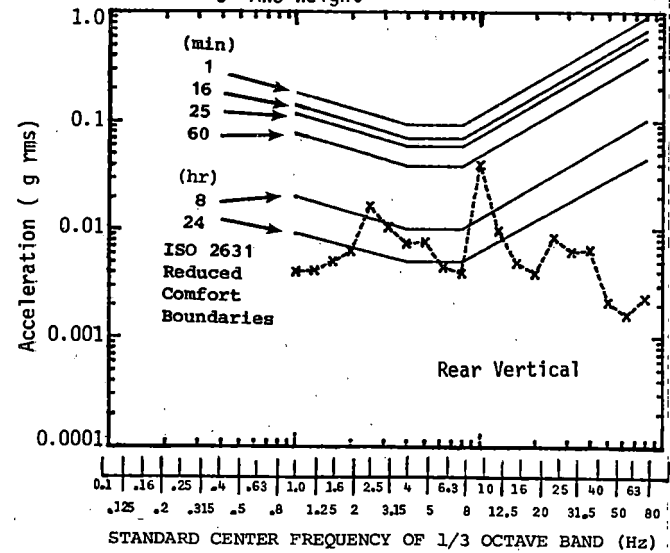
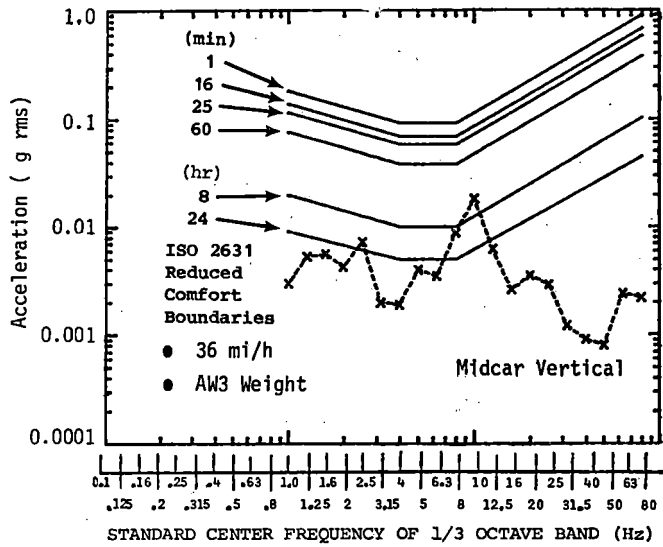
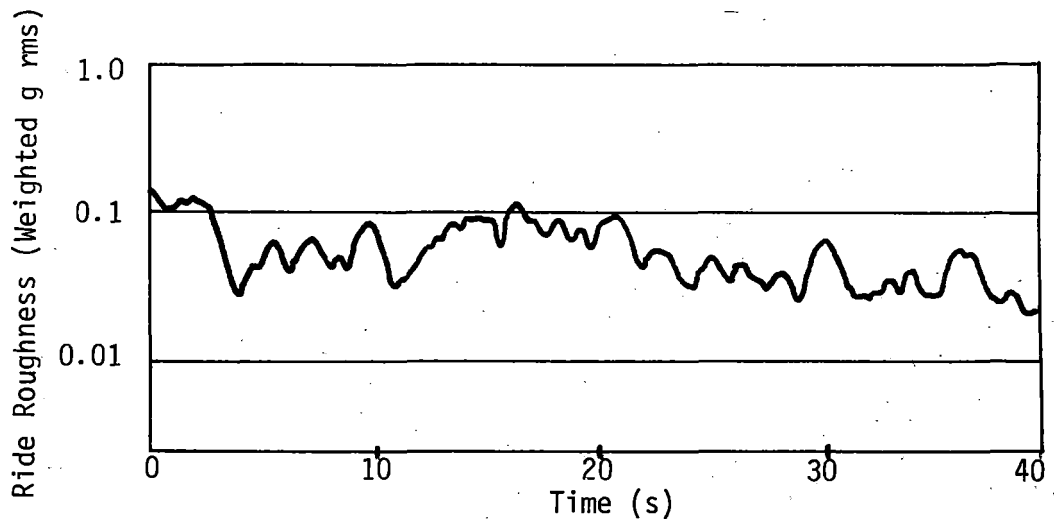


FIGURE 5-6

FIGURE 5-7

1/3 OCTAVE BAND VIBRATION LEVELS.



NOTE:

- Track Section III, Stations 25.5 to 28
- .1-second Average Window
- 62 mi/h
- AW3 Weight

FIGURE 5-8 RIDE ROUGHNESS TIME HISTORY, MIDCAR VERTICAL.

- At high vehicle loadings and at high speed, the vertical ride, particularly in the center of the car, was very poor, due to a dominant 10 Hz vibration.
- The TTT provides a very low level of excitation, due to the high quality of its track; revenue service track conditions may excite the 10 Hz vertical mode, even more than demonstrated in these tests, and provide an unacceptable ride.

EFFECT OF CONSTANT VEHICLE SPEEDS AND VEHICLE LOADING ON RIDE QUALITY

Objective

To determine the effects of vehicle speed and loading on ride quality.

Test Method

The vehicle was slowly accelerated on the tangent track in section III, stations 30 to 33. Unweighted accelerometer signals produced on strip charts were visually examined to determine the 'worst speeds' relative to adjacent speeds. The worst speeds were chosen, based on the 'blossoming' of accelerometer traces, as follows:

Vehicle Weight	AW0	AW3	AW4
		17	17
	24	24	24
	35	36	35
Worst	46	44	45
Speeds	48	48	48
(mi/h)	54	52	54
	57	57	57
	60	62	61

Test runs were then made maintaining these speeds through the test section. Data were recorded from all accelerometers; subsequent playback of the data through the appropriate weighting network and rectifying circuit (to produce a ride roughness time history) showed that as far as passenger comfort was concerned, the vehicle had no significant 'worst speeds'. The speeds selected were therefore representative of the vibration levels throughout the speed range.

To evaluate the effect of constant vehicle speeds, the averaged weighted rms ride roughness levels were calculated for a 20-second period for all accelerometer channels at all speeds at the AW3 loading. The time history data were weighted using the appropriate analog filter networks for vertical or lateral ride and were then processed in the frequency domain using the spectrum analyzer. The averaging function of the machine was used to obtain frequency spectra representative of the total time history. These spectra were then converted into a power spectral density presentation using the HP-85 desk top computer. A single average rms level was then calculated from the square root of the area under the power spectral density plot. Average values for each speed were compared to the values at 17 mi/h on a percent-change basis.

To evaluate the effect of vehicle loading, similar ride roughness levels were calculated, again for a 20-second period, for three of the speeds--24, 35, and 60 mi/h--for the vehicle loadings of AW0 and AW4.

Results

At AW3 loading, lateral and longitudinal ride roughness levels were low, even at the highest speed tested. However, vertical levels were very much higher, showing a steady increase with speed, with the highest levels occurring at the midcar vertical location. Table 5-1 shows the percent change of ride roughness levels relative to the lowest speed (17 mi/h). The table illustrates the vertical acceleration trends with speed. The lateral and longitudinal levels show a similar (though not as strong) trend. At 62 mi/h, the midcar vertical ride was poor, reaching a ride roughness value of 0.06 g rms.

Figure 5-9 shows the ride roughness levels, plotted against speed, for the forward car lateral location and midcar vertical location, and shows the strong relationship between speed and ride roughness.

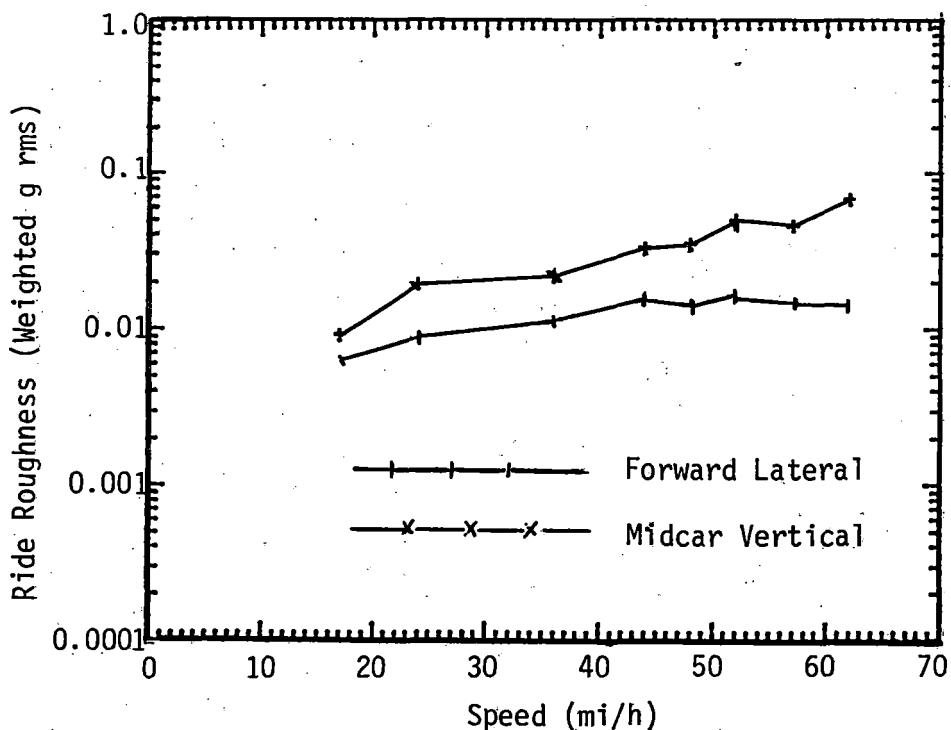


FIGURE 5-9 RIDE ROUGHNESS LEVELS, VARIATION WITH SPEED, AW3 WEIGHT.

TABLE 5-1. PERCENT CHANGE IN RIDE ROUGHNESS LEVEL DUE TO CHANGE IN SPEED (AW3 WEIGHT).

Speed (mi/h)	17	24	36	44	48	52	57	62
	Ride Roughness (g rms)	%	%	%	%	%	%	%
Fwd Vert.	0.0123	+18	+64	+106	+110	+150	+160	+210
Mid Vert.	0.0092	+112	+139	+262	+283	+443	+389	+640
Mid Left Vert.	0.0093	+82	+119	+214	+260	+328	+278	+532
Rear Vert.	0.0112	+32	+87	+152	+150	+221	+198	+291
Fwd Lat.	0.0059	+44	+80	+137	+122	+147	+142	+137
Mid Lat.	0.0051	+6	+16	+35	+37	+41	+47	+49
Rear Lat.	0.0064	+34	+72	+142	+94	+94	+75	+86
Longitudinal	0.0083	-2	+28	+42	+43	+53	+51	+47

The effect of vehicle loading on ride roughness is shown by the data in Table 5-2. The AW4 ride roughness data at three vehicle speeds are expressed as a percentage change from the corresponding values at AWO weight. There is no consistent trend in the data. For the vertical vibration case, heavier loading reduced the ride roughness levels at the two lower speeds, but increased them at the high speed. The lateral direction showed the reverse of this trend.

TABLE 5-2. PERCENT DIFFERENCE OF AW4 RIDE ROUGHNESS VALUES FROM THOSE OF AWO WEIGHT.

Speed (mi/h)	24	35	60
	%	%	%
Fwd Car and Vertical	-12	-8	+27
Mid Car and Vertical	-3	-3	+109
Mid Car left Vertical	-30	-20	+68
Rear car and Vertical	-23	-12	+47
Fwd car Lateral	+17	+18	-13
Mid car Lateral	+4	-10	-35
Rear Car Lateral	+20	+9	-21
Longitudinal	+4	+5	-32

Figure 5-10 shows the ride roughness level for the midcar left vertical directions, plotted against speed, for the two loadings of AWO and AW4. As with other vertical directions, the plot shows a crossover of ride roughness trends at 43 mi/h. Figure 5-11 shows the Fourier spectrum of the midcar vertical acceleration for the two loadings at 62 mi/h. There was a reduction of level at frequencies from 25 to 60 Hz at the highest loading, perhaps due to the damping effect of the lead ballast used to simulate passenger loading.

In conclusion, passenger comfort deteriorated as speed increased, but the higher loading of AW4 over AWO did not produce a consistent trend in passenger comfort.

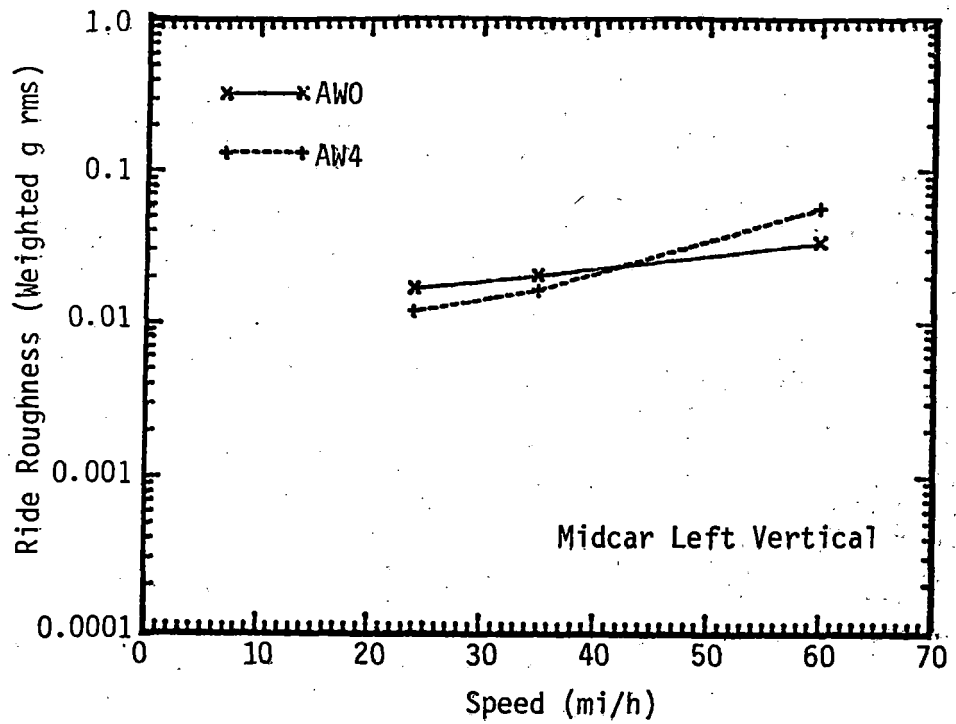


FIGURE 5-10 RIDE ROUGHNESS LEVELS, EFFECT OF 3 WORST SPEEDS.

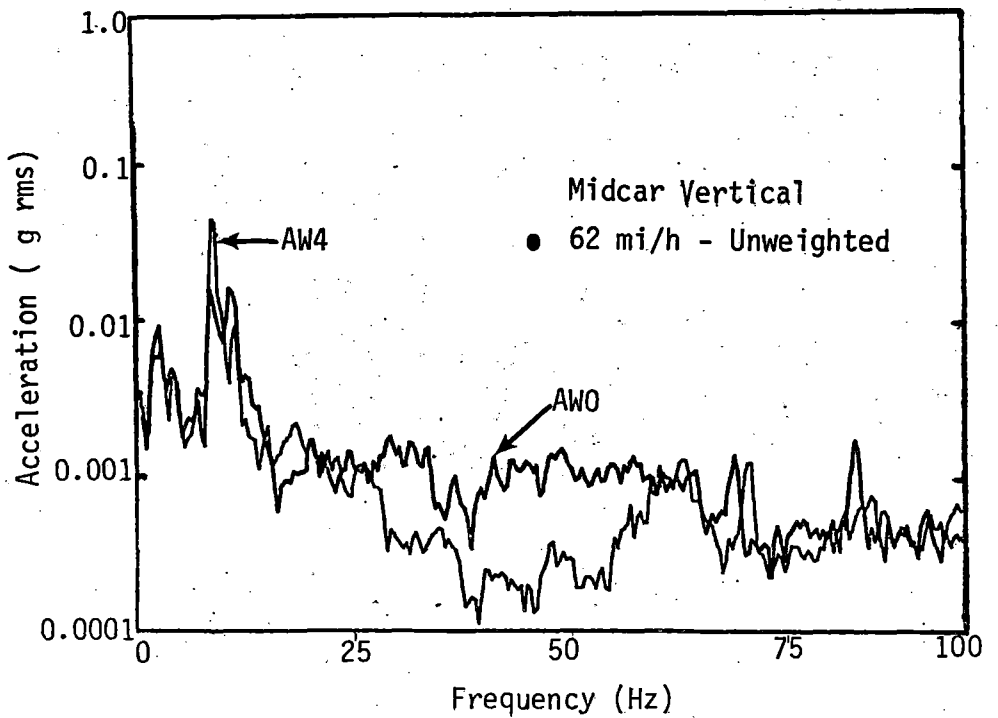


FIGURE 5-11 COMPARISON OF FREQUENCY SPECTRA AT TWO VEHICLE WEIGHTS.

EFFECT OF TRACK SECTION ON RIDE QUALITY

Objective

To determine the effect of track construction on ride quality.

Test Method

For each of seven track sections, ride roughness values, averaged over 20 seconds, were calculated for an AW3 weight vehicle at 62 mi/h. ISO 2631-weighted and rectified ride roughness time histories were also produced.

Results

The ride roughness level for each track section was calculated and an average for the seven sections was computed from the resulting values. The percentage differences between each track section and the average are shown in Table 5-3. The poorest vertical ride occurs on track section III, jointed rail with wood ties. The worst lateral and longitudinal ride occurs in track section I, welded rail with wood ties, and is probably caused by the perturbed track section at stations 11 to 15 of section I.

Figure 5-12 shows vertical and lateral ride roughness time histories for track section III; the data were weighted and rms-averaged over a 1-second time constant. The vertical levels are about 0.07 g but the lateral levels are lower at approximately 0.015 g. A similar time history for track section I is shown in Figure 5-13.

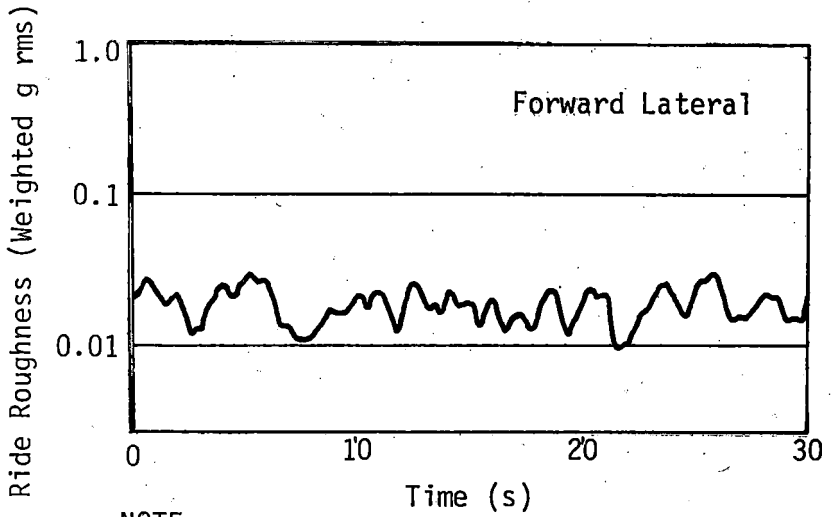
The lateral ride roughness time history for the perturbed track part of track section 1 shows fairly high transients caused by the perturbations (see Figure 5-13).

TABLE 5-3. PERCENT DIFFERENCES FROM AVERAGE RIDE ROUGHNESS LEVELS DUE TO EFFECT OF TRACK SECTION.

Track Section	I	II	III	IV	V	VI	VII	Average Ride Roughness(g rms)
Fwd Car and Vert	+18	+25	+27	-21	-27	-17	-6	0.0282
Mid Car and Vert	-13	+40	+62	-22	-22	-28	-15	0.0428
Mid Car L. Vert	-10	+32	+61	-22	-18	-28	-14	0.0389
Rear Car and Vert	+16	+19	+45	-20	-26	13	-11	0.0307
Fwd Car Lat	+13	-27	-3	-8	+19	-3	+9	0.0163
Mid Car Lat	+33	-9	-5	-24	+20	-10	-5	0.0090
Rear Car Lat	+40	-22	+11	-11	-24	-21	+25	0.0126
Longitudinal	+30	-1	+30	-12	-25	-26	+4	0.0103

Note:

62 mi/h
AW3 Weight



NOTE:

- Track Section III, Stations 25.5 to 28
- 1-second Averaging Window
- 62 mi/h
- AW3 Weight

51-9

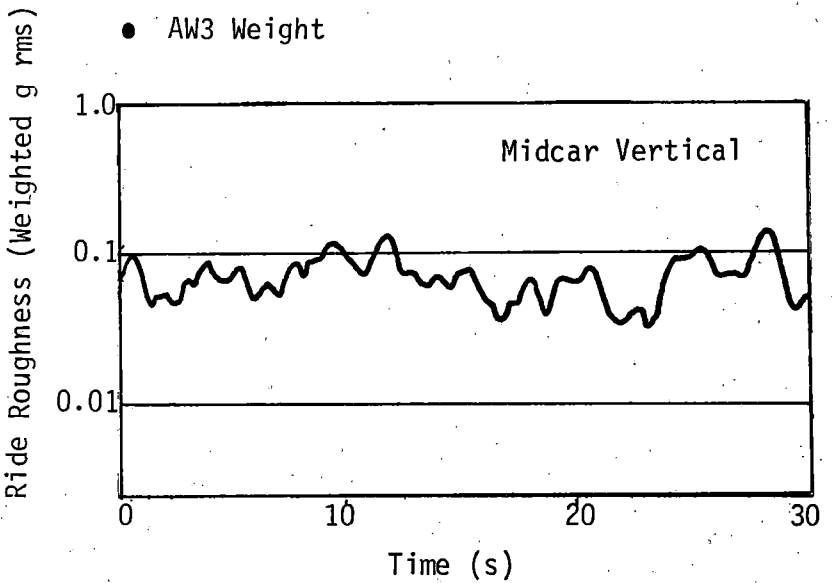
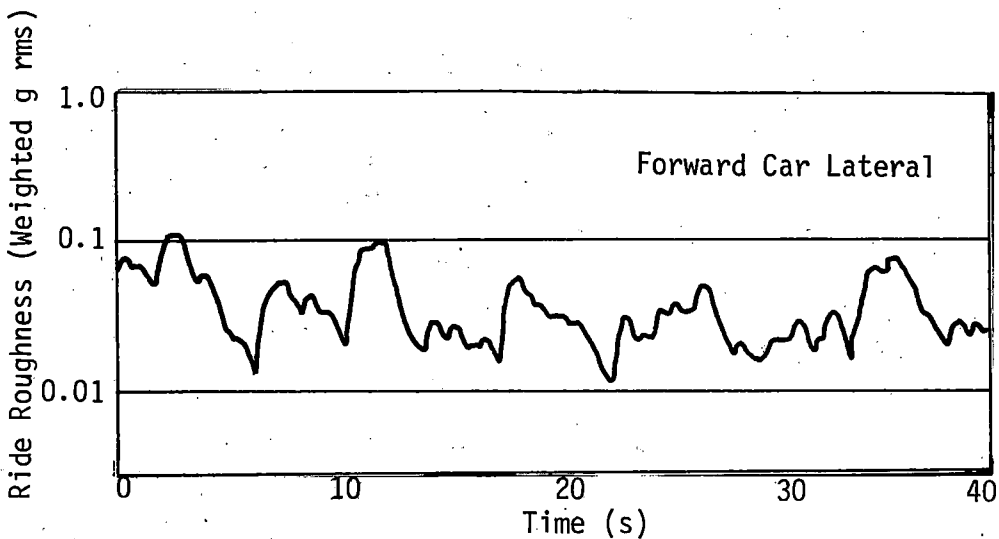


FIGURE 5-12 RIDE ROUGHNESS TIME HISTORIES.



NOTE:

- Track Section I, Stations 12 to 15
- 1-second Averaging Window
- 62 mi/h
- AW3 Weight

FIGURE 5-13 RIDE ROUGHNESS TIME HISTORY.

EFFECT OF ACCELERATION AND BRAKING ON RIDE QUALITY

Objective

To determine the most severe vibration levels encountered during acceleration and braking.

Test Method

Acceleration and braking tests were performed on the tangent track of section III, jointed rail with wood ties - stations 30 to 33, at AW3 vehicle weight. Accelerations were made at a P4 master controller setting from standing starts at station 30, with acceleration to a maximum speed of 58 mi/h at station 33. Braking tests using full service braking were conducted with the vehicle entering station 30 at 60 mi/h and braking to a complete stop.

Ride roughness time histories were produced for acceleration, blended braking, and friction braking from rectified and ISO 2631-weighted signals. Time histories were used, since the rapidly changing nature of acceleration and braking data is incompatible with one-third octave analysis or single-number vibration level characterization.

Results

In acceleration, vertical ride roughness levels increased gradually up to 0.03 g at 40 mi/h and remained constant thereafter. Lateral levels changed less uniformly, varying from 0.005 to 0.01 g during acceleration from 0 to 40 mi/h. Figure 5-14 shows both of these trends. Longitudinal acceleration levels were higher (0.02 g) in the 10 to 20 mi/h range than throughout the remainder of the speed range, where they were typically on the order of 0.006 g.

During braking, vertical and lateral ride roughness levels decreased gradually with speed, down from 0.03 and 0.008 g, respectively (Figure 5-15), however the longitudinal and midcar lateral levels did not decrease significantly until the vehicle came to a stop. Longitudinal levels for blended braking (0.015 g) were double the levels for friction braking.

For both acceleration and braking, vertical ride quality was smooth without significant transient motion; lateral levels were more transient (Figure 5-15). Acceleration and braking levels were similar to those for constant speeds, therefore it can be concluded that acceleration and braking have little effect on ride quality.

THE LOW FREQUENCY RIDE OF THE VEHICLE

The effects of vibrations in the frequency range less than 1 Hz are characteristically different than those frequencies affecting whole-body vibration, and are associated with motion sickness (kinetosis). These vibrations are not addressed by

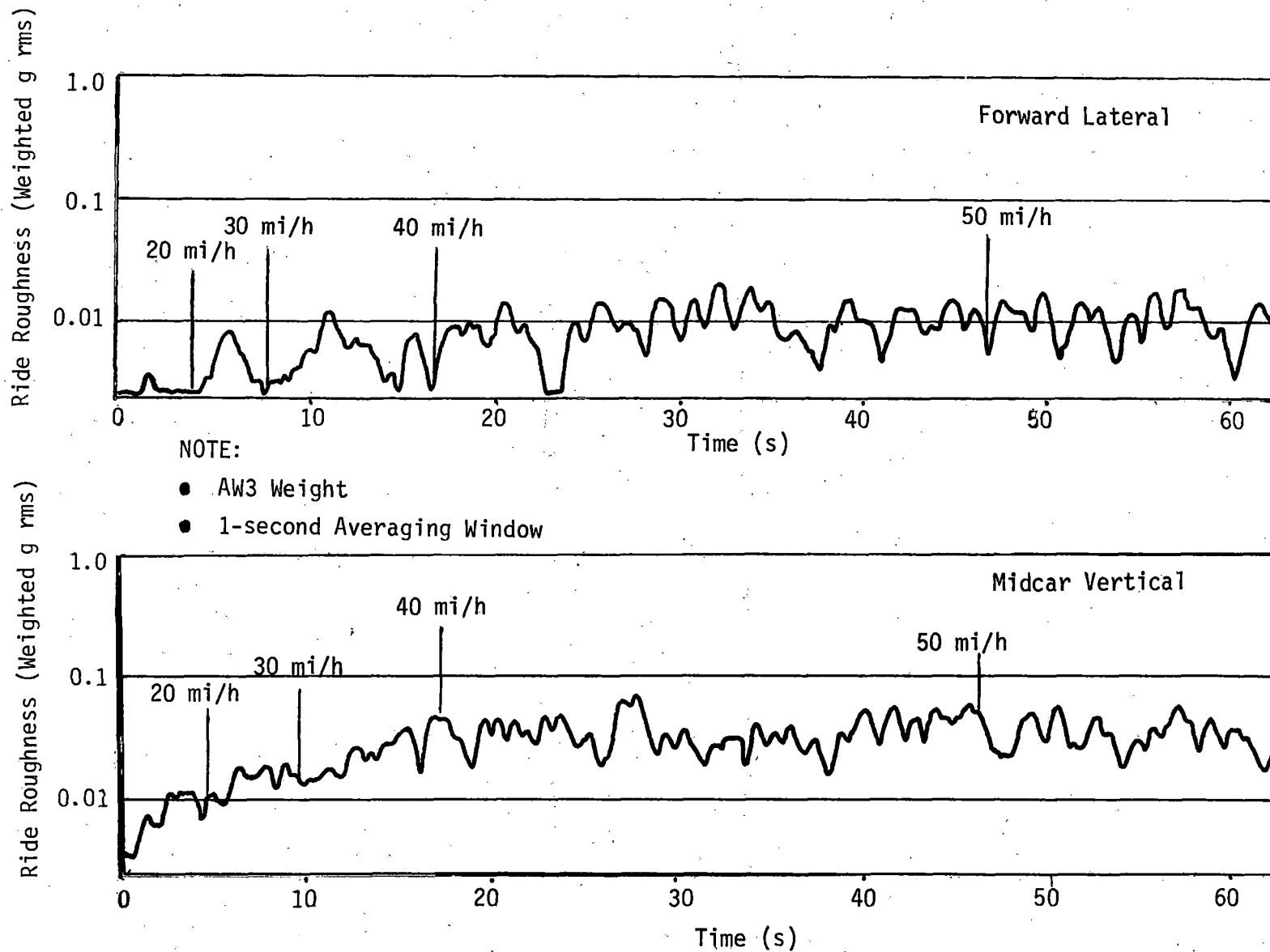


FIGURE 5-14 RIDE ROUGHNESS TIME HISTORIES, FORWARD LATERAL AND MIDCAR VERTICAL DURING ACCELERATION.

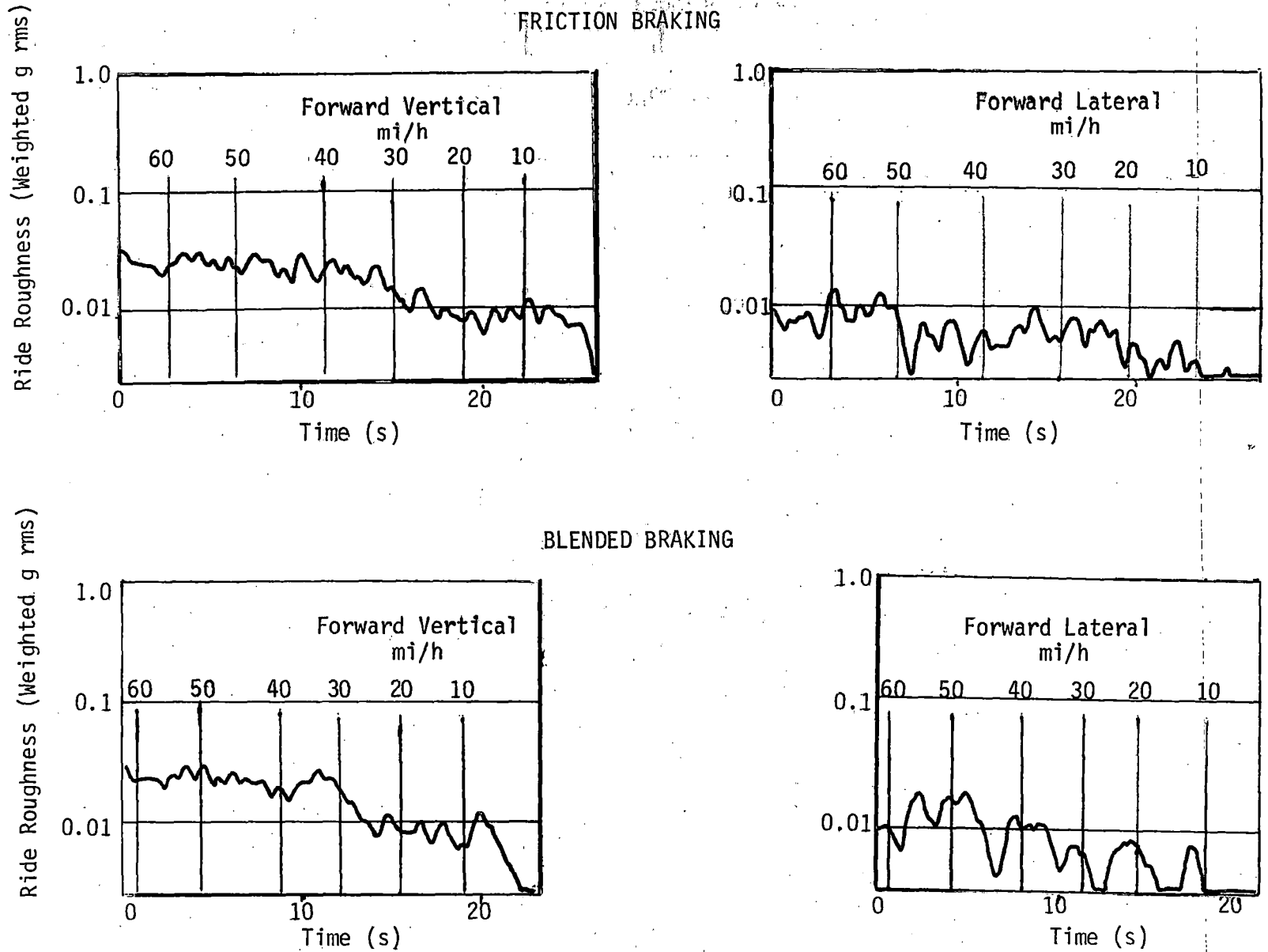


FIGURE 5-15 RIDE ROUGHNESS TIME HISTORIES DURING BLENDED AND FRICTION BRAKING.

ISO 2631, although it has been suggested⁴ that the constant comfort boundaries could be provisionally extended into this low frequency range, as shown by the broken horizontal lines in Figure 5-16 and 5-17. An alternate extension has been made by the use of boundaries of motion sickness incidence,⁵ shown in Figure 5-18; as with the ISO 2631 reduced comfort boundaries, these refer to one-third octave band levels.

Data from the Orange Line tests were processed into one-third octave bands with center frequencies from 0.1 to 0.8 Hz by synthesis from Fast Fourier analysis. Synthesis of one-third octave bands in this low frequency range required a data collection time of 250 seconds, and so the analysis was conducted on data collected with the vehicle making a circuit of the entire track.

Figures 5-16 and 5-17 show the forward car vertical, midcar vertical, forward car lateral and longitudinal vibration low frequency one-third octave bands, plotted with the higher frequency data. The data are from a circuit of the track at 62 mi/h, AW3 weight. Below 1 Hz center frequency the band levels are very low--in the region of 0.001 g rms. Referring to Figure 5-18 it can be seen that a minimum, 2 percent incidence of motion sickness requires a level of 0.02 g rms at a frequency of 0.2 Hz. Since the levels were of the order of one-twentieth of that magnitude in the motion sickness frequency band, we can conclude that motion sickness will not be a problem for the Orange Line cars.

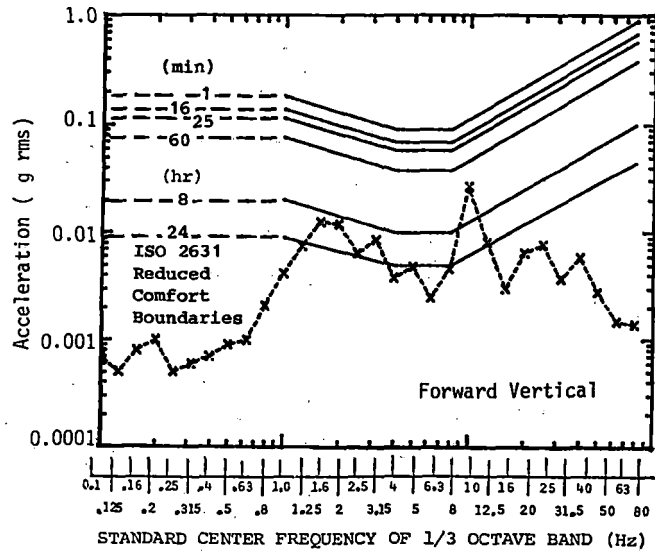
COMPARISON OF THE ORANGE LINE RIDE QUALITY TO THAT OF THE BLUE LINE

This section compares the ride of the Orange Line cars to that of a pair of Blue Line cars, tested on the TTT, in April/October 1979. The comparison has been limited to a vehicle weight of AW3 and the curved part of track section III. Of any sections tested, this section produced the greatest vertical accelerations on the Orange Line cars. Constant speed runs of 60 and 45 mi/h were used.

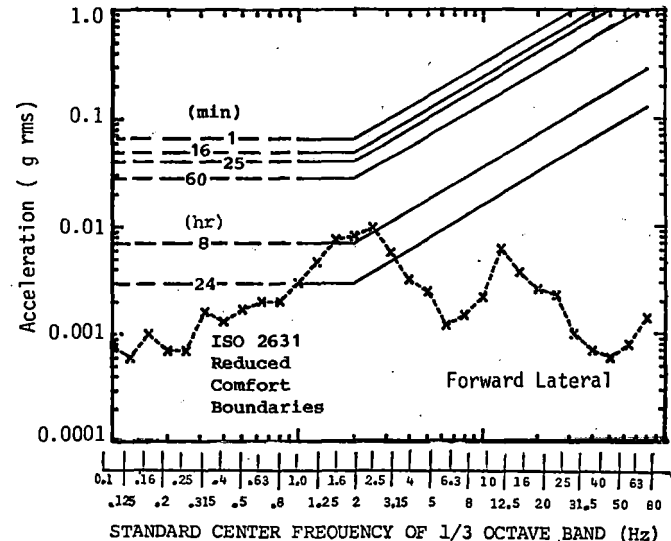
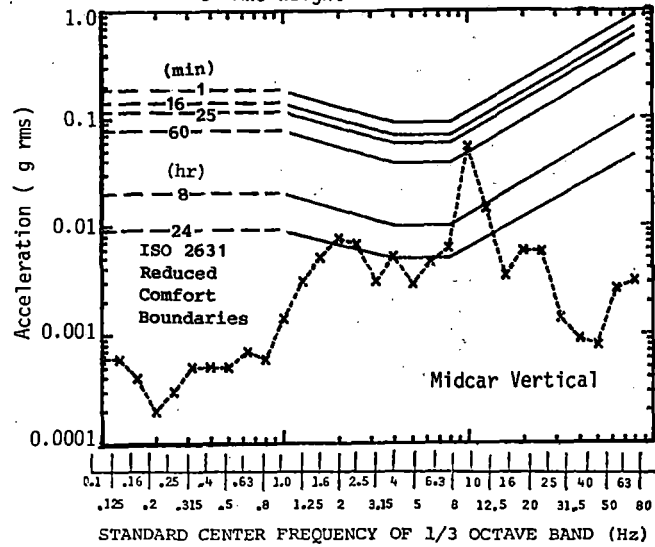
The Blue Line and Orange Line cars share a common modular approach to structural design, the principal differences between vehicles being that the Orange Line car is longer, with a correspondingly longer truck pivot spacing; it is also heavier and has a greater passenger load capability. Specifically, these differences are as follows:

⁴ Healey, A.J., "Digital Processing of Measured Vibration Data for Automobile Ride Evaluation," University of Texas at Austin, Austin, Texas.

⁵ Malone, W.L., and Vickery, J.M., Paper No. N76-16764, 1975 Ride Quality Symposium, NASA TM X-3295, NASA Langley Research Center, Hampton, VA., 1975.



Note:
 ● 62 mi/h
 ● AW3 Weight



Note:
 ● 62 mi/h
 ● AW3 Weight

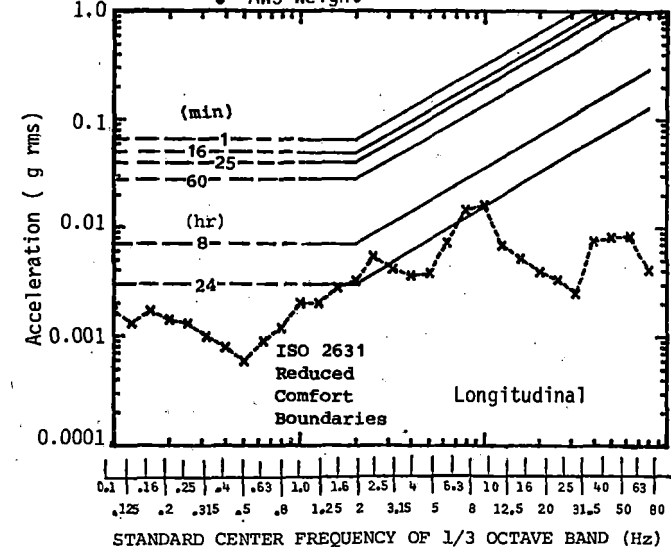
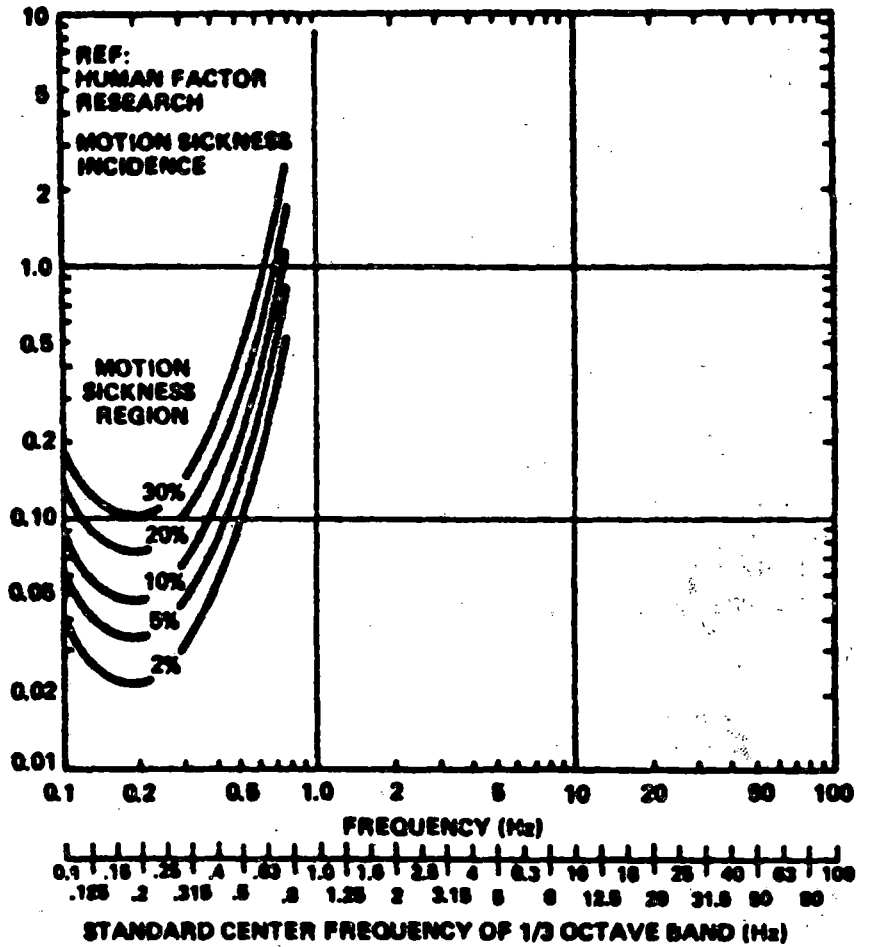


FIGURE 5-16

FIGURE 5-17

1/3 OCTAVE BAND VIBRATION LEVELS.



Note: This figure extracted from reference 5,
Malone, Op. cit.

FIGURE 5-18 CURVE OF CONSTANT MOTION SICKNESS INCIDENCE AS A
FUNCTION OF FREQUENCY.

	Orange Line	Blue Line
Overall Length	65' 2"	48' 10"
Truck Pivot Spacing	46' 6"	31' 4"
Empty Weight (AWO)	66,330 lbs	60,160 lbs
Standing Passenger Weight (AW3)	88,600 lbs	70,160 lbs

The longer beam length of the Orange Line car results in higher amplitude bending and rigid body responses, as detailed in the following comparison, which is based on one-third octave band analysis and ride roughness levels. For the vertical direction (midcar centerline), at 62 mi/h Orange Line and 60 mi/h Blue Line, the one-third octave spectrum shows a strong salient peak for both cars at the 10 Hz band (Figure 5-19) the level of this band for the Orange Line is 0.072 g rms and 0.036 g rms for the Blue Line.

Figure 5-20 shows the weighted one-third octave band levels at the higher speeds of 62 mi/h (Orange Line) and 60 mi/h (Blue Line). The weighted spectra show which band is the component most significant to the ride quality. Clearly, the 10 Hz band, for both the Orange and Blue Line cars, is most significant. Reduction of this band level would result in an improvement of ride quality.

For the lateral direction, again at 62 mi/h Orange Line, and 60 mi/h Blue Line (forward car lateral), the band levels are low (Figure 5-21). The Orange Line spectrum has a salient 2.5 Hz band at 0.011 g rms; the corresponding value for Blue Line was 0.002 g rms.

The weighted one-third octave band levels, (Figure 5-22), show that for the Orange Line cars, the 2.5 Hz band has the greatest influence on lateral ride quality; the Blue Line predominant frequency was 1.6 Hz. The levels, however, are low and give no cause for concern.

The ride roughness values for the same track sections and speeds are shown in Table 5-4. Also shown is the percent difference of Orange Line versus Blue Line values. Clearly, the Orange Line ride quality was worse than the Blue Line for both lateral and vertical directions at this speed. Comparison of the ride roughness levels to the exposure times for reduced comfort (Figure 5-1) shows that reduced comfort is reached in the center of the Orange Line cars after 15 minutes of travel at 60 mi/h. A corresponding level of reduced comfort at the same location for the Blue Line cars requires approximately 1 hour 15 minutes.

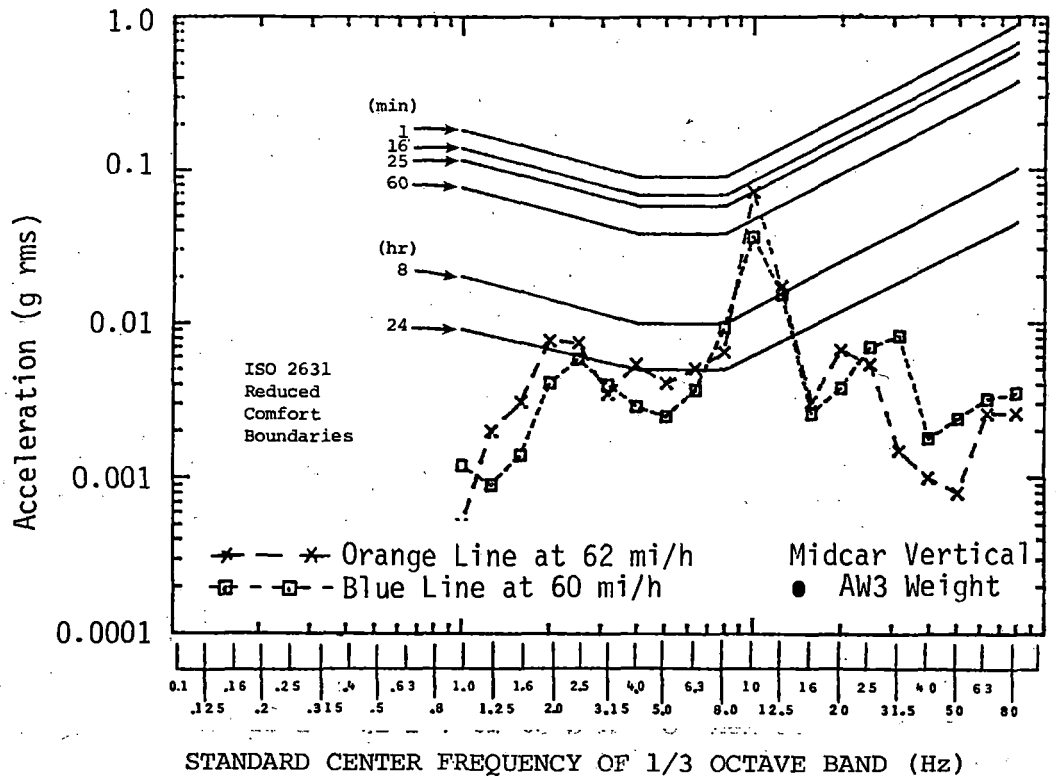


FIGURE 5-19

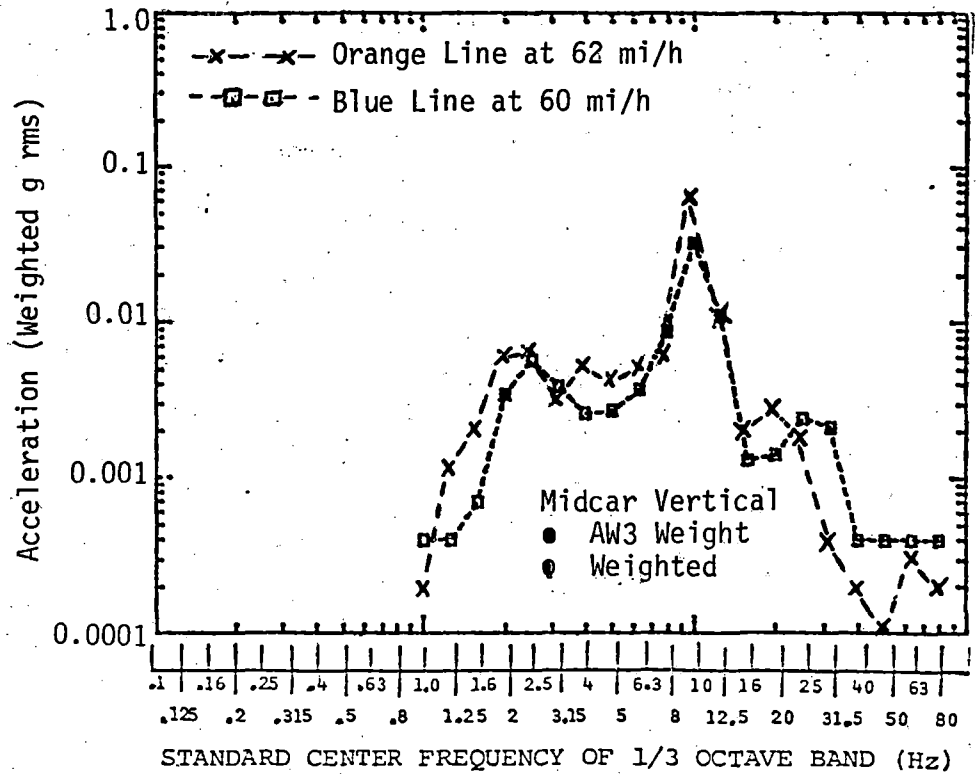


FIGURE 5-20

1/3 OCTAVE BAND VIBRATION LEVELS, COMPARING ORANGE AND BLUE LINE CARS.

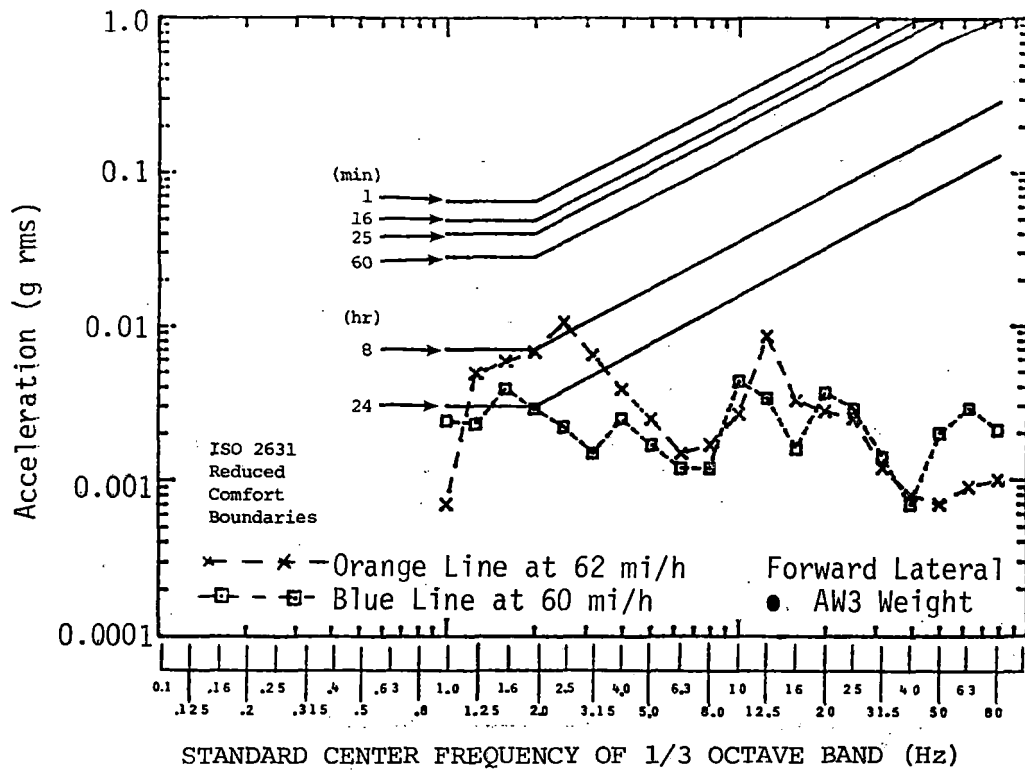


FIGURE 5-21

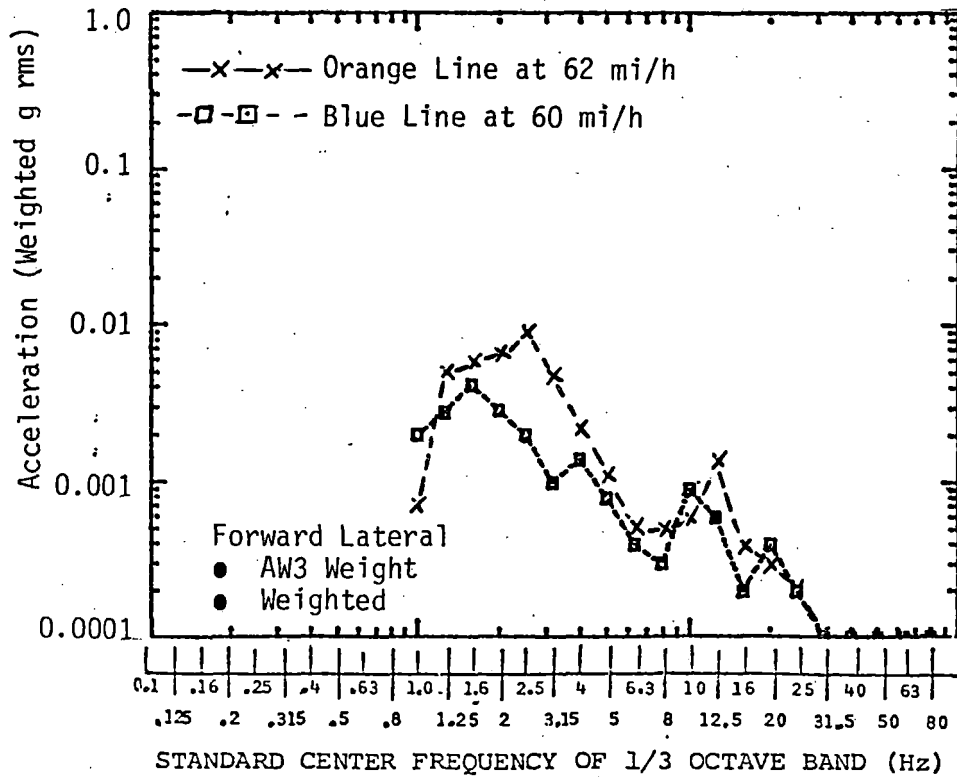


FIGURE 5-22

1/3 OCTAVE BAND VIBRATION LEVELS, COMPARING ORANGE AND BLUE LINE CARS.

TABLE 5-4. ISO 2631 LATERAL AND VERTICAL RIDE ROUGHNESS VALUES FROM 20 SECONDS OF DATA, CURVE PART OF TRACK SECTION III.

	Speed: Orange Line Cars = 62 mi/h			Speed: Orange Line Cars = 48 mi/h		
	Blue Line Cars = 60 mi/h			Blue Line Cars = 45 mi/h		
	(1) Blue Line (g rms)	(2) Orange Line (g rms)	$\frac{(2)-(1)}{(1)} \times 100\%$	(1) Blue Line (g rms)	(2) Orange Line (g rms)	$\frac{(2)-(1)}{(1)} \times 100\%$
Mid Car Vertical	0.0333	0.0689	107	0.0279	0.0401	44
Forward Car Vertical	0.0128	0.0369	188	0.0123	0.0245	99
Mid Car Lateral	0.0041	0.0087	112	0.0076	0.0076	0
Forward Car Lateral	0.0072	0.0153	113	0.0081	0.0088	9

SUMMARY

From the test results it was concluded that:

- The lateral and longitudinal ride of the Orange Line car was excellent.
- The vertical ride particularly at the center of the Orange Line car at high speed and loading, was very poor for a car on air springs.
- The Blue Line car showed similar characteristics but with a better ride.
- Both the Orange and Blue Line cars ride quality might be significantly improved if it is possible to detune the excitation of the body vibration mode from the suspension.

6 Acoustic Tests

Environmental considerations are playing an increasing role in the design of rapid transit cars, both in the areas of the influence of the vehicle itself on the passenger and wayside environment, and the elimination of toxic and carcinogenic materials used in its construction. Concern over the passenger environment has led to an increased awareness of the predominant sound transmission paths in the carbody, and the methods for the treatment of vehicle interiors with sound absorptive materials.

Traditionally, lead and asbestos materials have been used in the composition of transit vehicle brake shoes for the fade-free and squeal-free operating characteristics which they impart. Recent focus on the manufacturing and in-service particle emission hazards of components made of these materials has led to a search for suitable alternatives, and the general substitution of traditional materials with brake shoe compositions that are both lead-free and asbestos-free. Earlier tests of lead- and asbestos-free brake shoes at the TTC¹ showed that some compositions had inferior brake fade and squeal characteristics compared to compositions containing lead and asbestos.

Acoustic tests were carried out on the cars to gain information on the effectiveness of interior acoustic panels, to determine the predominant sound transmission paths through the carbody, and to evaluate the brake squeal properties of a series of brake shoe types. This section describes the acoustic tests carried out and discusses the results .

ABSORPTIVE PANEL AND DOOR TRANSMISSIBILITY EVALUATION

Objectives

The interior acoustic tests addressed two main objectives:

- To gain information on the effectiveness of car interior acoustic treatment.
- To identify the predominant sound transmission paths of the carbody in open field operating conditions.

Test Methods

The steady state sound pressure level inside a large enclosure represents the state of energy balance between the acoustic energy influx through the partitions, and the energy

1 FRA/TTC-80/05, Section 9.0.

absorption by objects and surfaces within the enclosure. For the same effective 'transmission loss' of the enclosure boundaries, a volume having little or no absorptivity will have a higher sound pressure level than one that contains absorptive material. The increase in sound pressure level is due to reverberation. Similarly, for identical absorptivity of the enclosure, the one with the higher boundary transmission loss will have a lower interior sound pressure level.

The Orange Line car has acoustically hard surfaces everywhere except for the ceiling panels, which are acoustic absorbers. This method of providing for absorptivity is the only practical one for a transit car; the disadvantages are the additional cost of the complex panel, and the greater difficulty in keeping it clean.

The effectiveness of the absorptive ceiling panels was evaluated by making comparative interior noise measurements between the standard ceiling configuration and one with the panels made ineffective. The panels were made non-absorptive by taping 1/8" thick Masonite panels to them, with the smooth side facing down. Test runs were made over sections of the TTT with wood tie/welded rail, wood tie/jointed rail, and concrete tie/welded rail construction (stations 14 through 17, 30 through 33, and 33 through 36, respectively). Vehicle speeds were 40 and 65 mi/h. Sound pressure measurements were recorded at one car interior point, the center of the rear side door vestibule (vehicle station 600.0), four feet above the floor. Comparison of one-third octave frequency domain plots and A-weighted sound pressure levels for the two configurations gave an evaluation of the effectiveness of the perforated ceiling panels as sound absorbing surfaces.

The transmission loss value of various typical carbody portions and cross-sections is reasonably well known. Not so well understood is the relative contribution of various panels and surfaces toward the attenuation of sound energy transmitted into the car. For tunnel operation, the doors can reasonably be considered the predominant sound transmission path; however, for the open field operation, there is some uncertainty as to the predominant energy path. Sound energy transmitted to the car interior is dependent on the transmission loss and the exterior incident sound pressure level; a better understanding of this relationship will aid in future design of transit cars.

The sound transmission loss tests carried out focused on the determination of the transmissibility properties of the side and end doors. The cars were operated over the same track sections as for the absorptivity tests, at 40 and 65 mi/h. Random incidence microphones with windshields were mounted under the carbody floor at vehicle station 600.0 of car 01209 (approximately at the center of the rear side doors), and between the cars, four feet above the end sills. An interior microphone was mounted on the centerline of the car at station 600.0, four feet above the floor. Details of the sound data acquisition

system are to be found in Appendix A. Sound pressure levels were recorded unweighted. The following vehicle configurations were evaluated:

- Datum case - Interior and exterior sound pressure level measurements were taken for the standard car configuration. The side and end doors were opened and closed normally to assure a natural door seal engagement. The heating, ventilating, and air-conditioning systems were made inoperative.
- End door covered - Rockwool/foil household insulation batts were applied over the end door from the outside, with the foil facing out; the air exhaust grills at the sides and top of the rear end door were also covered. Ducting tape was applied to seal the assembly airtight.
- Side doors and end door covered - Rockwool insulation was applied over the outside of the rear side doors, in addition to that already on the end door. Ducting tape was again applied to ensure that the assembly was airtight.
- Side doors open - All external applied insulation was removed from the side and end doors. The rear side doors were opened on both sides of the car. Wind noise in the interior microphone data was minimized by having car 01208 leading and moving the microphone station further toward the rear of car 01209, away from the immediate vicinity of the door openings.

Results

Sound pressure level data were processed in two ways:

- a. Unweighted data were played back on a sound-recording tape recorder and into a sound level meter, which was used to apply an A-weighting function. The A-weighted data were recorded on a sound level recorder to produce strip-chart time histories of the sound pressure levels through each track section. Average levels were estimated throughout the track section, for each vehicle configuration and speed, from the time histories; these values are tabulated in Table 6-1.
- b. Selected sound pressure level data were processed in the frequency domain using a General Radio type 1921 one-third octave analyzer. The data were synthesized into 30 one-third octave frequency bands over a range of center frequencies from 12.5 to 10 kHz. An 8-second integration time was used and the data were processed unweighted. The one-third octave sound pressure level data were then plotted using an X-Y analog plotter.

As a first step in obtaining a representative data set for this frequency domain analysis, the undercar sound pressure levels were examined for each of the track sections at 40 and 65 mi/h. The one-third octave plots for these test runs are

Table 6-1. A-WEIGHTED SOUND PRESSURE LEVELS, AVERAGED OVER EACH TRACK SECTION.

SPEED: 65 mi/h

Microphone Location/ Car Configuration	Sound Pressure Levels (dBA) for Stations:		
	14-17	30-33	33-36
Under-Car	114	112	112
Between Cars	101	98	98
Inside/Standard Carbody	77	73	73
Inside/Side Doors Open	86	83	82
Inside/Masonite Panels	77	76	73
Inside/All Doors Insulated	73	71	71
Inside/End Doors Insulated	75	73	73
SPEED: 40 mi/h			
Under-Car	105	101	100
Between Cars	94	88	86
Inside/Standard Carbody	71	67	65
Inside/Side Doors Open	80	76	72
Inside/Masonite Panels	70	69	65
Inside/All Doors Insulated	66	63	63
Inside/End Doors Insulated	68	65	65

illustrated in Figure 6-1 for a vehicle speed of 40 mi/h, and in Figure 6-2 for 65 mi/h. The plots show that the general trends of sound pressure level distribution across the frequency spectrum are similar for each track section, with the data for track stations 14-17 showing the highest sound pressure levels in the predominantly audible frequency range from 200 Hz to 4 kHz. On this basis, the track section from stations 14 through 17 was selected for a detailed one-third octave analysis of the interior sound pressure levels for each vehicle configuration.

The effectiveness of the absorptive ceiling panels was examined by comparing the interior sound pressure levels obtained for the standard carbody with those obtained when the panels were blanked off. The one-third octave plot comparison is shown in Figure 6-3. If the absorptive panels were effective, then the standard carbody data (dotted lines) could be expected to give lower sound pressure levels across the frequency spectrum than for the Masonite configuration (solid lines). The plots show that the absorptive panels gave marginally lower interior sound pressure levels for one-third octave bands with center frequencies from 500 Hz upward; in actuality, the differences are less than the general repeatability of the frequency analysis. On this basis, the absorptive panels can be considered to give little or no improvement to the interior sound pressure levels for the frequency spectra experienced on the TTT. This conclusion is supported by the

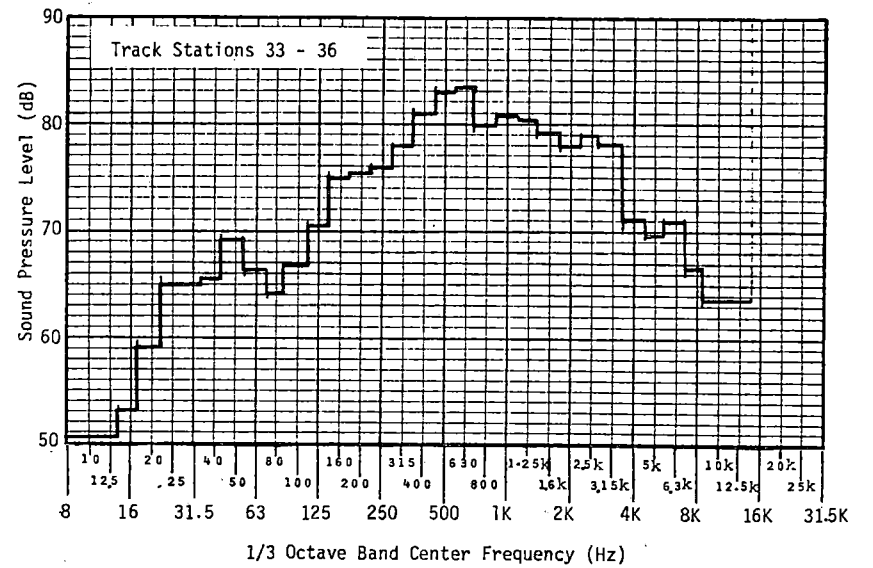
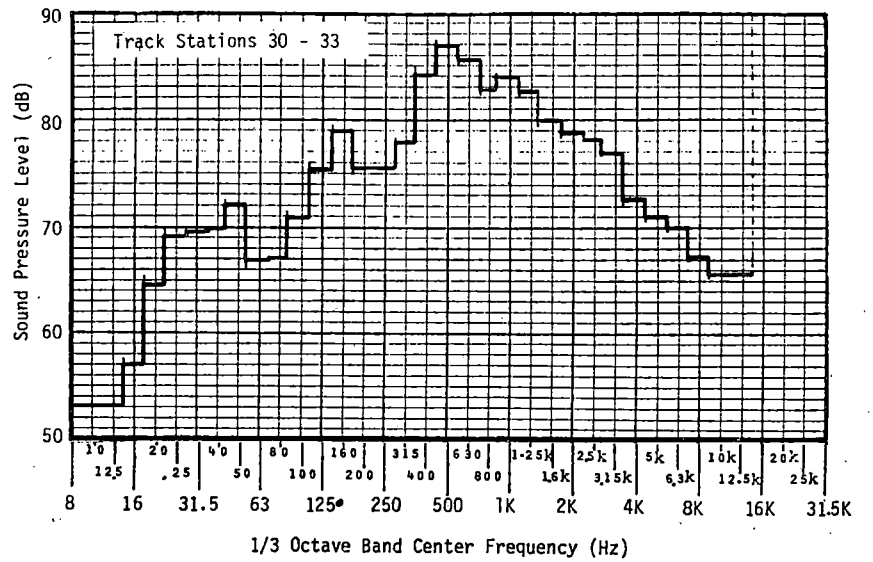
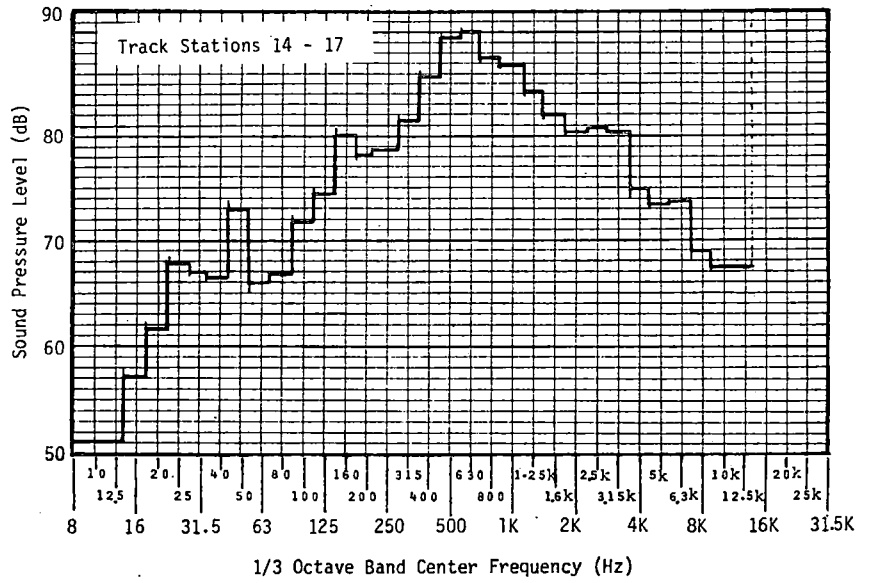


FIGURE 6-1 UNDERCAR SOUND PRESSURE LEVELS AT 40 MI/H.

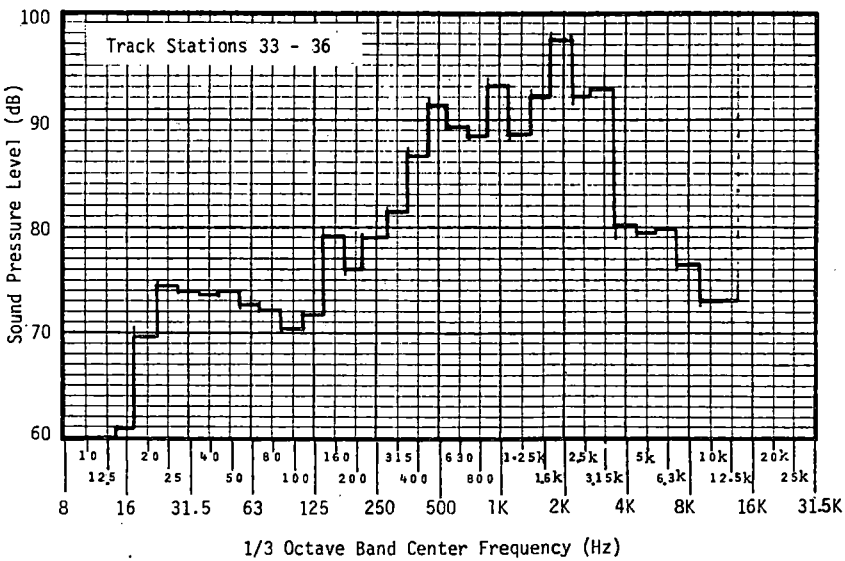
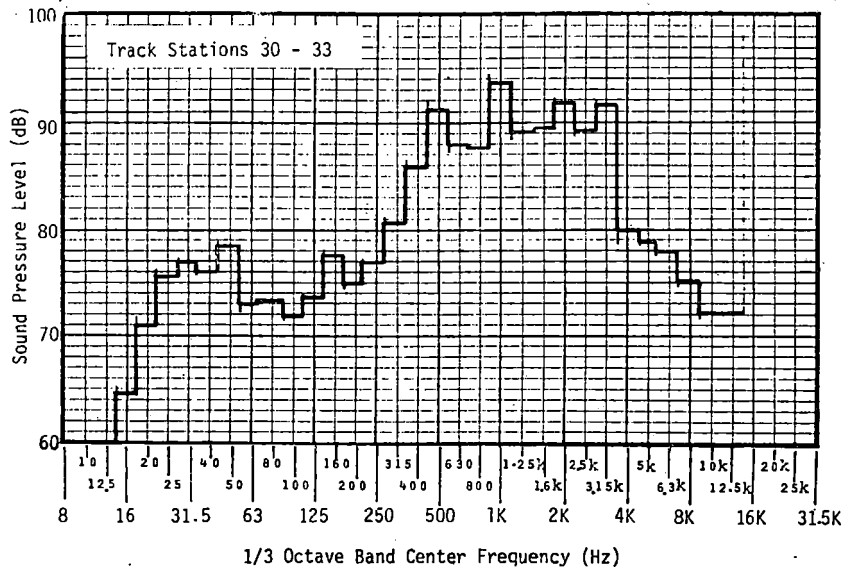
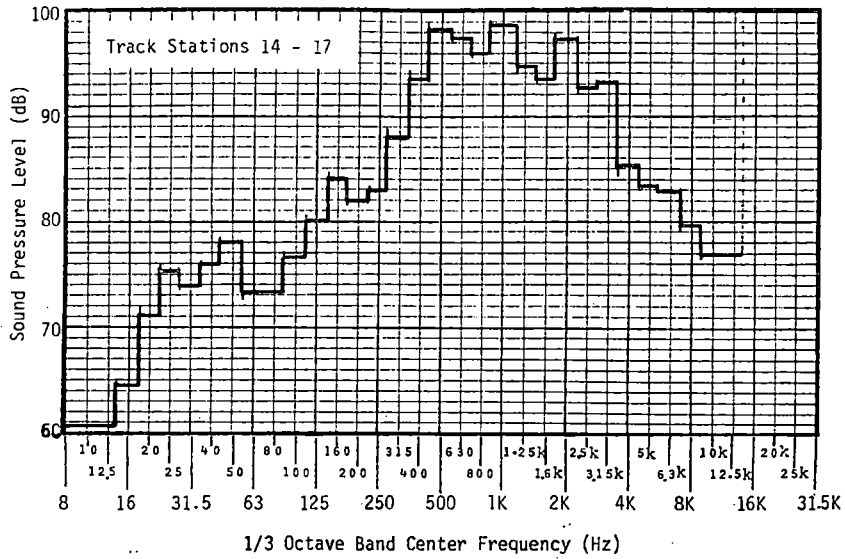


FIGURE 6-2 UNDERCAR SOUND PRESSURE LEVELS AT 65 MI/H.

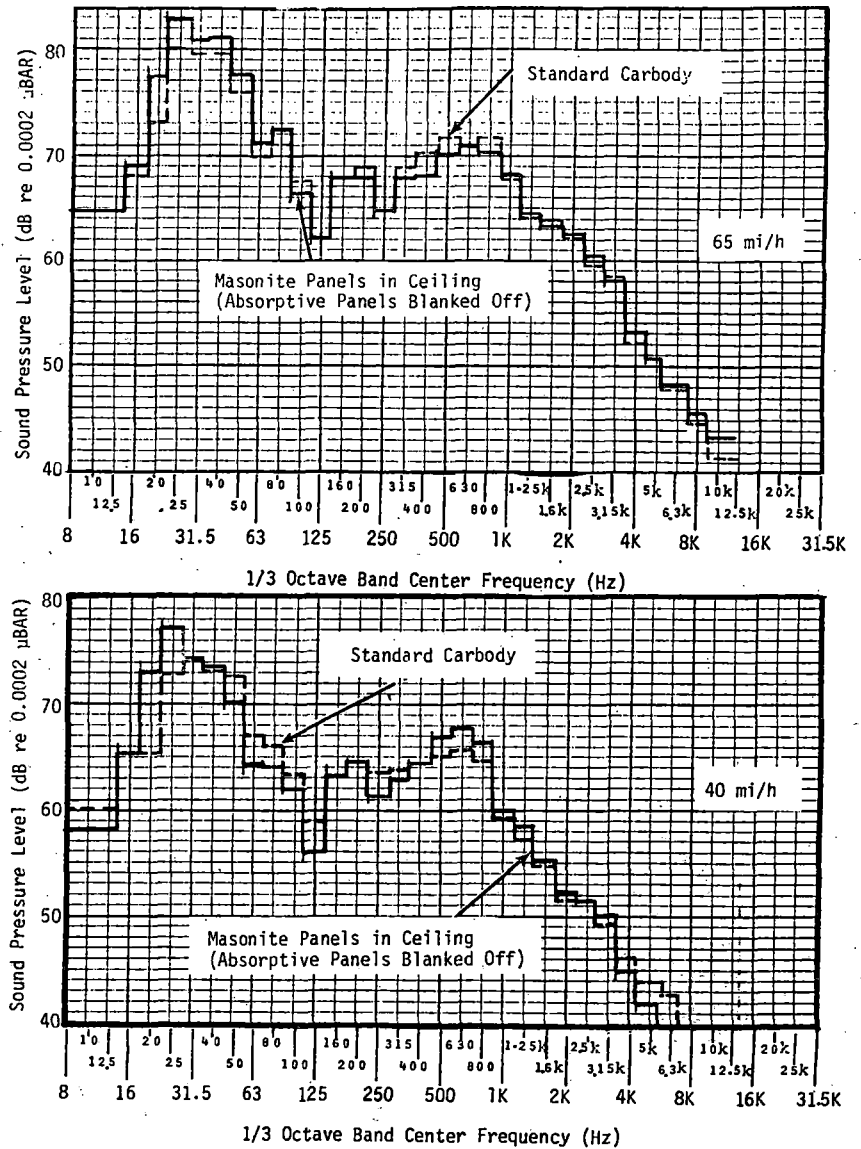


FIGURE 6-3 EFFECT OF ABSORPTIVE CEILING PANELS ON INTERIOR SOUND PRESSURE LEVELS, TRACK STATIONS 14-17.

averaged A-weighted levels for each track section (Table 6-1), which show a negligible change in level between the standard carbody and the Masonite panel configuration, except for rail stations 30-33 where there is a 3dB improvement due to the absorptive panels at 65 mi/h. Larger changes (2-3dB) are apparent in the lower frequency bands from 8 to 100 Hz center frequencies, however these are in the predominantly subaudible frequency ranges and are not of concern here. Pressure level changes at these frequencies are probably the result of aerodynamic turbulence around the door openings.

The exterior sound pressure level spectra for the data set chosen, 40 and 65 mi/h through track sections 14-17, are shown in Figure 6-4 for the under-car and between-cars microphone locations, compared to the standard carbody interior sound pressure levels. The one-third octave levels for all other vehicle configurations in the following figures are compared to the standard carbody interior data. Average A-weighted exterior

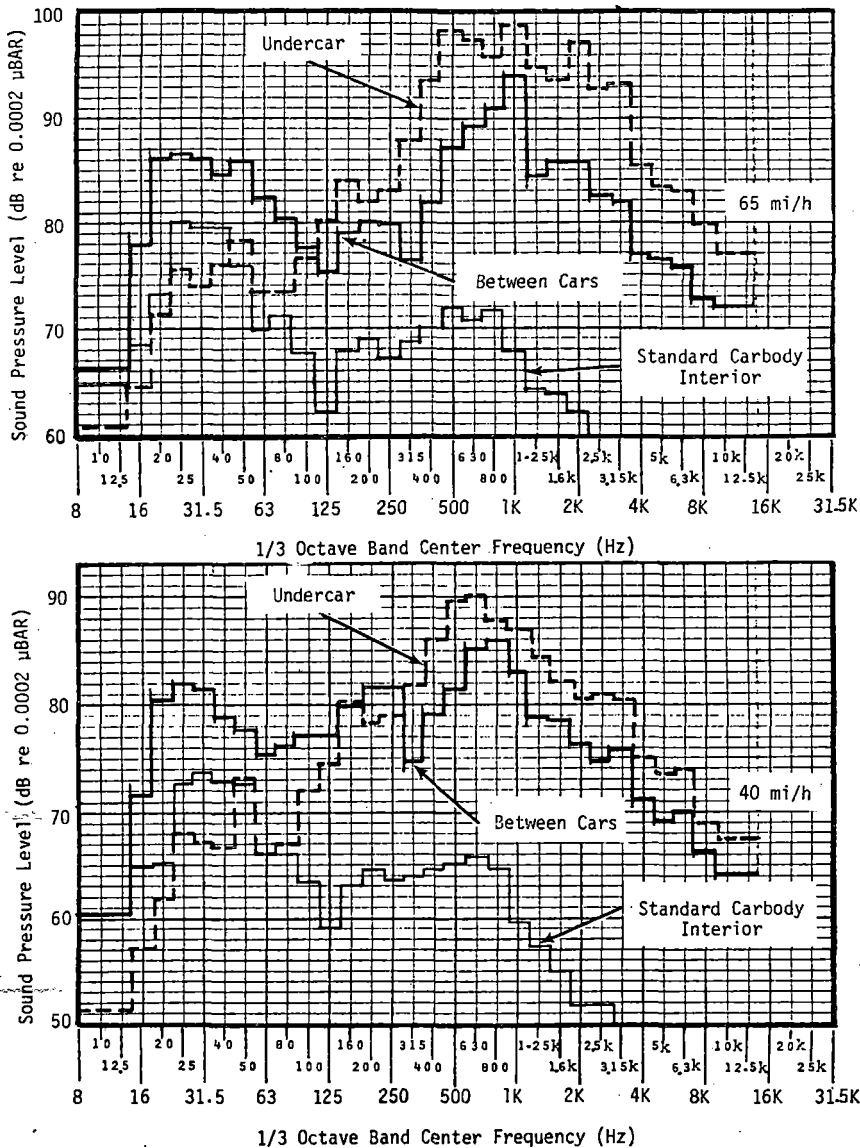


FIGURE 6-4 EXTERIOR SOUND PRESSURE LEVELS COMPARED TO STANDARD CARBODY INTERIOR LEVELS, TRACK STATIONS 14-17.

sound pressure levels were in the range 100-105 dBA at 40 mi/h, and 112-114 dBA at 60 mi/h for the undercar microphone location; the equivalent levels for the between-cars location were 86-94 dBA and 98-101 dBA for 40 and 65 mi/h, respectively.

Compared with the standard carbody case, operating with the side doors open produced a similar distribution of sound pressure level across the frequency spectra, but with an increase in sound pressure level of approximately 10 dB within each frequency band. These trends are illustrated in Figure 6-5. Considering the averaged A-weighted data of Table 6-1, the increase in overall sound pressure level due to opening the doors was 7-9 dBA, for all cases.

Two insulated door configurations were evaluated, (1) with external insulation applied to all doors and (2) with insulation applied to the end doors only. The sound pressure level trends with frequency are illustrated in the one-third octave

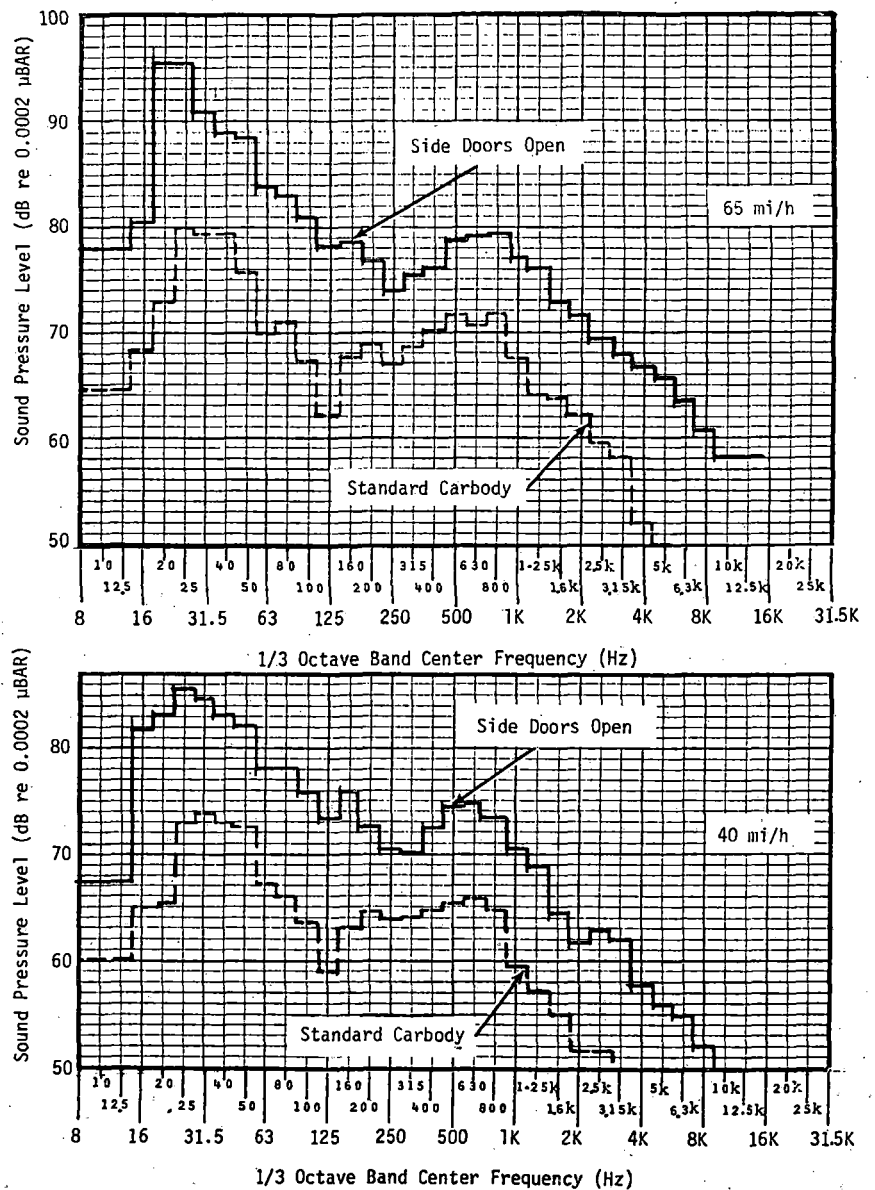


FIGURE 6-5 INTERIOR SOUND PRESSURE LEVELS WITH SIDE DOORS OPEN, TRACK STATIONS 14-17.

plots, Figures 6-6 and 6-7. As might be expected, both configurations gave a reduction in interior sound pressure level, with the most significant change due to insulating both the side and end doors. The improvement was more apparent for the 40 mi/h data, where a 2 to 4 dB reduction in sound pressure level was experienced for one-third octave bands from 250 Hz to 4 kHz center frequencies, than for the 65 mi/h cases. From the averaged A-weighted sound pressure level data, the standard carbody levels were in the range 65-71 dBA at 40 mi/h, compared to 63-66 dBA for the 'all doors insulated' case. At 65 mi/h, the average level ranges were 73-77 dBA for the standard carbody, and 71-73 dBA for the insulated case.

Summarizing, the absorptive panels were not effective when subjected to the sound pressure level spectra for open field operation. However, this result may be radically different when operating in other environments, i.e., tunnels, or with a passenger load. The overall effectiveness of the panels cannot

01-9

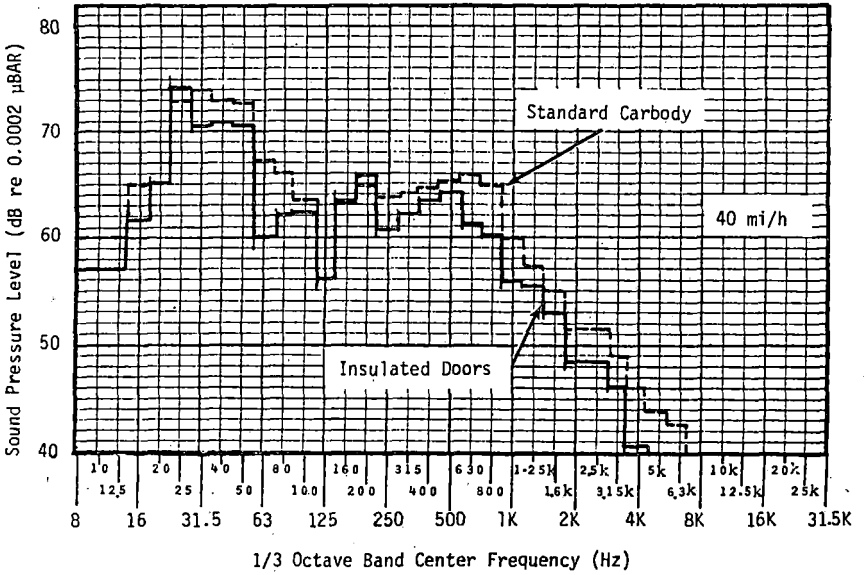
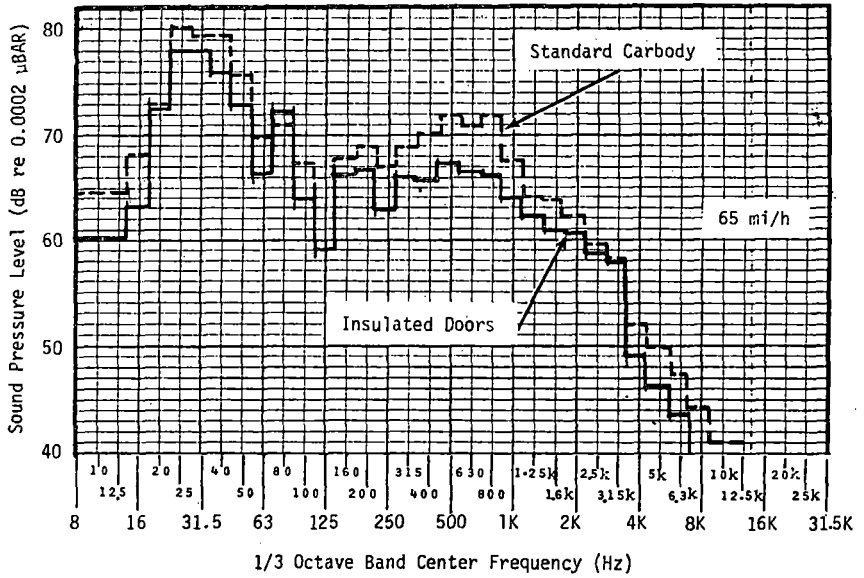


FIGURE 6-6 INTERIOR SOUND PRESSURE LEVELS WITH ALL DOORS INSULATED, TRACK STATIONS 14-17.

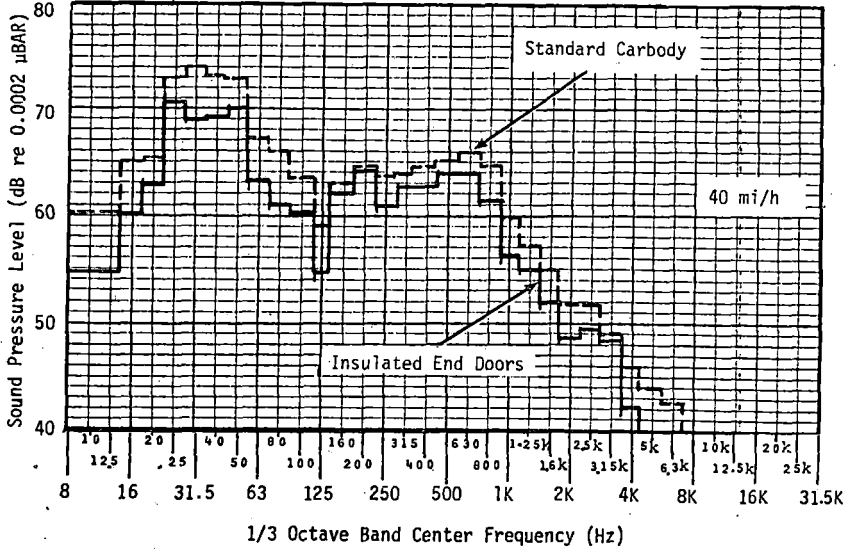
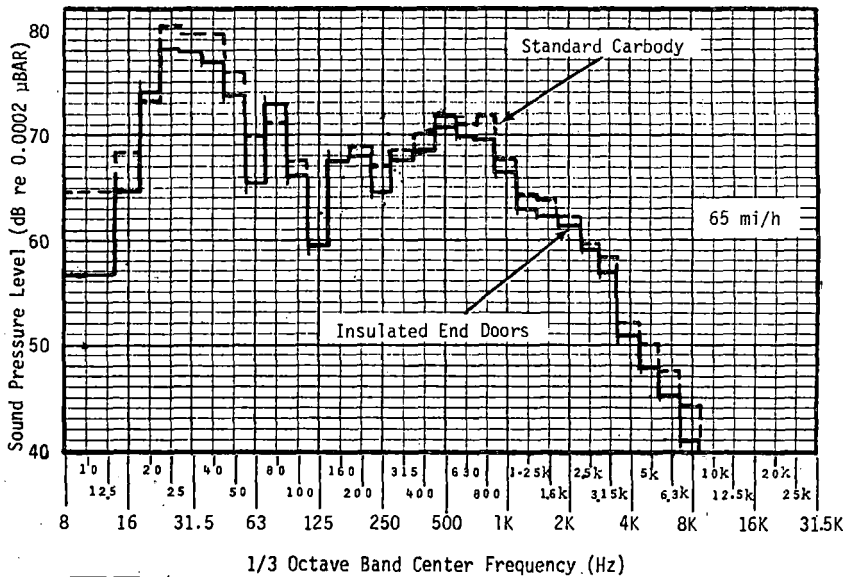


FIGURE 6-7 INTERIOR SOUND PRESSURE LEVELS WITH END DOORS INSULATED, TRACK STATIONS 14-17.

be discounted on the basis of these limited tests. The added door insulation was effective in reducing the noise transmitted through the doors, however, the reason for the improvement, whether improved sealing, less transmissibility through the doors, or a combination of both, is not apparent. The sound pressure levels were measured at one point only, the center of the door vestibule, and so the overall effectiveness of the insulation was not assessed. Further tests--for example, a similar insulation exercise, carried out on the vehicle windows--might help to establish whether the reduced transmissibility was due to the insulation of the glass or the door, or the improved sealing of the opening. From this exercise, the practicality of reducing door acoustic transmissibility properties could be properly assessed.

BRAKE SQUEAL

Objectives

The objectives of the brake squeal tests were:

- To determine the brake squeal characteristics of alternate brake shoe types, with the goal of selecting the shoe with the least objectionable noise characteristics for revenue service. An added proviso was that the shoes should provide the required full service and emergency braking rates without modification of the braking system.
- To determine the wayside sound pressure levels and the predominant frequencies associated with brake squeal.

Test Method

Four sets of brake shoes were submitted for evaluation by Hawker Siddeley Canada Inc. and Westinghouse Air Brake Company (WABCO), as detailed in Table 6-2.

TABLE 6-2. BRAKE SHOE TYPES.

<u>Supplier</u>	<u>Configuration/Material</u>
WABCO	V-222/W-539
WABCO	V-239/W-539
WABCO	V-239/W-560
TBL Ltd.	TBL-693

One set, the WABCO V-239/W-560, was withdrawn from the test program after an initial evaluation because, in the opinion of the WABCO representative, they produced excessive brake squeal.

Each of the remaining types was evaluated in a new and worn condition; for the worn configuration the shoes were machined to within 1/4" of their condemning limit. Before it was tested, each brake shoe type was seated to the wheels by sub-

jecting it to a number of friction-only braking stops. The criterion used to define adequate brake shoe seating was that at least 90 percent of the brake shoe area should show wear marks. After the seating procedure had been performed, full service friction-only braking stops were made to establish the correct brake cylinder pressures. The pressures were adjusted to compensate for the changes in brake shoe coefficient of friction due to the different material compositions. Adjustments were made until the full service braking characteristics from 50 mi/h matched those of the standard configuration, which used the V-222/W-539 shoes.

Noise measurements were made onboard car 01209 and at the wayside. The two onboard microphone locations were external, on the carbody side-skirt, at the level of the bottom of the side sill. One microphone was located in line with the rear truck kingpin and the other was mounted midway between the trucks. The wayside microphone locations were 15 ft and 50 ft from the track centerline, on the outside of the TTT, at rail station 38. The microphones were mounted on tripods at axle height. Sound pressure levels were recorded in the linear, unweighted mode. The tests were conducted on a section of tangent track with welded rail and concrete ties.

Test runs were made by initiating full service friction braking from 50 mi/h, such that the vehicles came to a stop with their 'B' ends opposite the wayside microphone locations. Test runs were made initially for the onboard microphone configuration and then repeated for the wayside locations.

Braking was initiated in two ways. In order to achieve a consistent stopping point opposite the wayside microphones, stops were initiated by using a wayside obstruction to operate the truck-mounted emergency tripcock; in this case, emergency brake pressures were reset to match the desired full service brake pressure. A fracture of the tripcock operating arm midway through the test necessitated changing the brake application method to manual, driver control. This gave less consistent stopping points and affected the data as discussed in the 'Results' discussion which follows. The tripcock failure was considered to be due to abnormal use and was discounted as a component failure problem.

At least five runs were made for each test case to achieve a measure of repeatability; for each run the air compressor and the heating, ventilating, and air conditioning systems were deactivated before applying the brakes, and were reactivated after the vehicle had stopped. Brake shoe temperatures were maintained in the 140° to 180° F range; these were monitored by means of thermocouples, installed one per hole (drilled in each brake shoe on the left-hand side of car 01209), and recorded during each run. The tests were conducted at AW3 vehicle weight.

Results

The test results were greatly influenced by inconsistencies

in the brake squeal phenomenon. The number of wheels at which brake squeal occurred for any test configuration seemed to be random. This, together with inconsistencies in the point at which the vehicle stopped, made the sound pressure levels at the source and their distance from the wayside microphone locations uncontrollable variables. Therefore, the noise levels recorded at the microphones showed a considerable variance in sound pressure level from run to run. In view of these inconsistencies, sound pressure level data, both onboard and wayside, were reviewed on a 'worst case' basis. The data were played back and recorded on a sound level recorder as time history traces, in unweighted form. The maximum sound pressure levels during the braking run were tabulated from these traces. The worst cases for each brake configuration and microphone location are presented in Figures 6-8 in bar graph format. Variance of sound pressure levels for any configuration, from run to run, was a maximum of 10 dB. A review of the data contained in these two figures, made in conjunction with an aural playback of the data tapes, shows the following trends:

- The WABCO V-239 shoes with W-560 composition gave the highest onboard sound pressure levels, with a maximum value of 120 dB at the rear truck. These shoes were subsequently withdrawn from the test, therefore no wayside or worn shoe data is available.
- The two configurations of WABCO shoes with W-539 composition--V-222, a two-piece shoe, and V-239, a one-piece shoe--gave comparable sound pressure levels when they were new (112 to 114 dB at the truck and 104 dB at the 15-ft, wayside location). However, the V-239 configuration showed markedly reduced sound pressure levels when worn (8 to 10 dB less at the wayside), whereas the V-222 configuration showed no improvement. An aural review of the data tapes showed that there was little or no brake squeal noise with the worn V-239 configuration.
- The TBL-693 shoes were by far the quietest of all the shoes evaluated. The sound pressure levels at the truck were a maximum of 107 dB and wayside levels were less than 80 dB. An aural playback showed that there were no incidences of brake squeal.

Frequency-domain analysis was carried out on a number of brake squeal records. Four-second time slices were processed, using an analog one-third octave analyzer and an x-y plotter, to produce one-third octave plots with band center frequencies from 8 Hz to 12.5 kHz. The data were processed in linear, unweighted form. A review of the plots shows that sound pressure levels across the frequency range varied from run to run, because of inconsistencies in the brake squeal phenomenon discussed earlier. However, for all brake squeal records, a dominant sound pressure level can be seen at the band centered on 3.15 kHz, with some activity in the adjacent 4 kHz band. Two typical brake squeal one-third octave plots are presented in Figure 6-9 for the 15-ft and 50-ft wayside microphone locations. The dominant 3.15 kHz band sound pressure levels can be

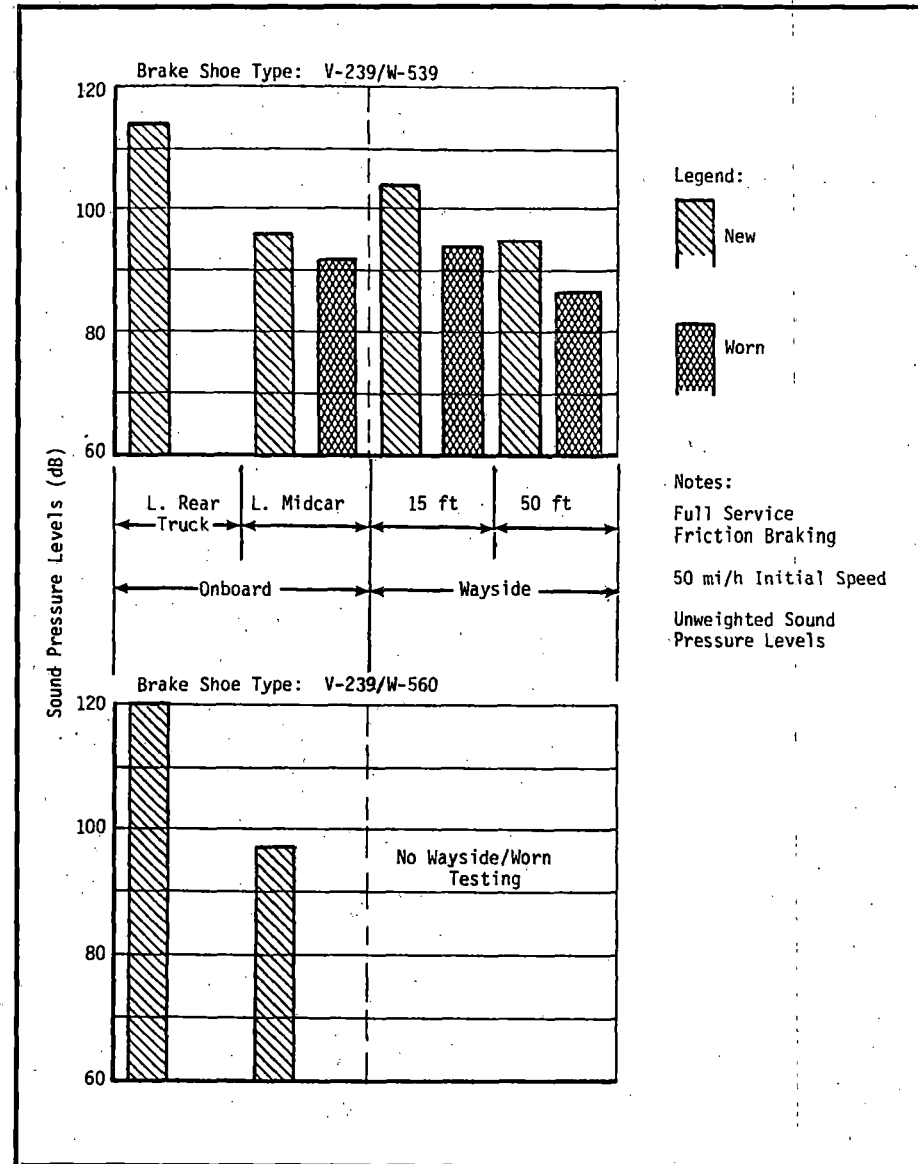
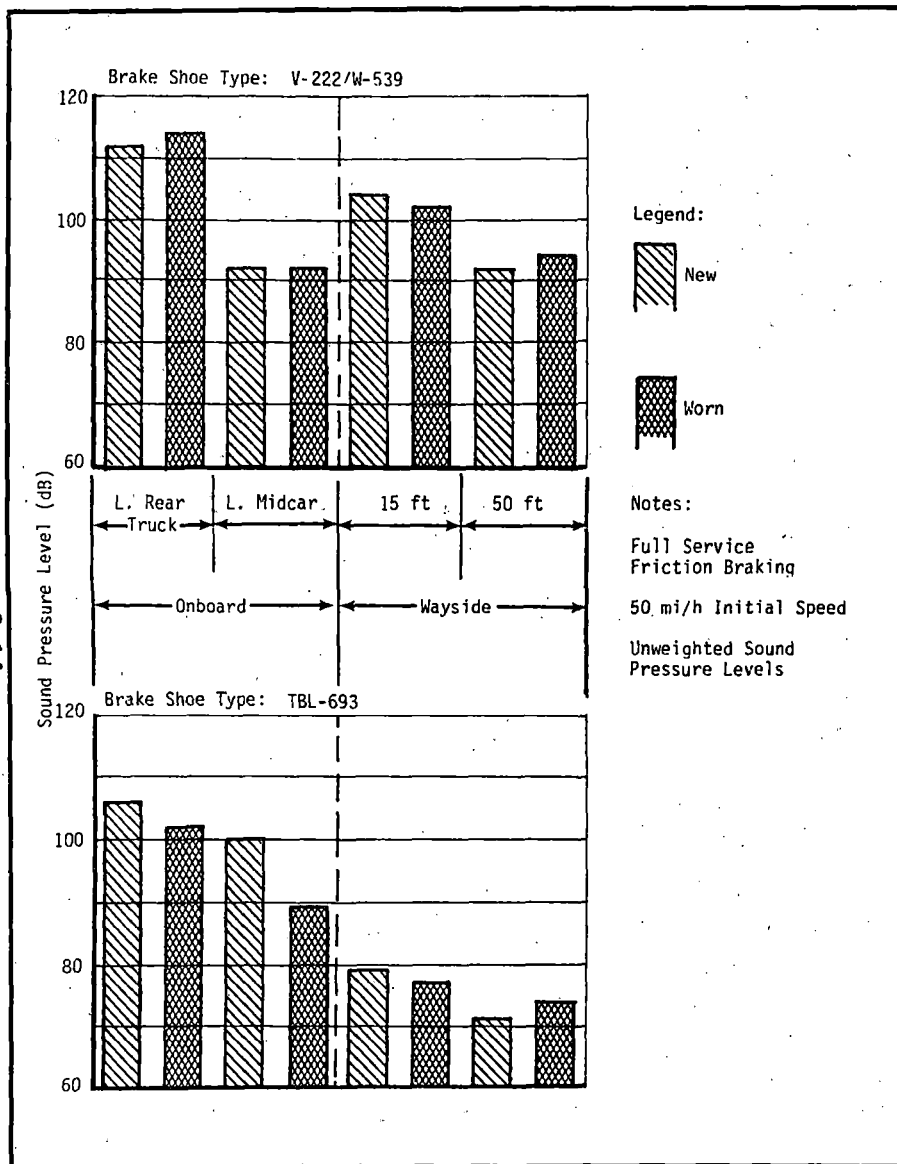


FIGURE 6-8 MAXIMUM NOISE LEVELS, ONBOARD AND WAYSIDE.

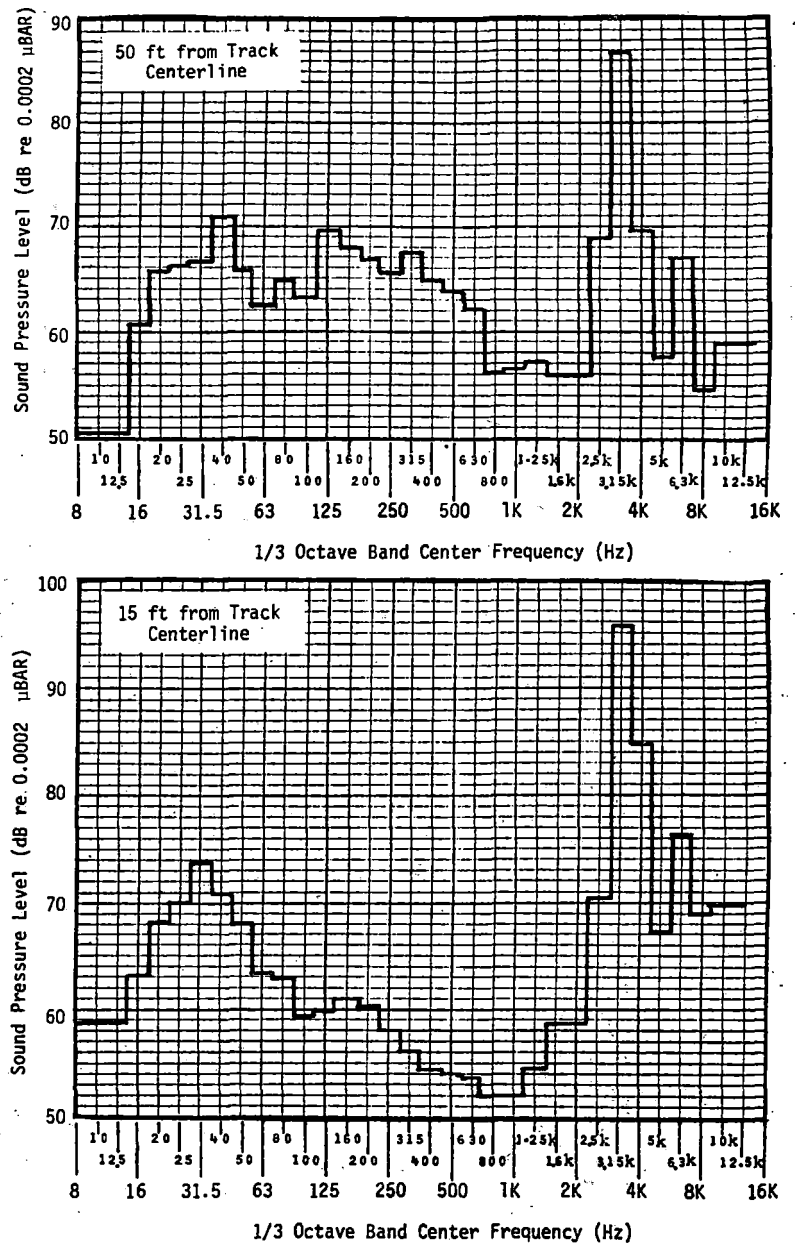


FIGURE 6-9 TYPICAL WAYSIDE FREQUENCY SPECTRA DURING BRAKE SQUEAL (UNWEIGHTED)

seen to be 15 to 20 dB higher than the general level; this was undoubtedly the frequency band of the squeal.

A review of the braking performance was conducted for each shoe configuration tested to determine whether braking performance was degraded by any of the brake shoe types. The performance runs in this test phase were conducted from an initial speed of 50 mi/h, using full service friction braking and emergency braking activated by the motorman's deadman. Typical deceleration characteristics for the standard V-222/W-539 shoes are shown in Figure 6-10 for full service and emergency braking along with the TBL-693 and V-239/W-539 shoes. The data presented are for 'new' shoes and brake shoe temperatures in the 100°-150° F range. No obvious trends could be determined between 'new' and 'worn' shoe configurations or with temperatures up to the 180° F test limit. Average deceleration

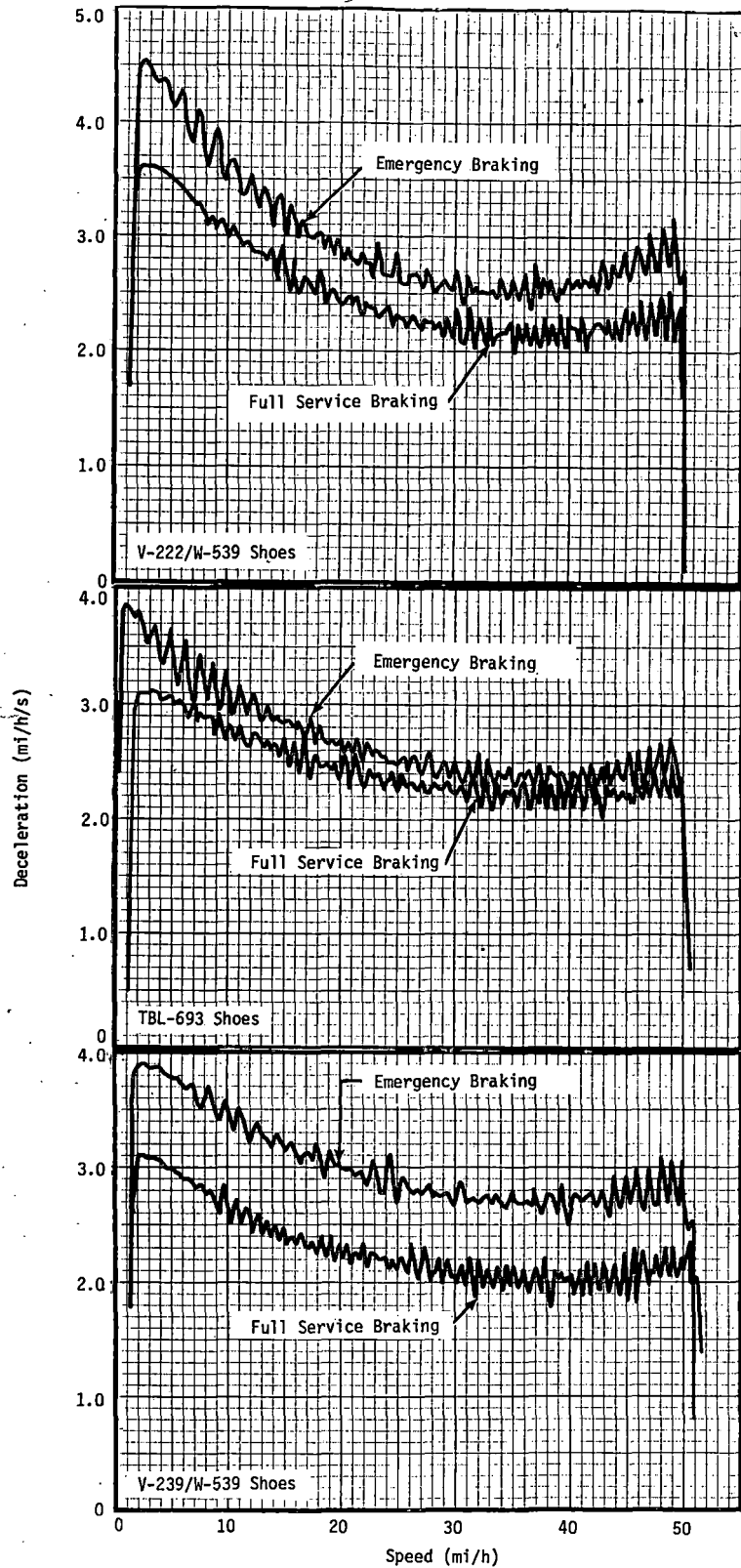


FIGURE 6-10 FRICTION BRAKING CHARACTERISTICS.

levels were computed for a series of stops from 50 mi/h for both full service friction and emergency braking. The averages were calculated from stopping distances and times. These are presented in Table 6-3.

TABLE 6-3. AVERAGE DECELERATION LEVELS FROM 50 MI/H.

Shoe Type	Average Deceleration (mi/h/s)	
	Full Service Friction Braking	Emergency Braking
V-222/W-539	2.60	3.05
TBL-693	2.45	2.81
V-239/W-539	2.63	2.99

The following points can be determined from the data presented:

- None of the brake shoes tested could meet the specification requirements for full service friction or emergency braking, (deceleration levels of 2.75 and 3.25 mi/h/s, respectively), from 50 mi/h. This confirms the results of the performance tests for friction-only and emergency braking described in section 4.0, where the required levels could not be attained at speeds over 40 mi/h.
- The V-222/W-539 and V-239/W-539 shoes had comparable braking performance from 50 mi/h, while the TBL-693 shoes showed a performance decrement on the order of 0.2 mi/h/s on average deceleration, for both full service friction and emergency operation.

Summarizing the findings of the brake squeal tests:

- The TBL-693 brake shoes were free of brake squeal effects in both new and worn configurations, but had a deceleration penalty of 0.2 mi/h/s from 50 mi/h, compared to the standard shoes.
- Both of the WABCO W-539 composition shoes suffered from brake squeal when new, but the V-239 configuration two-piece shoe was dramatically improved when worn. They offer comparable braking performance which is, however, still below the deceleration requirements of the vehicle specification.
- The predominant frequency excited by the brake squeal phenomenon lies in the one-third octave band centered on 3.15 kHz.

Appendix A

INSTRUMENTATION, DATA ACQUISITION, AND DATA PROCESSING

This appendix describes the onboard instrumentation sensors, the data acquisition methods, and data processing techniques used for the Orange Line test program. The system described is that which is common to the standardized transit vehicle evaluation tests carried out at the TTC. Other special engineering tests which have individual instrumentation requirements are described in the appropriate sections of the report describing those tests.

INSTRUMENTATION

Instrumentation requirements were divided into three basic groups according to the type of test to be performed:

- Performance (acceleration, braking, spin/slide, train resistance, energy consumption, and duty cycle).
- Vehicle Dynamics (ride quality, component-induced vibration).
- Acoustics (brake squeal, door panel losses, absorptive panel evaluation).

Performance Tests

Performance test objectives were met with a series of special transducers mounted on the cars, supplemented by a limited number of built-in vehicle sensors. The measurement numbers, standard outputs, and sensor descriptions of each sensor for the performance tests are shown in Table A-1. The sensors can be classed as (1) those typically used to assure the correct operation of the vehicles and (2) those used to characterize the vehicles' performance. In the first category are parameters such as motor currents, brake cylinder pressures, load weigh signals, brake relay indicators (functioning of the spin/slide protection system), and axle speeds. The second category includes measurements such as longitudinal acceleration, time, speed and distance (performance evaluation), line voltage and current (energy consumption), axle speeds (spin/slide protection system efficiency), and brake shoe temperatures (friction braking duty cycles).

Longitudinal acceleration was measured by means of a servo-accelerometer mounted on the carbody of car 01209. Accurate speed and distance measurements were made by means of a ninth wheel assembly, mounted on the rear truck of car 01209. This assembly allows a sprung, damped suspension to push a wheel of known diameter against the rail head. A gear wheel

TABLE A-1 INSTRUMENTATION SENSOR LISTING, PERFORMANCE*.

CHANNEL NUMBER	PARAMETER	STANDARD OUTPUT NAME	MEASUREMENT NUMBER	SENSOR TYPE	MEASUREMENT RANGE	MAXIMUM CUTOFF FREQUENCY
1	IRIG-B Time	T/A	01411	Time Code Generator	---	1 KHz
2	Line Voltage	LVD/A	01101	Resistive Divider	1000 Volts	100 Hz
3	Line Current (A-Car)	LCD/A	01102	Hall Effect Sensor	2000 Amps	100 Hz
4	Motor Current (A-Car, Front)	MACD/AF	01103	Hall Effect Sensor	1000 Amps	100 Hz
5	Motor Current (A-Car, Rear)	MACD/AR	01104	Hall Effect Sensor	1000 Amps	100 Hz
6	Loadweigh (A-Car)	LW/A	01206	Derived Signal	85-122 PSIG	100 Hz
7	Straight Air Pipe (A-Car)	SAP/A	01207	Derived Signal	33.33 PSIG	100 Hz
8	Brake Cylinder Pressure (A-Car, Rear)	BCP/AR	01202	Strain Gage	50 PSIG	100 Hz
9	Line Current (B-Car)	LCD/B	01105	Hall Effect Sensor	2000 Amps	100 Hz
10	Motor Current (B-Car, Front)	MACD/BF	01106	Hall Effect Sensor	1000 Amps	100 Hz
11	Motor Current (B-Car, Rear)	MACD/BR	01107	Hall Effect Sensor	1000 Amps	100 Hz
12	Loadweigh (B-Car)	LW/B	01208	Derived Signal	85-122 PSIG	100 Hz
13	Straight Air Pipe (B-Car)	SAP/B	01209	Derived Signal	33.33 PSIG	100 Hz
14	Brake Cylinder Pressure (B-Car, Rear)	BCP/BR	01204	Strain Gage	50 PSIG	100 Hz
15	Controller Setting	CS/B	01301	Resistive Divider	B4/P4	100 Hz
16	Vehicle Speed	VS/B	01401	Electromagnetic Sensor	100 MPH	10 Hz
17	9th Wheel Speed	VS/B5	01410	Electromagnetic Sensor	100 MPH	10 Hz
18	9th Wheel Distance	D/A	01421	Pulse Generator	10 Ft/Step	10 Hz
19	Automatic Location Detector	ET/A2	01423	Displacement Sensor	---	---
20	Vehicle Acceleration	AP/B	02001	Servo Accelerometer	+5.4 MPHPS	3.15 Hz
21	Wheel/Slip (A-Car)	W/SA	01126	Contact Closure	Digit Hi/Lo	100 Hz
22	Wheel/Slip (B-Car)	W/SB	01127	Contact Closure	Digit Hi/Lo	100 Hz
23	Brake Pipe (B-Car)	BPP/B	01205	Contact Closure	Digit Hi/Lo	100 Hz
24	---	---	---	---	---	---
25	---	---	---	---	---	---
26	---	---	---	---	---	---
27	Tape Speed Reference	---	---	---	---	---
28	Voice	---	---	---	---	---

* TESTS: Acceleration, Braking, Duty Cycle, Train Resistance

TABLE A-1 INSTRUMENTATION SENSOR LISTING, PERFORMANCE** (CONTINUED).

CHANNEL NUMBER	PARAMETER	STANDARD OUTPUT NAME	MEASUREMENT NUMBER	SENSOR TYPE	MEASUREMENT RANGE	MAXIMUM CUTOFF FREQUENCY
1	IRIG-B Time	T/A	01411	Time Code Generator	---	1 KHz
2	Line Voltage	LVD/A	01101	Resistive Divider	1000 Volts	100 Hz
3	Line Current (A-Car)	LCD/A	01102	Hall Effect Sensor	2000 Amps	100 Hz
4	Motor Current (A-Car, Front)	MACD/AF	01103	Hall Effect Sensor	1000 Amps	100 Hz
5	Motor Current (A-Car, Rear)	MACD/AR	01104	Hall Effect Sensor	1000 Amps	100 Hz
6	Axle #1 Speed (A-Car)	VS/A1	01402	Electromagnetic Sensor	100 MPH	10 Hz
7	Brake Cylinder Pressure (A-Car, Front)	BCP/AF	01201	Strain Gage	50 PSIG	100 Hz
8	Brake Cylinder Pressure (A-Car, Rear)	BCP/AR	01202	Strain Gage	50 PSIG	100 Hz
9	Line Current (B-Car)	LCD/B	01105	Hall Effect Sensor	2000 Amps	100 Hz
10	Motor Current (B-Car, Front)	MACD/AF	01106	Hall Effect Sensor	1000 Amps	100 Hz
11	Motor Current (B-Car, Rear)	MACD/AR	01107	Hall Effect Sensor	1000 Amps	100 Hz
12	Axle #2 Speed (A-Car)	VS/A2	01403	Electromagnetic Sensor	100 MPH	10 Hz
13	Brake Cylinder Pressure (B-Car, Front)	BCP/BF	01203	Strain Gage	50 PSIG	100 Hz
14	Brake Cylinder Pressure (B-Car, Rear)	BCP/BR	01204	Strain Gage	50 PSIG	100 Hz
15	Axle #3 Speed (A-Car)	VS/A3	01404	Electromagnetic Sensor	100 MPH	10 Hz
16	Axle #4 Speed (A-Car)	VS/A4	01405	Electromagnetic Sensor	100 MPH	10 Hz
17	9th Wheel Speed	VS/B5	01410	Electromagnetic Sensor	100 MPH	10 Hz
18	9th Wheel Distance	D/A	01421	Pulse Generator	10 Ft/Step	10 Hz
19	Axle #1 Speed (B-Car)	VS/B1	01406	Electromagnetic Sensor	100 MPH	10 Hz
20	Vehicle Acceleration	AP/B	02001	Servo Accelerometer	+5.4 MPHPS	3.15 Hz
21	Wheel/Slip (A-Car)	W/SA	01126	Contact Closure	Digit Hi/Lo	100 Hz
22	Wheel/Slip (B-Car)	W/SB	01127	Contact Closure	Digit Hi/Lo	100 Hz
23	Axle #2 Speed (B-Car)	VS/B2	01407	Electromagnetic Sensor	100 MPH	10 Hz
24	Axle #3 Speed (B-Car)	VS/B3	01408	Electromagnetic Sensor	100 MPH	10 Hz
25	Axle #4 Speed (B-Car)	VS/B4	01409	Electromagnetic Sensor	100 MPH	10 Hz
26	Controller Setting	CS/B	01301	Resistive Divider	B4/P4	---
27	Tape Speed Reference	---	---	---	---	---
28	Voice	---	---	---	---	---

** TESTS: Spin/Slide

mounted on the wheel, together with a magnetic pickup, provided a signal output with 60 pulses per revolution of the wheel; by conditioning and counting these pulses, outputs are provided which are proportional to speed and distance and are unaffected by vehicle wheel slips.

Accurate time information was provided by an IRIG time code generator which provided a continuous time-of-day code; performance time-to-stop measurements were also made with a stop-watch. Brake shoe temperatures were monitored by means of Chromel-constantan thermocouples mounted (in holes drilled in each brake shoe) so that the thermocouple junction was approximately 1/8" from the friction surface of the shoe; a brake shoe on the

left hand side of each axle of car 01209 was instrumented in this way.

Track location information was provided by a series of steel targets mounted on the track crossties at 1,000 ft intervals, in conjunction with a capacitive displacement sensor mounted under car 01209. Upon detection of a steel target, the displacement sensor gave a momentary output which was then annotated on the chart records and the voice channel of the analog tape recorder, to identify the specific track station.

Vehicle Dynamics

Accelerometers were installed on the carbody floor of vehicle 01209 to meet the requirements of the vehicle dynamics test phase. Vertical and lateral +0.5 g servo-accelerometers were mounted over each truck kingpin and at the carbody longitudinal center, together with a longitudinal accelerometer at the center location. Table A-2 contains a summary of the parameters measured for the ride quality test objectives.

Acoustics

The acoustic instrumentation was independent of other instrumentation on the engineering tests and included equipment for indicating and recording sound pressure levels and equipment for data analysis. Data were recorded unweighted, and later processed to A-weighted sound pressure levels for one-third octave frequency analysis and sound pressure level time histories.

The recording system used two Brüel and Kjaer (B&K) 4134 pressure response type microphones, fitted with windshields for external applications. Since, for these tests, sound was to come from multiple and/or moving sources, the pressure response type of microphone was selected over the free field microphone type; the latter suffer a much more dramatic loss of sensitivity for off-axis incidence. The microphone signals were input to two B&K 2209 sound level meters. The dynamic range of the sound signal was first reduced in the input stage to the meter by means of a selectable high-pass filter set to the 10 Hz position. The dynamic range was then further reduced by means

TABLE A-2 INSTRUMENTATION SENSOR LISTING, RIDE QUALITY.

CHANNEL NUMBER	PARAMETER	STANDARD OUTPUT NAME	MEASUREMENT NUMBER	SENSOR TYPE	MEASUREMENT RANGE	MAXIMUM CUTOFF FREQUENCY
1	IRIG-B Time	T/A	01411	Time Code Generator	---	1 KHz
2	Line Voltage	LVD/A	01101	Resistive Divider	1000 Volts	100 Hz
3	Line Current (A-Car)	LCD/A	01102	Hall Effect Sensor	2000 Amps	100 Hz
4	Motor Current (A-Car, Front)	MACD/AF	01103	Hall Effect Sensor	1000 Amps	100 Hz
5	Motor Current (A-Car, Rear)	MACD/AR	01104	Hall Effect Sensor	1000 Amps	100 Hz
6	Forward Centerline Vertical	AC/A1	02101	Servo Accelerometer	+0.5 g	100 Hz
7	Brake Cylinder Pressure (A-Car, Rear)	BCP/AR	01202	Strain Gage	50 PSIG	100 Hz
8	---	---	---	---	---	---
9	Line Current (B-Car)	LCD/B	01105	Hall Effect Sensor	2000 Amps	100 Hz
10	Motor Current (B-Car, Front)	MACD/BF	01106	Hall Effect Sensor	1000 Amps	100 Hz
11	Motor Current (B-Car, Rear)	MACD/BR	01107	Hall Effect Sensor	1000 Amps	100 Hz
12	Forward Centerline Lateral	AC/A2	02102	Servo Accelerometer	+0.5 g	100 Hz
13	Brake Cylinder Pressure (B-Car, Rear)	BCP/BR	01204	Strain Gage	50 PSIG	100 Hz
14	---	---	---	---	---	---
15	Mid-Car Centerline Vertical	AC/A4	02104	Servo Accelerometer	+0.5 g	100 Hz
16	Vehicle Speed	VS/A	01401	Electromagnetic Sensor	100 MPH	10 Hz
17	9th Wheel Speed	VS/B5	01410	Electromagnetic Sensor	100 MPH	10 Hz
18	9th Wheel Distance	D/A	01421	Pulse Generator	10 Ft/Step	10 Hz
19	Mid-Car Centerline Lateral	AC/A5	02105	Servo Accelerometer	+0.5 g	100 Hz
20	Vehicle Acceleration (Mid Centerline Longitudinal)	AP/B	02001	Servo Accelerometer	+5.4 MPHPS	100 Hz
21	Automatic Location Detector	ET/A2	01423	Displacement Sensor	---	100 Hz
22	Event	ET/A1	01422	Switch	---	---
23	Mid-Car Centerline Vertical (Left)	AC/A6	02106	Servo Accelerometer	+0.5 g	100 Hz
24	Rear Centerline Vertical	AC/A7	02107	Servo Accelerometer	+0.5 g	100 Hz
25	Rear Centerline Lateral	AC/A8	02108	Servo Accelerometer	+0.5 g	100 Hz
26	Controller Setting	CS/B	01301	Resistive Divider	B4/P4	100 Hz
27	Tape Speed Reference	---	---	---	---	---
28	Voice	---	---	---	---	---

of a B&K 1616 one-third octave band filter set to the 'Linear' mode. In this mode a high-pass filter of 100 dB/decade slope and 3 dB attenuation at 22.4 Hz was applied to the signal. This was necessary because the sound onboard a moving transit vehicle has a broad band nature. The frequency spectrum shows significant components in both the "infra-sound band" (from 1 to 20 Hz) and the "audio-frequency band" (from 20 Hz to 20 kHz). The frequency spectrum has very high levels at the low frequency end (of the order of 30 dB). Because the NAGRA IV SJ recorder used had a dynamic range of 60 dB, it could not record the complete signal range. Therefore, the low frequency infra-sound content of the signals was filtered out, such that only the audio-frequency band content was recorded. The -3 dB point of the high-pass filter, at 22.4 Hz, corresponds to the shoulder of the 25 Hz center frequency one-third octave band.

From the filter the signals were returned to the B&K 2209 Sound Level Meters, where they were amplified by the output filters and presented as signal inputs to a Nagra IV SJ recorder. The sound level signals were then recorded in the 'Linear' mode with no frequency weighting applied.

Sound recording system levels were calibrated in the field with a B&K 4230 Sound Level Calibrator before each test. The calibrator produces a known tone (94 dB at 1kHz) which was applied directly to the microphones. Noise data were analyzed in both time and frequency domains. Strip chart time histories were produced using a B&K Graphic Level Recorder type 2306, which has the data-playback capability of applying pen response characteristics to simulate 'impulse', 'fast', and 'slow' meter settings. A General Radio type 1921 Real Time Analyzer was used to produce one-third octave plots, unweighted, and with 'A' weighting characteristics applied by means of an analog filter network.

DATA ACQUISITION

The onboard analog data acquisition system for the Performance and Ride Quality tests consisted of signal conditioning, filters, strip chart recorders, and one 28-track tape recorder. A schematic of the basic system is shown in Figure A-1. The data acquisition system, as installed onboard the MBTA vehicle, is shown in Figures A-2 and A-3.

Signal Conditioning And Monitoring Electronics

The signal conditioning system, an ENDEVCO 4470 unit, provided excitation voltages for transducers, sensors, and for preconditioning circuits. The 4470 also provided amplifications as required to normalize all analog signals to a +5 V level. The SM-1 signal monitor provides real-time static monitoring (digital multimeter) and dynamic monitoring (oscilloscope) of any analog data signals. The signal conditioning system is

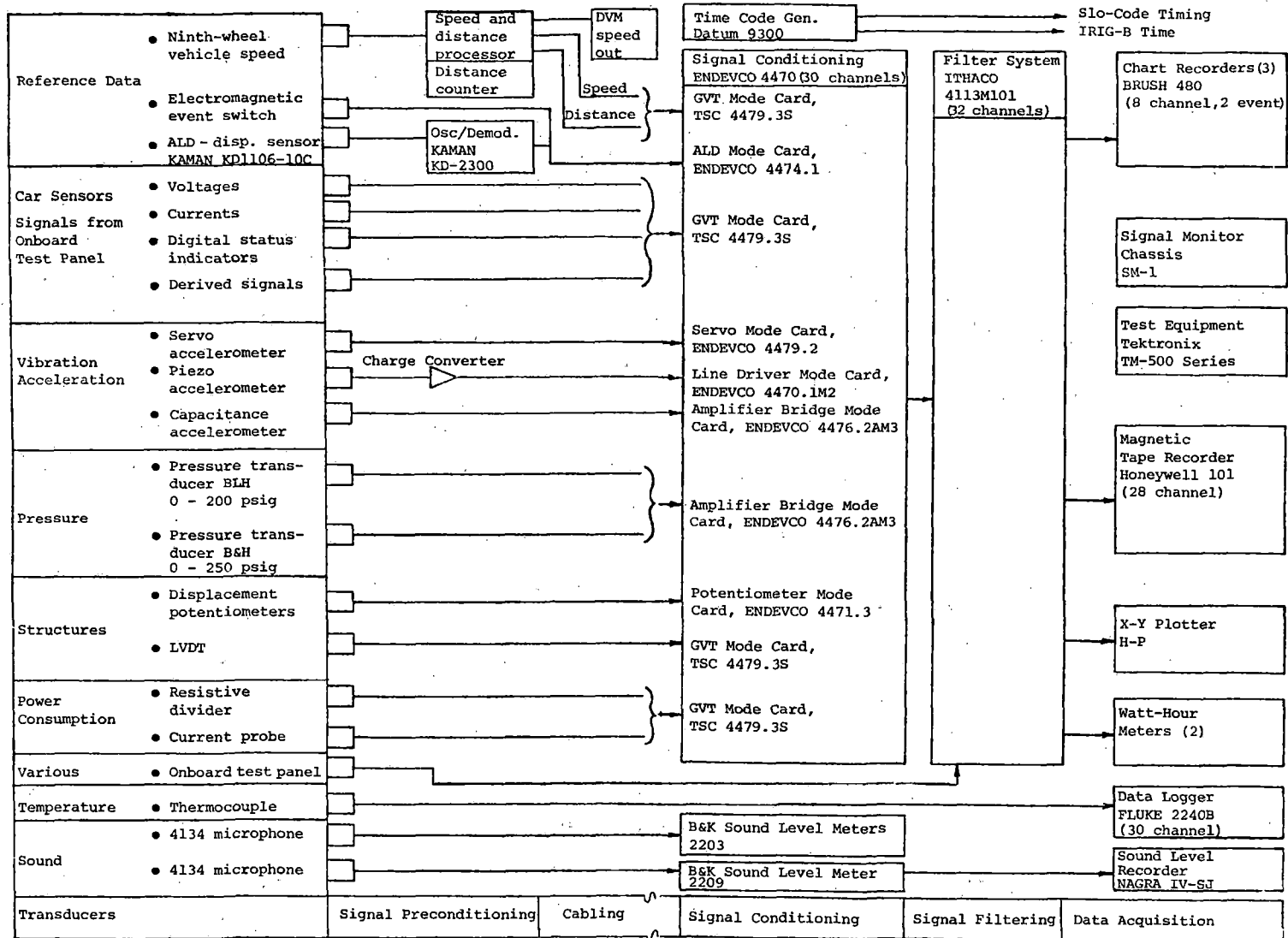


FIGURE A-1 DATA ACQUISITION SYSTEM, BLOCK DIAGRAM.

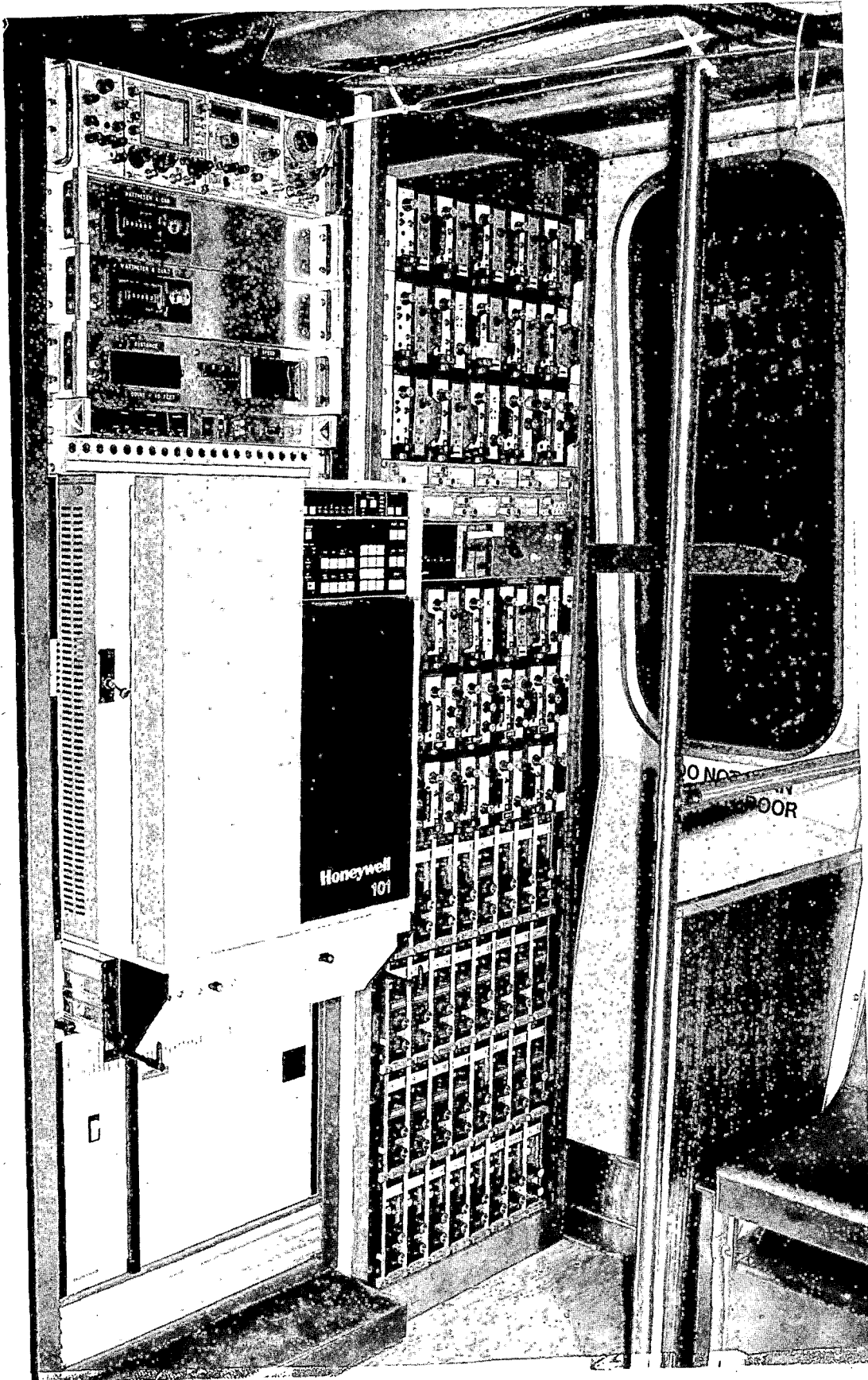


FIGURE A-2 DATA ACQUISITION SYSTEM.

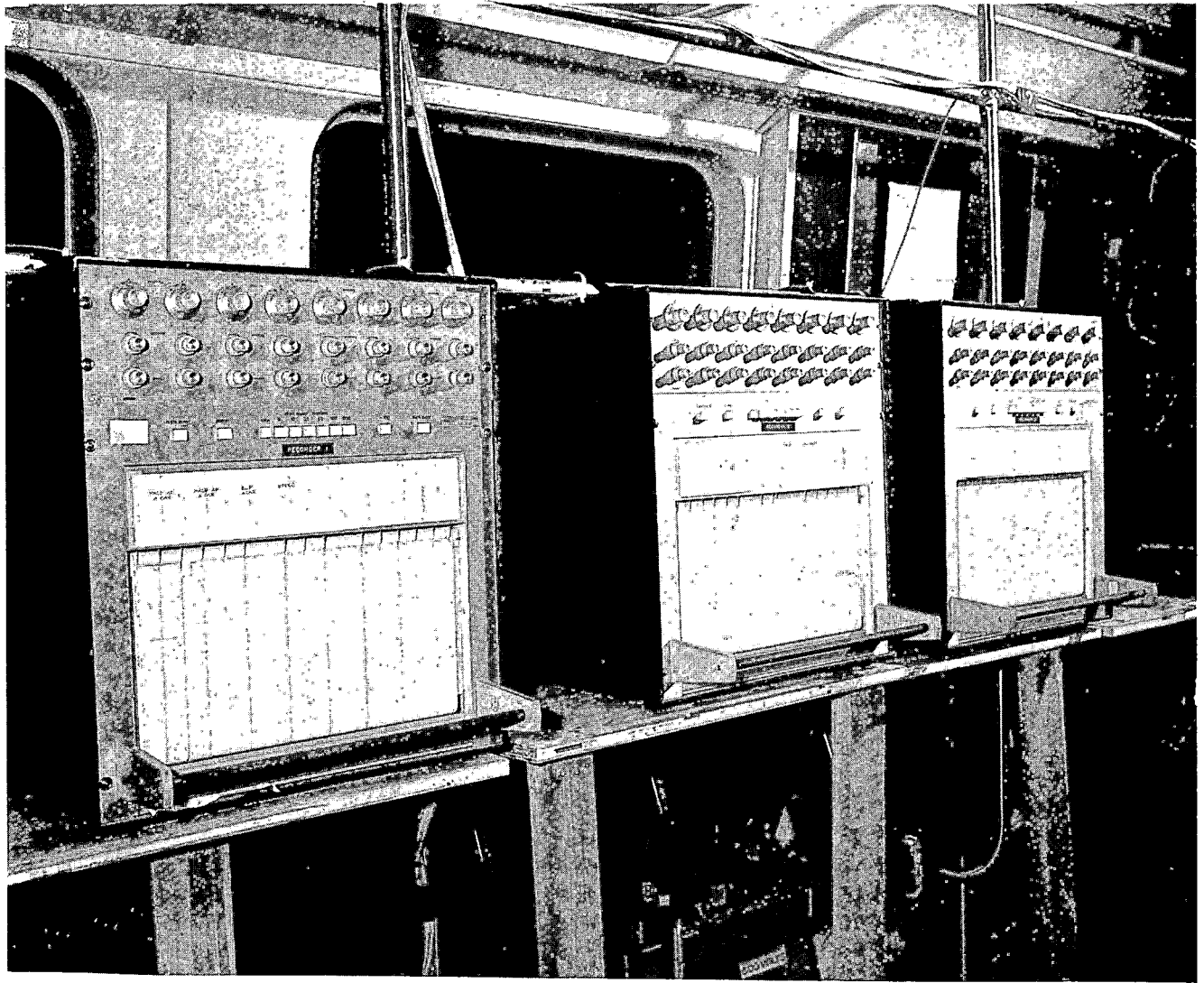


FIGURE A-3 DATA ACQUISITION SYSTEM.

described below, and the signal monitoring system is described in detail in a standard instrumentation manual.¹

The ENDEVCO 4470 has 35 separate channels, each of which is composed of a modular unit and a plug-in 'mode' card. Seven rack adapters provide for mounting of the modules in a standard 19" rack, five modules per adapter, with interconnections for power, signal input, signal output, and monitor and calibration functions. The modular unit is a package containing circuit instrument power supply, calibration circuits, and interconnections for each plug-in mode card.

The mode card contains circuit components designed for a specific type of signal conditioning. Conditioning functions of the measurement system are all routed through the mode card, and the function of a particular module is 'specialized' by the card installed. Any module can be used to perform any conditioning function by installing the appropriate card. Cards may have a standard circuit configuration or a custom circuit. The variety of card types used to condition incoming signals is evident in Figure A-2.

Signal Filtering Electronics

An Ithaco type 4113 system was used to enhance the signal-to-noise ratio of the measurement systems and to minimize signal 'aliasing' during digitization. The system is made up of 32 separate channels of low-pass filter networks. Each channel is switch-selectable between 4-pole Bessel (linear phase delay) or 4-pole Butterworth (maximum flat amplitude response) filter characteristics. The cutoff frequency of each channel can be varied from 1 Hz to 1 MHz. Each of the separate filters (Ithaco 4113M101) is an integral modular unit. Eight of these modules were installed in a rack-mounted adapter which provided a common a.c. power input, switch, indicator lamp, and fuse.

Strip Chart Recorders

The strip chart recorders that were used to monitor test progress online consisted of three Brush (model 480) 8-channel recorders.

Tape Recorder

The analog type recorder was a Honeywell model 101 portable magnetic tape recorder/reproducer with microcomputer control. The tape heads were 28-track, IRIG configuration. The tape recorder setup for MBTA testing is listed in Table A-3.

1 General Vehicle Test Instrumentation Manual, Report No. UMTA-MA-06-0025-77-77.

TABLE A-3. TAPE RECORDER CONFIGURATION.

Track	Record/Reproduce	Data
#1	Direct	IRIG-B time code
#2 #26	FM	Data channels
#27	FM Shorted input to record center frequency as a reference signal	
#28	Voice	Voice

The FM data channels were adjusted so that full-scale signal equalled 40 percent deviation, at a tape speed of 1 7/8 inches per second. The center frequency was 3.375 kHz, with +40% = 4.725 kHz and -40% = 2.025 kHz.

X-Y Plotter

A Hewlett-Packard 70048 X-Y analog plotter was used onboard the cars during the performance test phase, to plot acceleration/deceleration versus speed from conditioned inputs from the data acquisition system.

Ninth Wheel Speed And Distance Processor

The ninth wheel speed and distance processor was fabricated by Garrett Airesearch, Inc. The processor applies excitation to an electromagnetic sensor (mounted on the ninth wheel assembly under the car) and, in turn, receives pulses from the sensor caused by a 60-tooth gear (attached to the ninth wheel) rotating in its magnetic field. As the gear rotates, the sensor produces a pulsed signal whose frequency is proportional to the rotational speed of the wheel. The processor accepts this signal and produces an analog output voltage proportional to speed, together with a staircase function distance signal. The circuitry within the processor can apply scaling factors to suit the circumference of the ninth wheel and the number of pulses per revolution from the toothed gear wheel. The staircase distance signal is comprised of a series of ten additive step functions which reset to zero output voltage after every tenth step. A scaling factor can be set in the processor to equate each step to 0.1, 1, or 10 ft.

Energy Consumption Watt-Hour Meter

Energy consumption data were acquired by means of a watt-hour chassis designed and constructed at the TTC. The chassis has an analog multiplier to provide an output, from the scaled inputs of voltage and current sensors, proportional to instantaneous power. The output of the multiplier was then integrated with respect to time by an integrating voltage-frequency converter. This device produced a pulse frequency

proportional to applied voltage. Each pulse represented an increment of energy, the sum of which represented total energy. Output from the frequency converter was then conditioned in a divider/counter driver circuit, using three scalable counters and a monostable multivibrator. This driver circuit acted as a pulse stretcher to increase the pulse width to the 20 ms minimum required to drive a 6-digit mechanical counter (one for each car of a married pair), which totalled power consumption over the duration of a test run. A functional description of the system² and a circuit diagram of the watt/hour meter chassis³ are maintained by the TTC.

DATA PROCESSING

Data Processing was conducted in a variety of methods, with consideration given to the complexity and length of each specific task in order to reduce the total data processing task. As a result, digital data analysis requirements were reduced to a minimum and emphasis was placed on treating raw data, direct from the analog data tapes, using hardware such as a spectrum analyzer. The following paragraphs describe the techniques used for each test phase.

Performance Data

Acceleration and deceleration performance characteristic plots were obtained onboard the cars using scaled analog inputs to an X-Y plotter. The plotter was patched in parallel with the tape recorder and the Brush charts, allowing data plots to be produced as the test runs were conducted. Scaling of the plotter was obtained from (1) a known offset of the longitudinal accelerometer for the acceleration input, and (2) from an oscillator input to the speed and distance processor (representing a known speed) for the vehicle speed input. Energy consumption data were tabulated from the digital displays of the onboard watt-hour meters. Spin/slide protection system efficiency was determined directly from the Brush Chart oscillograph records by the use of numerical integration techniques.

Drift test data were digitized at 32 samples per second and plotted, speed versus time, on a DEC 11/60 computer, using a time history format. Average acceleration values were calculated from velocity and time pairs selected from the plots. An acceleration time history was then plotted from these values, from which a train-resistance versus speed plot was calculated, using the known vehicle weight with an allowance for rotating inertia.

2 "Functional Description of Watt-Hour Meter" TTC Memo IE/DG/76-109, November 23, 1976.

3 "Drawing Number Sk-RDL-4255", Transportation Test Center, January 4, 1977.

Ride Quality Data

The basis for the assessment of ride quality was the ISO 2631 Guide for the Evaluation of Human Exposure to Whole-Body Vibration, (ISO 2631-1974, International Organization for Standardization).

To characterize the ride quality of the cars, three data processing methods were used:

- One-third octave band vibration levels,
- ISO 2631-weighted vibration level (ride roughness) time histories, and
- ISO 2631-weighted rms single-number characterization (ride roughness level).

The one-third octave band levels were obtained by synthesis from the Fourier spectrum produced by the Fourier Transform algorithm performed on an HP 3582A Spectrum Analyzer. The frequency ranges of interest are as follows:

- One-third octave bands from 0.1 to 0.8 Hz center frequency (motion sickness range), and
- One-third octave bands from 1.0 to 80 Hz center frequency (whole-body vibration range).

The one-third octave band characteristics were taken from the International Electromechanical Commission, Publication 225 Octave, Half-Octave, and Third-Octave Band Filters Intended for the Analysis of Sounds and Vibrations. The publication defines the exact center frequency (F_m) of each third-octave as:

$$F_m = 10^{10 \frac{N}{10}}$$

where:

N = the band #, a positive or negative integer or zero

Also, the passband of each filter is defined by the upper and lower limiting frequencies:

$$F_2 = F_m \sqrt[6]{2} \approx 1.1225 F_m$$

and

$$F_1 = F_m / \sqrt[6]{2} \approx 0.8909 F_m$$

where:

F_2 = upper limiting frequency

F_1 = lower limiting frequency

In the range of interest in ride quality there are 30, one-third octave bands, as shown in Table A-4.

TABLE A-4. ONE-THIRD OCTAVE BAND CENTER FREQUENCIES.

Band Numbers	Preferred Frequencies	Pass-Band $F_2 - F_1$	
(N)	(Hz)	(Hz)	
-10	0.1	0.0231	Motion Sickness Range
- 9	0.125	0.0291	
- 8	0.16	0.0367	
- 7	0.2	0.0462	
- 6	0.25	0.0581	
- 5	0.315	0.0732	
- 4	0.4	0.0921	
- 3	0.5	0.116	
- 2	0.63	0.146	
- 1	0.8	0.183	
0	1	0.183	Whole Body Vibration Range
1	1.25	0.291	
2	1.6	0.367	
3	2	0.462	
4	2.5	0.581	
5	3.15	0.732	
6	4	0.921	
7	5	1.16	
8	6.3	1.46	
9	8	1.83	
10	10	2.31	
11	12.5	2.91	
12	16	3.67	
13	20	4.62	
14	25	5.81	
15	31.5	7.32	
16	40	9.21	
17	50	11.16	
18	63	14.6	
19	80	18.3	

Note that the passband of the highest frequency band is almost 1000 times as wide as that of the lowest frequency band. Because of this very great difference of passband width, the synthesis from the Fourier Spectrum is made more difficult. The Fast Fourier Transform (FFT) analyzer produced a 256-spectral-line display over the frequency range selected. In order to have a minimum of 5 spectral lines falling in every 1/3 octave band for subsequent synthesis, the FFT analysis was performed by taking multiple passes over three ranges:

- 0.0 to 1.0 Hz - for motion sickness.
- 0.0 to 10.0 Hz - for motion sickness.
- 0.0 to 100.0 Hz - for whole body vibration.

The corresponding spectral line spacing, and the time taken to collect one pass at each range, is as follows:

<u>Range(Hz)</u>	<u>Line Spacing(Hz)</u>	<u>Time(s)</u>
0.0 to 1.0	0.004	250
0.0 to 10.0	0.04	25
0.0 to 100.0	0.4	2.5

When analyzing the whole-body vibration range it was the practice to take 8 passes at 2.5 seconds each, with the analyzer set at the 100 Hz upper frequency, a total of $8 \times 2.5 = 20$ seconds of data. For the 10 Hz upper frequency, one pass of 25 seconds was taken. Thus, both ranges covered approximately the same quantity of data.

When analyzing the motion sickness range it was the practice to take one pass with the analyzer at 1 Hz upper frequency (250 seconds of data), 8 passes at 10 Hz upper frequency (200 seconds of data), and 64 passes at 100 Hz upper frequency (160 seconds of data). Because the time required to produce the motion sickness range was so long, the analysis was restricted to recordings made when the cars circled the entire track.

Synthesis of the one-third octave bands from the spectral time display on the analyzer was performed on an HP 85 desk top computer connected to the analyzer by the HP-IB interface bus. A modified version of a one-third octave analysis program for the audio range (contained in HP application note 245-3) was used. The data from the Fourier spectrum was added together within each one-third octave band on the basis of power. The criterion for addition was that if a spectral line lay inside the passband it was added. Allowance was made for the Hann window applied to the signal. The modified program was checked with both a white noise source and a single frequency signal.

The ISO 2631-weighted rms values (or ride roughness levels) were obtained by first weighting the signal with an electronic network having a passband shape of characteristics shown in Table A-5. Two weighting networks were used, one for vibrations in the vertical direction and one for longitudinal and lateral vibrations. The weighted signal was then applied to the spectrum analyzer and a Fourier spectrum produced. The rms value was obtained in a way similar to obtaining one-third octave band values except that the bandwidth was broadened to cover the frequency range of interest.

The ISO-weighted (ride roughness) vibration time histories were produced by rectifying and smoothing the signals produced by the ISO weighting networks. The output was then applied to a B&K portable level graphic recorder to produce a strip chart. The rectifying network had an averaging time constant of approximately 1 second. With the graphic level recorder's "Recording Mode" switch set to "DC Log" mode and with a 50-dB, logarithmic potentiometer installed, strip charts of weighted vibration level with 1 g rms full-scale and a range of 50 dB could be produced. Paper speed was 3 mm/sec. Both the characteristics of the weighting network and the rectifying circuits

were functionally checked with single-frequency sine waves.

TABLE A-5. WEIGHTING FACTORS RELATIVE TO THE FREQUENCY RANGE OF MAXIMUM ACCELERATION SENSITIVITY* FOR THE VIBRATION ISO 2631 RESPONSE CURVES.

Center Frequency of 1/3 octave band	Vertical (z) Vibrations		Longitudinal and Lateral (x,y) Vibrations	
	Weighting Factor	Attenuation (dB)	Weighting Factor	Attenuation (dB)
1.0	0.50	= - 6	1.00	= 0
1.25	0.56	= - 5	1.00	= 0
1.6	0.63	= - 4	1.00	= 0
2.0	0.71	= - 3	1.00	= 0
2.5	0.80	= - 2	0.80	= - 2
3.15	0.90	= - 1	0.63	= - 4
4.0	1.00	= 0	0.50	= - 6
5.0	1.00	= 0	0.40	= - 8
6.3	1.00	= 0	0.315	= -10
8.0	1.00	= 0	0.25	= -12
10.0	0.80	= - 2	0.2	= -14
12.5	0.63	= - 4	0.16	= -16
16.0	0.50	= - 6	0.125	= -18
20.0	0.40	= - 8	0.10	= -20
25.0	0.315	= -10	0.08	= -22
31.5	0.25	= -12	0.063	= -24
40.0	0.20	= -14	0.050	= -26
50.0	0.16	= -16	0.040	= -28
63.0	0.125	= -18	0.0315	= -30
80.0	0.10	= -20	0.025	= -32

* 4 to 8 Hz in the case of vertical vibration
 1 to 2 Hz in the case of lateral vibration

Appendix B

MBTA ORANGE LINE REVENUE SERVICE PROFILE SIMULATIONS

The following tables, B-1 and B-2, detail the test runs made to simulate a round trip revenue service run on the MBTA Orange Line. The distances between stations, the maximum speeds attained, and the station dwell times are those detailed by MBTA for the Orange Line, from Oak Grove to Forest Hills and return. Only the track gradients differed.

TABLE B-1 MBTA ORANGE LINE REVENUE SERVICE PROFILE SIMULATION - SOUTHBOUND.

Depart Station Name	Station Marker	First Speed mi/h	Station Marker	Next Speed mi/h	Station Marker	Next Speed mi/h	Station Marker	Next Speed mi/h	Arrive Station Name	Dwell Time Sec.
Oak Grove	5.000	40	9.160	0					Malden	25
Malden	9.160	40	18.420	0					Wellington	20
Wellington	18.420	40	24.680	0					Sullivan Sq.	20
Sullivan Sq.	24.680	40	29.060	0					Community Coll.	15
Community Coll.	29.060	25	29.760	40	33.350	0			North Station	20
North Station	33.350	30	34.760	0					Haymarket	20
Haymarket	34.760	40	35.930	25	36.600	0			State	20
State	36.600	40	37.545	0					Washington	20
Washington	37.545	40	38.890	0					Essex	20
Essex	38.890	25	41.860	0					Dover	15
Dover	41.860	25	45.930	0					Northampton	15
Northampton	45.930	25	47.930	15	49.290	0			Dudley	30
Dudley	49.290	15	50.120	25	7.420	0			Egleston	15
Egleston	7.420	25	10.240	0					Green Street	15
Green Street	10.240	25	12.950	15	14.200	0			Forest Hills	15
Forest Hills	14.200	15	14.750	0					Forest Hills Tail Track	END

TABLE B-2 MBTA ORANGE LINE REVENUE SERVICE PROFILE SIMULATION - NORTHBOUND.

Forest Hills Tail Track	14.610	15	13.850	0					Forest Hills	15
Forest Hills	13.850	25	9.890	0					Green Street	15
Green Street	9.890	25	7.082	0					Egleston	15
Egleston	7.082	25	50.690	10	49.610	6	48.780	0	Dudley	30
Dudley	48.780	10	48.180	25	45.580	0			Northampton	15
Northampton	45.580	25	41.490	0					Dover	15
Dover	41.490	25	40.780	15	39.040	40	38.180	0	Essex	20
Essex	38.180	40	36.830	0					Washington	20
Washington	36.830	40	35.500	0					State Street	20
State Street	35.500	40	34.330	0					Haymarket	20
Haymarket	34.330	40	32.910	0					North Station	20
North Station	32.910	40	29.540	20	28.630	0			Community Coll.	15
Community Coll.	28.630	40	24.260	0					Sullivan Sq.	20
Sullivan Sq.	24.260	40	18.000	0					Wellington	20
Wellington	18.000	40	8.730	0					Malden	25
Malden	8.730	40	5.990	25	5.739	15	4.840	0	Oak Grove	END